Published for SISSA by Springer

Received: *June 4, 2024*
Accepted: *August 14, 2024*
Published: *September 2, 2024*

Search for dark mesons decaying to top and bottom quarks in proton-proton collisions at $\sqrt{s} = 13$ TeV with the ATLAS detector

The ATLAS collaboration

E-mail: atlas.publications@cern.ch

Abstract: A search for dark mesons originating from strongly-coupled, SU(2) dark flavor symmetry conserving models and decaying gaugephobically to pure Standard Model final states containing top and bottom quarks is presented. The search targets fully hadronic final states and final states with exactly one electron or muon and multiple jets. The analyzed data sample corresponds to an integrated luminosity of 140 fb^{-1} of proton-proton collisions collected at $\sqrt{s} = 13$ TeV with the ATLAS detector at the Large Hadron Collider. No significant excess over the Standard Model background expectation is observed and the results are used to set the first direct constraints on this type of model. The two-dimensional signal space of dark pion masses m_{π_D} and dark rho-meson masses m_{ρ_D} is scanned. For $m_{\pi_D}/m_{\rho_D} = 0.45$, dark pions with masses $m_{\pi_D} < 940$ GeV are excluded at the 95% CL, while for $m_{\pi_D}/m_{\rho_D} = 0.25$ masses $m_{\pi_D} < 740$ GeV are excluded.

Keywords: Beyond Standard Model, Dark Matter, Exotics, Hadron-Hadron Scattering

ArXiv ePrint: 2405.20061

https://doi.org/10.1007/JHEP09(2024)005

JHEP09(2024)005

Contents

1 Introduction

The Standard Model (SM) can be extended by a new strongly-coupled, confining gauge theory with fermion representation which transforms under the electroweak group. The appeal of such an extension is that dark matter can arise in the form of composite mesons or baryons of the new strongly-coupled theory. In addition, these models often exhibit an automatic accidental symmetry protecting against dark matter decay. Consequently, candidates for strongly-coupled dark matter include dark mesons, dark quarkonia-like states, glueballs and dark baryons [1, 2]. The search presented here targets one set of models incorporating this

JHEP09(2024)005

concept: Stealth Dark Matter [3]. Here, the new strongly-coupled dark sector consists of vector-like fermions that can transform under the new dark group but also interact with both the electroweak sector of the SM and the Higgs boson. The result is the emergence of a quantum chromodynamics (QCD)-like dark sector as the direct analog to the QCD meson and baryon sector. This leads to several intriguing phenomenological consequences: as long as the vector-like mass is dominant over the chiral mass, the new dark sector is only weakly constrained by precision electroweak or Higgs coupling measurements, while the Higgs interactions break the dark sector global symmetry and thus allow dark mesons to decay into pure SM states [4]. This search focuses on the low-energy effective theories developed in ref. [5], which incorporate the leading interactions between dark mesons of a strongly-coupled SU(2) dark flavor symmetry preserving dark sector and the SM. These models contain a stable dark scalar baryon which could account for the stable dark matter observed in cosmological measurements [3].

The simplified model targeted in this search contains only the two phenomenologically relevant sets of dark mesons: a lighter pseudoscalar triplet of dark pions, π_D, and an additional triplet of dark rho vector mesons, ρ_D, which are both expected at a scale around or slightly above the electroweak scale. Following standard theoretical assumptions, the triplets are completely mass-degenerate and the dark sector can be fully described by three parameters: the mass of the dark pions m_{π_D}, the mass of the dark rho mesons m_{ρ_D}, and the number of dark colors N_D. Since the phenomenological consequences remain unchanged for values of N_D that are not excessively large, N_D is fixed to $N_D = 4$ throughout this search following the typical choice made for Stealth Dark Matter [3].

Contrary to QCD, the vector-like nature of the dark sector allows to either gauge the full $\mathrm{SU(2)}_L$ weak interaction symmetry group or just the underlying U(1) group, which leads to two distinct models of kinetic mixing of dark mesons with the SM, $\mathrm{SU(2)}_L$ and $\mathrm{SU(2)}_R$. The phenomenological consequences manifest themselves in the allowed decay channels and production cross-sections of dark pions, where the $\mathrm{SU(2)}_L$ models result in considerably larger cross sections than the $\mathrm{SU(2)}_R$ models. Dark pions are always pair-produced either via Drell-Yan-type processes or resonantly via kinetic mixing of SM electroweak gauge bosons with the ρ_D that then subsequently decays into a pair of dark pions, as shown in figure 1. The kinetic mixing parameter ϵ depends on the number of dark colors as shown in figure 1(a) (see also ref. [4]). Throughout nearly all of the parameter space investigated in this search, the resonant production dominates the production of dark pions. Once the choice of $N_D = 4$ is made, the production cross-section depends trivially on the ratio of the dark pion and dark rho-meson masses, for which the symbol $\eta_D = m_{\pi_D}/m_{\rho_D}$ is used, equivalent to the η defined in ref. [4]. For gaugephobic $\mathrm{SU(2)}_L$ models, a given dark pion mass and η_D-parameter fully specify the model, including the dark pion decay branching fractions.

This search considers only models with $\eta_D < 0.5$ where the decay $\rho_D^{\pm,0} \to \pi_D^{\pm}\pi_D^{0,\mp}$ has a branching fraction of nearly 1.0, while for models with $\eta_D > 0.5$ this decay is kinematically forbidden and the dark rho meson can only decay to pairs of leptons or quarks. Previous searches for resonances in the dilepton spectrum both in ATLAS [6] and CMS [7] have placed strong constraints on such models [4]. The bounds for models with $\eta_D < 0.5$ are considerably weaker [2]. This is the first search in any collider experiment optimized for this specific type of model.

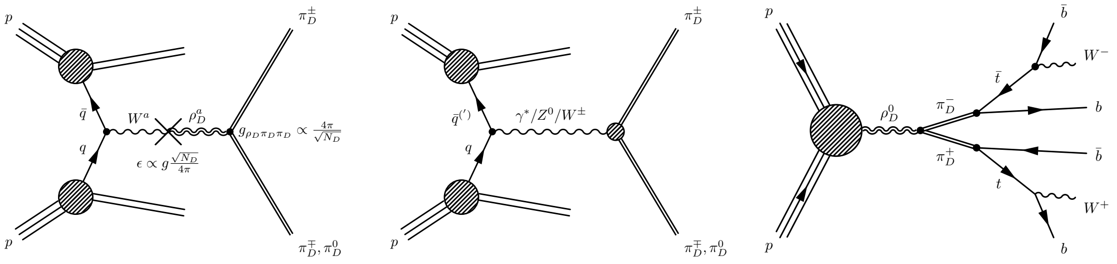

(a) (b) (c)

Figure 1. Examples of leading Feynman diagrams of dark pion pair production. The diagram in (a) shows resonant production via kinetic mixing with the W-field resulting in either a neutral or charged dark rho meson, a mixing with the B-field that can only result in a neutral dark rho meson is also possible, (b) shows Drell-Yan-type pair production of dark pions, and (c) shows an illustrative diagram of the dark pion decay into a top and a bottom quark for dark pion production.

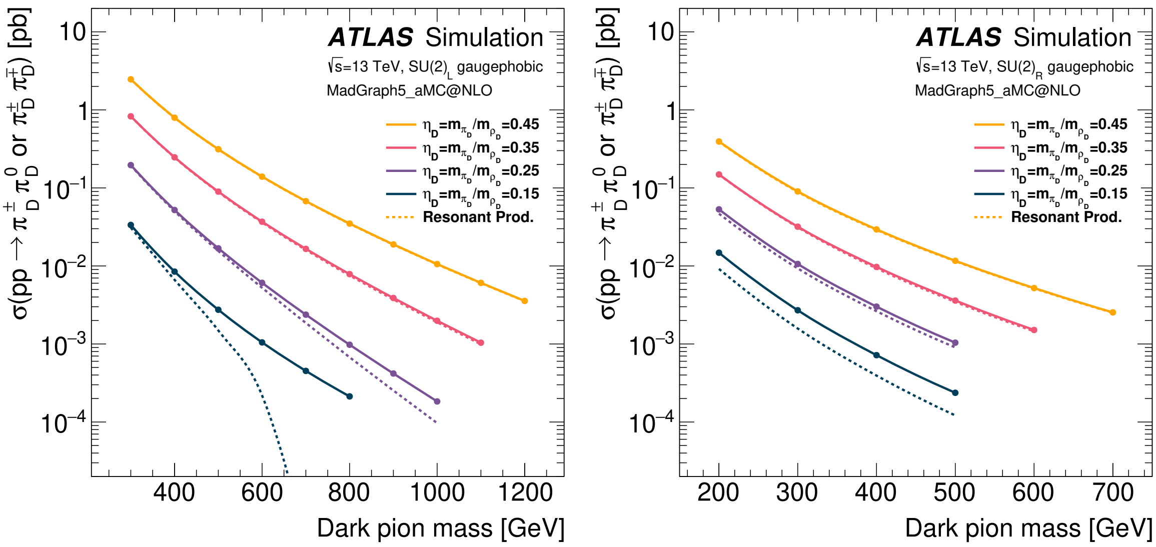

(a) (b)

Figure 2. Pair-production cross-sections for dark pions as a function of dark pion mass for four different values of η_D in (a) an $\mathrm{SU}(2)_L$ model and (b) an $\mathrm{SU}(2)_R$ model. The dashed colored lines indicate the contribution of the resonant production mode to the total dark pion production cross-section.

Figure 2 shows the pair-production cross-sections for dark pions in $\mathrm{SU}(2)_L$ and $\mathrm{SU}(2)_R$ models. The contribution of resonant production to the total production cross-section is indicated by the dashed lines. A variety of different decay channels are open to dark pions in the available parameter space. The most relevant channels and their branching fractions are shown in figure 3. For gaugephobic models the decay to top and bottom quarks dominates at high masses, while decays to bottom and charm quarks, τ-leptons and gauge bosons are relevant at lower dark pion masses.

This search is the result of the analysis of $140\,\mathrm{fb}^{-1}$ of proton-proton (pp) collisions collected by the ATLAS detector during Run 2 of the Large Hadron Collider (LHC). Since

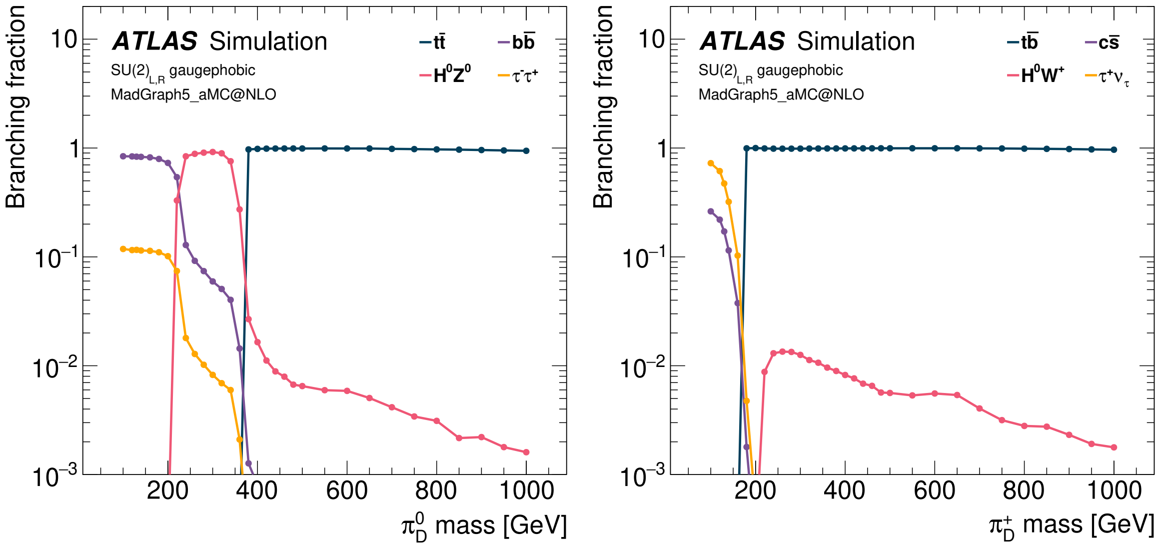

(a) (b)

Figure 3. Branching fractions of the available decays of dark pions from gaugephobic SU$(2)_L$ and SU$(2)_R$ models are shown for (a) neutral dark pions and (b) positively charged dark pions. Channels with small branching fractions are suppressed for clarity.

the dark pions are pair-produced in the model considered, the experimental signatures are either three top quarks and one bottom quark ($tttb$) or two top quarks and two bottom quarks ($ttbb$).[1] About one third of dark pions in the SU$(2)_L$ models are neutral, resulting in the $tttb$ event signature being twice as likely as the $ttbb$ signature. These processes can give rise to several different final states depending on the hadronic or semileptonic decay mode of each of the top quarks. The search is performed in the *all-hadronic* channel, targeting fully hadronic top quark decays where the signal results in eight to ten jets of which at least four originate from bottom quarks, and in the *one-lepton* channel, corresponding to final states with exactly one electron or muon in addition to up to four jets from b-quarks.

The results are interpreted as limits on the production cross-section of dark pion pairs as a function of m_{π_D} and η_D.

2 ATLAS detector

The ATLAS detector [8] at the LHC covers nearly the entire solid angle around the collision point.[2] It consists of an inner tracking detector surrounded by a thin superconducting

[1]The label "$tttb$" is used to indicate both $t\bar{t}t\bar{b}$ as well as its charge conjugate, $t\bar{t}\bar{t}b$; whereas "$ttbb$" refers to $t\bar{t}b\bar{b}$.

[2]ATLAS uses a right-handed coordinate system with its origin at the nominal interaction point (IP) in the center of the detector and the z-axis along the beam pipe. The x-axis points from the IP to the center of the LHC ring, and the y-axis points upwards. Polar coordinates (r, ϕ) are used in the transverse plane, ϕ being the azimuthal angle around the z-axis. The pseudorapidity is defined in terms of the polar angle θ as $\eta = -\ln\tan(\theta/2)$ and is equal to the rapidity $y = \frac{1}{2}\ln\left(\frac{E+p_z c}{E-p_z c}\right)$ in the relativistic limit. Angular distance is measured in units of $\Delta R \equiv \sqrt{(\Delta y)^2 + (\Delta\phi)^2}$.

solenoid, electromagnetic and hadronic calorimeters, and a muon spectrometer incorporating three large superconducting air-core toroidal magnets.

The inner-detector system (ID) is immersed in a 2 T axial magnetic field and provides charged-particle tracking in the range $|\eta| < 2.5$. The high-granularity silicon pixel detector covers the vertex region and typically provides four measurements per track, the first hit generally being in the insertable B-layer (IBL) installed before Run 2 [9, 10]. It is followed by the SemiConductor Tracker (SCT), which usually provides eight measurements per track. These silicon detectors are complemented by the transition radiation tracker (TRT), which enables radially extended track reconstruction up to $|\eta| = 2.0$. The TRT also provides electron identification information based on the fraction of hits (typically 30 in total) above a higher energy-deposit threshold corresponding to transition radiation.

The calorimeter system covers the pseudorapidity range $|\eta| < 4.9$. Within the region $|\eta| < 3.2$, electromagnetic calorimetry is provided by barrel and endcap high-granularity lead/liquid-argon (LAr) calorimeters, with an additional thin LAr presampler covering $|\eta| < 1.8$ to correct for energy loss in material upstream of the calorimeters. Hadronic calorimetry is provided by the steel/scintillator-tile calorimeter, segmented into three barrel structures within $|\eta| < 1.7$, and two copper/LAr hadronic endcap calorimeters. The solid angle coverage is completed with forward copper/LAr and tungsten/LAr calorimeter modules optimized for electromagnetic and hadronic energy measurements respectively.

The muon spectrometer (MS) comprises separate trigger and high-precision tracking chambers measuring the deflection of muons in a magnetic field generated by the superconducting air-core toroidal magnets. The field integral of the toroids ranges between 2.0 and 6.0 T m across most of the detector. Three layers of precision chambers, each consisting of layers of monitored drift tubes, cover the region $|\eta| < 2.7$, complemented by cathode-strip chambers in the forward region, where the background is highest. The muon trigger system covers the range $|\eta| < 2.4$ with resistive-plate chambers in the barrel, and thin-gap chambers in the endcap regions.

The luminosity is measured mainly by the LUCID–2 [11] detector that records Cherenkov light produced in the quartz windows of photomultipliers located close to the beampipe.

Events are selected by the first-level trigger system implemented in custom hardware, followed by selections made by algorithms implemented in software in the high-level trigger [12]. The first-level trigger accepts events from the 40 MHz bunch crossings at a rate below 100 kHz, which the high-level trigger further reduces in order to record complete events to disk at about 1 kHz.

A software suite [13] is used in data simulation, in the reconstruction and analysis of real and simulated data, in detector operations, and in the trigger and data acquisition systems of the experiment.

3 Data and simulated event samples

This analysis is performed using data from pp collisions with $\sqrt{s} = 13$ TeV recorded by the ATLAS detector in 2015–2018. Only events for which all relevant subsystems were operational are considered. The data correspond to an integrated luminosity of $140.1 \pm 1.2\,\text{fb}^{-1}$ [14].

Monte Carlo (MC) simulated event samples are used for the estimate of background from SM processes and to model the targeted signal models. The details of the event generation are provided in sections 3.1 and 3.2 for signal and background samples, respectively. The generation of all simulated event samples includes the effect of multiple pp interactions per bunch crossing, as well as changes in detector response due to interactions in bunch crossings before or after the one containing the hard interaction, modeled by overlaying simulated inelastic events on the physics event. These two effects are referred to as pileup. The simulated event samples are processed with the GEANT4-based ATLAS detector simulation [15, 16]. All samples are weighted to match the pileup distribution observed in data and are processed with the same reconstruction algorithms as data.

3.1 Signal samples

Signal samples are generated in a grid over a two-dimensional space, varying the dark pion mass m_{π_D} between 300–1200 GeV and the η_D-parameter between 0.15–0.45. The matrix element calculation for the pair production of dark pions is performed at next-to-leading order (NLO) in QCD based on the model described in ref. [4] using MADGRAPH5_aMC@NLO v2.4.3 [17] interfaced with PYTHIA8.212 [18] for the modeling of parton showering, hadronization and underlying event using the A14 set of tuned parameters ("tune") [19] and the NNPDF2.3LO [20] set of parton distribution functions (PDF).

The decays of bottom and charm hadrons are simulated using the EVTGEN v1.6.0 program [21]. An additional set of signal samples, with parameter values near the expected exclusion contour of the all-hadronic channel, is generated at NLO in QCD using MADGRAPH5_aMC@NLO v2.9.9 [17] interfaced with PYTHIA8.306 [22] using the A14 tune and NNPDF2.3LO PDF set. Kinematic distributions match in both setups. All signal cross-sections are extracted from MADGRAPH5_aMC@NLO v2.9.9. The number of dark colors N_D is set to 4 for all signal points. The dark pion decays are simulated using the narrow width approximation and contain all possible decay channels from figure 3.

3.2 Background samples

The dominant SM background process in the all-hadronic channel is multijet production. This background is estimated with data-driven methods while MC simulation is used to estimate the remaining SM processes. The background in the one-lepton channel is estimated from MC simulations and is dominated by top quark pair-production ($t\bar{t}$), often in association with heavy-flavor quarks ($t\bar{t}$+HF). Other important backgrounds are the production of a vector boson in association with jets (V + jets) and single top-quark production (single top) which is dominated by the associated production of a top quark with a W boson but also contains single top-quark production in the s- and t-channels. Smaller background contributions stem from $t\bar{t}$ produced in association with additional bosons or quarks ($t\bar{t}t\bar{t}$, $t\bar{t}V$, $t\bar{t}H$, and other $t\bar{t}$+X) and multiboson production. The configurations used to produce the background samples are described below and are summarized in table 1. For all background samples, except those generated with SHERPA, the EVTGEN v.1.6.0 or v1.7.0 program is used to simulate the decays of bottom and charm hadrons.

JHEP09(2024)005

Process	Generator	PDF	Showering	Tune	Cross section
$t\bar{t}$	PowhegBox v2	NNPDF3.0nlo	Pythia8	A14	NNLO+NNLL
$t\bar{t}b\bar{b}$	Powheg Box Res	NNPDF3.0nlo	Pythia8	A14	NLO
V + jets	Sherpa v2.2.11	NNPDF3.0nnlo	Sherpa	Def.	NLO
Single top	PowhegBox v2	NNPDF3.0nlo	Pythia8	A14	NLO+NNLL
$t\bar{t}t\bar{t}$	MadGraph5_aMC@NLO v2.4.3	NNPDF3.1nlo	Pythia8	A14	NLO
$t\bar{t}V$	MadGraph5_aMC@NLO v2.3.3	NNPDF3.0nlo	Pythia8	A14	NLO
$t\bar{t}H$	PowhegBox v2	NNPDF3.0nlo	Pythia8	A14	NLO
Other $t\bar{t}$+X	MadGraph5_aMC@NLO	NNPDF2.3lo	Pythia8	A14	NLO
Multiboson	Sherpa v2.2.1/v2.2.2	NNPDF3.0nnlo	Sherpa	Def.	NLO

Table 1. Overview of the configuration of all nominal background samples used in the analysis; details and definitions are provided in the text.

3.2.1 $t\bar{t}$ background

The production of $t\bar{t}$ events is modeled using the PowhegBox v2 [23–26] generator that provides matrix elements at NLO in QCD with the NNPDF3.0nlo [27, 28] set PDFs and the h_{damp} parameter, which controls the matching in Powheg and effectively regulates the high-p_{T} radiation against which the $t\bar{t}$ system recoils, set to 1.5 m_{top} [29]. The functional form of the renormalization and factorization scales are set to the default scale $\sqrt{m_{\mathrm{top}}^2 + p_{\mathrm{T}}^2}$. The events are interfaced with Pythia8.230 for the parton shower and hadronization, using the A14 set of tuned parameters and the NNPDF2.3lo PDF set. The $t\bar{t}$ sample is normalized to the cross section prediction at next-to-next-to-leading order (NNLO) in QCD including the resummation of next-to-next-to-leading-logarithmic (NNLL) soft-gluon terms calculated using Top++2.0 [30–36]. For pp collisions at a center-of-mass energy of $\sqrt{s} = 13\,\mathrm{TeV}$, this cross section corresponds to $\sigma(t\bar{t})_{\mathrm{NNLO+NNLL}} = 832 \pm 51\,\mathrm{pb}$ using a top-quark mass of $m_{\mathrm{top}} = 172.5\,\mathrm{GeV}$.

The inclusive $t\bar{t}$ sample described above is complemented by a dedicated sample in which a pair of top quarks is produced in association with two b-quarks. Events are simulated with the Powheg Box Res [37] generator and OpenLoops 1 [38–40], using a pre-release of the implementation of this process in Powheg Box Res provided by the authors [41], with the NNPDF3.0nlo PDF set. It is interfaced with Pythia8.240, using the A14 set of tuned parameters and the NNPDF2.3lo PDF set. The four-flavor scheme is used with the b-quark mass set to 4.95 GeV. The factorization scale and h_{damp} parameter are both set to $0.5 \times \Sigma_{i=t,\bar{t},b,\bar{b},j} m_{\mathrm{T},i}$, and the renormalization scale is set to $\sqrt[4]{m_{\mathrm{T}}(t) \cdot m_{\mathrm{T}}(\bar{t}) \cdot m_{\mathrm{T}}(b) \cdot m_{\mathrm{T}}(\bar{b})}$. This $t\bar{t}b\bar{b}$ sample is used in the one-lepton channel where the dominant background comes from $t\bar{t}$ production, whereas the multijet-dominated all-hadronic channel relies on the five-flavor scheme inclusive sample alone.

Previous studies have seen improved agreement between data and prediction in $t\bar{t}$ events, particularly for the top-quark p_{T} distribution, when comparing with NNLO calculations [42]. Top-quark pair differential calculations at NNLO QCD accuracy including electroweak (EW) corrections have become available [43]. Hence, a small improvement to the modeling is incorporated by correcting the $t\bar{t}$ and the $t\bar{t}b\bar{b}$ samples to match their top/antitop-quark

JHEP09(2024)005

p_{T} and the top-quark mass distribution to the accuracy predicted at NNLO in QCD and NLO in EW.

Events in the $t\bar{t}$ and $t\bar{t}b\bar{b}$ samples are classified according to the flavor of the particle jets not originating from the top quark. The particle jets are reconstructed from the simulated stable particles using the anti-k_t algorithm [44, 45] with a radius parameter $R = 0.4$, and are required to have $p_{\mathrm{T}} > 15\,\mathrm{GeV}$ and $|\eta| < 2.5$. Events are labeled as $t\bar{t}+ \geq 1b$ if at least one particle jet is matched within $\Delta R < 0.4$ to b-hadrons with $p_{\mathrm{T}} > 5\,\mathrm{GeV}$ that do not arise from the decay of top quarks. In the remaining events, if at least one particle jet is matched within $\Delta R < 0.4$ to additional c-hadrons with $p_{\mathrm{T}} > 5\,\mathrm{GeV}$, the events are classified as $t\bar{t}+ \geq 1c$. All other events are labeled as $t\bar{t} + \mathrm{light}$. The $t\bar{t}b\bar{b}$ sample is used for the $t\bar{t}+ \geq 1b$ category meaning that all $t\bar{t} + \mathrm{light}$ and $t\bar{t}+ \geq 1c$ events are rejected from this sample. Likewise, only the $t\bar{t} + \mathrm{light}$ and $t\bar{t}+ \geq 1c$ events are retained from the inclusive $t\bar{t}$ sample.

3.2.2 Other backgrounds

The production of $V +$ jets is simulated with the Sherpa v2.2.11 [46] generator using NLO matrix elements for up to two partons, and leading-order (LO) matrix elements for up to five partons calculated with the Comix [47] and OpenLoops 1 libraries. They are matched with the Sherpa parton shower [48] using the MEPS@NLO prescription [49–52] and the set of tuned parameters developed by the Sherpa authors. The Hessian NNPDF3.0nnlo PDF set is used and the samples are normalized to a prediction that is NNLO in QCD [53].

The associated production of a top quark with a W bosons (tW) is modeled using the PowhegBox v2 [24–26, 54] generator at NLO in QCD using the five-flavor scheme and the NNPDF3.0nlo PDF set. The diagram removal scheme [55] is used to remove interference and overlap with $t\bar{t}$ production. The related uncertainty is estimated by comparing with an alternative sample generated using the diagram subtraction scheme [29, 55]. Single top-quark t-channel production is modeled using the PowhegBox v2 [24–26, 56] generator at NLO in QCD using the four-flavor scheme and the corresponding NNPDF3.0nlo PDF set. Single top-quark s-channel production is modeled using the PowhegBox v2 [24–26, 57] generator at NLO in QCD in the five-flavor scheme with the NNPDF3.0nlo PDF set. All single top-quark events are processed through Pythia8.230 using the A14 tune and the NNPDF2.3lo PDF set.

The production of $t\bar{t}t\bar{t}$ events is modeled using the MadGraph5_aMC@NLO v2.4.3 generator which provides matrix elements at NLO in QCD with the NNPDF3.1nlo [27] PDF set. The functional form of the renormalization and factorization scales is set to $0.25 \times \sum_i \sqrt{m_i^2 + p_{\mathrm{T},i}^2}$, where the sum runs over all the particles generated from the matrix element calculation, following ref. [58]. Top quarks are decayed at LO using MadSpin [59, 60] to preserve all spin correlations. The events are interfaced with Pythia8.230 for the parton shower and hadronization, using the A14 set of tuned parameters and the NNPDF2.3lo PDF set.

The production of $t\bar{t}V$ events is modeled using the MadGraph5_aMC@NLO v2.3.3 generator at NLO in QCD with the NNPDF3.0nlo PDF set. The events are interfaced to Pythia8.210 using the A14 tune and the NNPDF2.3lo PDF set.

The production of $t\bar{t}H$ events is modeled using the POWHEGBOX v2 [23–26, 61] generator at NLO in QCD with the NNPDF3.0NLO PDF set. The events are interfaced to PYTHIA8.230 using the A14 tune and the NNPDF2.3LO PDF set.

Further rare top-quark-pair backgrounds ttt, $t\bar{t}ZZ$, $t\bar{t}WW$, $t\bar{t}WZ$, $t\bar{t}WH$ and $t\bar{t}HH$ are all produced using the NLO in QCD MADGRAPH5_aMC@NLO generator interfaced with PYTHIA8 using the A14 set of tuned parameters and scaled to NLO cross sections [62].

Samples of diboson final states (VV) are simulated with the SHERPA v2.2.1 or v2.2.2 [46] generator depending on the process, including off-shell effects and Higgs-boson contributions, where appropriate. Semileptonic final states, where one boson decays leptonically and the other hadronically, are generated using matrix elements at NLO accuracy in QCD for up to one additional parton and at LO accuracy for up to three additional parton emissions. Samples for the loop-induced processes $gg \to VV$ are generated using LO-accurate matrix elements for up to one additional parton emission. The matrix element calculations are matched and merged with the SHERPA parton shower based on Catani-Seymour dipole factorization [47, 48] using the MEPS@NLO prescription. The virtual QCD corrections are provided by the OPENLOOPS 1 library. The NNPDF3.0NNLO PDF set is used, along with the dedicated set of tuned parton-shower parameters developed by the SHERPA authors.

4 Object and event selections

For each event, interaction vertices are reconstructed from ID charged particle tracks, where the tracks are required to have transverse momenta (p_{T}) greater than 500 MeV [63]. Candidates for the primary vertex are required to have at least two associated tracks. If multiple vertices are reconstructed, the vertex with the largest sum of the squares of the transverse momenta of associated tracks is taken as the primary vertex. Events that fail the primary vertex reconstruction are rejected.

Electrons are reconstructed from energy deposits in the electromagnetic calorimeter that are matched to charged-particle tracks in the ID [64]. They are identified using a likelihood-based (LH) identification which employs calorimeter and tracking information to discriminate between electrons and jets and that combines this likelihood and the likelihood of it originating from background processes into a single discriminant. Only electron candidates with $p_{\mathrm{T}} > 10\,\mathrm{GeV}$ within $|\eta| < 1.37$ or $1.52 < |\eta| < 2.47$ are considered. Electrons are required to be well isolated using criteria based on the properties of the topological clusters in the calorimeter and of ID tracks around the reconstructed electron. Further requirements of $|z_0 \sin\theta| < 0.5\,\mathrm{mm}$ and $|d_0|/\sigma(d_0) < 5$ are placed on the longitudinal and transverse impact parameters to select electrons originating from the primary vertex. Electrons are further categorized as "baseline" or "signal". For the all-hadronic channel, baseline electrons are identified by the *LooseAndBLayer* likelihood-based identification working point and are required to fulfill the *Loose* isolation criteria [64, 65]. Events containing a baseline electron candidate satisfying these baseline criteria are rejected. For the one-lepton channel, baseline electrons are identified with the *Medium* working point [64] and are not subject to any isolation requirement. Signal electrons are identified by the *Tight* working point and are subject to the *Tight* track-based isolation criteria [64]. The p_{T}-requirement of the signal electrons is increased to $p_{\mathrm{T}} > 28\,\mathrm{GeV}$. Signal electrons constitute a subset of the baseline electrons.

Muon candidates are reconstructed by combining tracks in the MS with tracks in the ID and are subject to cut-based identification criteria which are based on the numbers of hits in the different ID and MS subsystems, and on the significance of the charge-to-momentum ratio q/p [66]. All muon candidates are required to be within the acceptance region of the ID at $|\eta| < 2.5$ and to have $p_{\mathrm{T}} > 10\,\mathrm{GeV}$. Muons are required to satisfy isolation requirements based on the properties of ID tracks around the reconstructed muon [66]. Similarly to electrons, requirements on the longitudinal and transverse impact parameters, $|z_0 \sin\theta| < 0.5\,\mathrm{mm}$ and $|d_0|/\sigma(d_0) < 3$, are also applied. Baseline muons are identified in the all-hadronic channel by the *Loose* quality working point and are required to fulfill the *Loose* isolation criteria [66]. Events containing a muon candidate satisfying these baseline criteria are rejected. In the one-lepton channel, baseline muons are identified by the *Medium* quality working point [66] and are not subject to any isolation criteria. For the selection of signal muons the *Medium* quality working point is applied and the muon candidates are required to fulfill the *Tight* isolation criteria based on the $p_T^{\mathrm{varcone30}}$ variable defined in ref. [66] and have $p_{\mathrm{T}} > 28\,\mathrm{GeV}$. Signal muons constitute a subset of the baseline muons. Events are selected for the one-lepton channel if they contain exactly one signal and no additional baseline leptons (electrons or muons).

Jet candidates are reconstructed using a particle-flow reconstruction algorithm [67] combining charged particle tracks from the ID and three-dimensional topological energy clusters [68] in the calorimeter. Jets are reconstructed using the anti-k_t algorithm [44] implemented in the FastJet package [45] with a fixed radius parameter $R = 0.4$ using charged constituents associated with the primary vertex and neutral particle flow objects as inputs. In order to minimize the contribution from pileup jets, a requirement on the jet-vertex tagger [69] is made for jets with p_{T} below $60\,\mathrm{GeV}$.

Slight differences in the efficiency of the association of jets to vertices in data and simulation are addressed by applying scale factors to simulation. Jet energy scale corrections, derived from MC simulation, are used to calibrate the average energies of jet candidates to the scale of their constituent particles [70]. Remaining differences between data and simulated events are evaluated and corrected for using in situ techniques, which exploit the transverse momentum balance between a jet and a reference object such as a photon, Z boson, or multijet system in data. After these calibrations, all jets in the event with $p_{\mathrm{T}} > 20\,\mathrm{GeV}$ must satisfy a set of loose jet-quality requirements [71] designed to reject jets originating from sporadic bursts of detector noise, large coherent noise or isolated pathological cells in the calorimeter system, hardware issues, beam-induced background or cosmic-ray muons [72]. In the one-lepton channel, the jets are required to satisfy $|\eta| < 2.5$, while in the all-hadronic channel, they are required to satisfy $|\eta| < 2.8$ to match the η range of the H_T trigger. If these jet requirements are not met, the jet is discarded.

Jets are tagged as containing a b-hadron (b-tagged) by a deep neural network algorithm trained on a simulated hybrid sample composed of $t\bar{t}$ and $Z' \to t\bar{t}$ events [73, 74] at a working point corresponding to a 77% b-jet efficiency, as measured on an inclusive $t\bar{t}$ sample. This working point has a rejection factor of 5 and 170 on charm and light-flavored jets, respectively. Flavor-tagging efficiency differences between data and simulation are corrected by a reweighting procedure detailed in refs. [75–77].

To resolve any reconstruction ambiguities between electrons, muons and jets, an overlap removal procedure is applied in a prioritized sequence, based on baseline leptons and jets, as follows. First, if a electron shares the same ID track with another electron, the electron with lower p_{T} is discarded, and then any electron sharing the same ID track with a muon is rejected. Next, jets are rejected if they lie within $\Delta R = 0.2$ of an electron. Similarly, jets within $\Delta R = 0.2$ of a muon are rejected if the jet has fewer than three associated tracks or if the muon is matched to the jet through ghost association [44]. Finally, electrons that are close to a remaining jet are discarded if their distance from the jet is $\Delta R < 0.4$, while for muons the distance is $\Delta R < \min(0.4, 0.04 + 10\,\mathrm{GeV}/p_{\mathrm{T}})$.

Large-R jets are reclustered from the calibrated $R = 0.4$ jets described above using the anti-k_t algorithm with a fixed radius parameter of $R = 1.2$ [78]. The large-R jets aim to fully contain the dark pion decay products and the R parameter is optimized for the dark pion mass range of the targeted signal points. For the one-lepton channel the signal lepton is added to the $R = 0.4$ jet collection before the reclustering, which then proceeds in the same way as in the all-hadronic channel. After reclustering, the large-R jet containing the lepton is referred to as J^{lep} and the leading fully hadronic large-R jet J^{had}. Both large-R jets originate from the same reclustering procedure, ensuring there is no overlap between the two.

Events are selected for the all-hadronic channel using triggers on H_{T}, defined as the scalar sum of the transverse momenta of all the reconstructed jets in the event with $|\eta_{\mathrm{jet}}| < 2.8$ [79]. The H_{T}-trigger threshold was 850 GeV in 2015 and the first half of 2016, and was increased to 1000 GeV in the latter half of 2016 for the remainder of Run 2. Since the trigger decision is based on H_{T} computed from trigger-level jet momenta (which lack a detailed calibration), the triggers show a slow onset behavior with respect to H_{T} computed from jet momenta of fully calibrated jets. A requirement of $H_{\mathrm{T}} > 1150\,\mathrm{GeV}$ ensures that the trigger is fully efficient to minimize systematic uncertainties resulting from imprecise modeling of the onset behavior in simulation. The H_{T} variable computed from fully calibrated jets is used for the remainder of this search.

Events are selected for the one-lepton channel using a combination of single-lepton triggers [80–83]. The single-lepton triggers require the presence of a muon or an electron with p_{T} higher than a certain threshold and, in some cases, impose identification and lepton-isolation requirements. The lowest p_{T} threshold was 24 (20) GeV for electrons (muons) during the 2015 data-taking period and 26 GeV for both electrons and muons in the data-taking periods from 2016 to 2018. The efficiencies of the single-lepton triggers range between 20% and 50% in the simulated signal samples. To account for small differences in the single-lepton trigger efficiency between data and simulation, all triggered simulated events receive an event weight to match data.

The analysis strategy relies on the reconstruction of each dark pion using a large-R jet. In the all-hadronic channel, events are required to have six or more $R = 0.4$ jets with $p_{\mathrm{T}} > 25\,\mathrm{GeV}$, in addition to the $H_{\mathrm{T}} > 1150\,\mathrm{GeV}$ requirement and the lepton veto. At least three jets within the ID acceptance ($|\eta| < 2.5$) must be b-tagged. At least two large-R jets with jet mass $m_{\mathrm{jet,R=1.2}} > 190\,\mathrm{GeV}$ are required in all events. Events for the one-lepton channel are required to have at least five jets, out of which at least three have to be b-tagged, and to have $H_{\mathrm{T}} > 300\,\mathrm{GeV}$. Here the H_{T} is defined similar to the all-hadronic channel, however only jets with $|\eta_{\mathrm{jet}}| < 2.5$ are considered. Events passing all selection requirements

JHEP09(2024)005

Variable	All-hadronic channel	One-lepton channel
$\mathrm{N_{lep}}$(baseline)	0	1
$\mathrm{N_{lep}}$(signal)	—	1
$\mathrm{N_{jets}}(R = 0.4)$	≥ 6	≥ 5
$\mathrm{N_{jets}}(R = 1.2)$	≥ 2	—
$\mathrm{N}_{b\text{-jets}}$	≥ 3	≥ 3
H_T	$\geq 1150\,\mathrm{GeV}$	$\geq 300\,\mathrm{GeV}$

Table 2. Summary of the preselection criteria for the all-hadronic and one-lepton channels, in terms of the number of baseline and signal leptons, $R = 0.4$ and $R = 1.2$ jets, number of b-jets, and H_T. The definitions of the physics objects for the two channels are given in the text. Signal leptons constitute a subset of the baseline leptons.

JHEP09(2024)005

listed here are considered preselected for the analysis. The preselection requirements are summarized for both the analysis channels in table 2.

5 Analysis strategy

Preselected events are separated into signal, control, and validation regions based on the properties of the large-R and small-R jets in the event, as well as the signal lepton for the one-lepton channel. Signal regions (SRs) are signal-enriched regions while the control regions (CRs) are used to estimate the SM background contributions. The validation regions (VRs) are used to validate the background estimation methods. The analysis strategies for the all-hadronic and one-lepton channels are detailed below.

5.1 All-hadronic channel

In the all-hadronic channel, the leading two large-R jets define the overall SR, where the leading large-R jet satisfies $m_{\mathrm{jet,R=1.2}} > 300\,\mathrm{GeV}$ and the sub-leading large-R jet satisfies $m_{\mathrm{jet,R=1.2}} > 250\,\mathrm{GeV}$ as shown in figure 4 for distributions after preselection. To suppress multijet events containing, for example, gluon to $b\bar{b}$ splitting, a selection on $m_{bb}/p_{\mathrm{T},bb}$, defined as the ratio of the mass to the transverse momentum of the pair of b-tagged jets closest to the center of the large-R jet, is applied to both large-R jets. In signal events $m_{bb}/p_{\mathrm{T},bb}$ is expected to take on larger values than in background events, thus a cut of $m_{bb}/p_{\mathrm{T},bb} > 0.25$ is required. Further, both large-R jets must satisfy a bb_i tag, where the ΔR between the leading ($i = 1$) or sub-leading ($i = 2$) large-R jet and the second closest b-tagged jet, defined as $\Delta R\,(j, b_2)$, is less than 1.0 and thus both b-tagged jets are well contained within the volume of the large-R jet. This variable is designed to suppress $t\bar{t}$ events where the second closest b-jet arises from the other top quark in the event and can thus have a large ΔR with the large-R jet. In signal, on the other hand, the decay products of the dark pion always include two b-quarks no matter whether the $tttb$ or $ttbb$ final state is considered and the ΔR therefore tends to be small. The overall SR is then subdivided into nine separate bins in the leading versus sub-leading large-R jet mass plane. A large-R jet is considered $\pi_{D,i}$ tagged if its mass

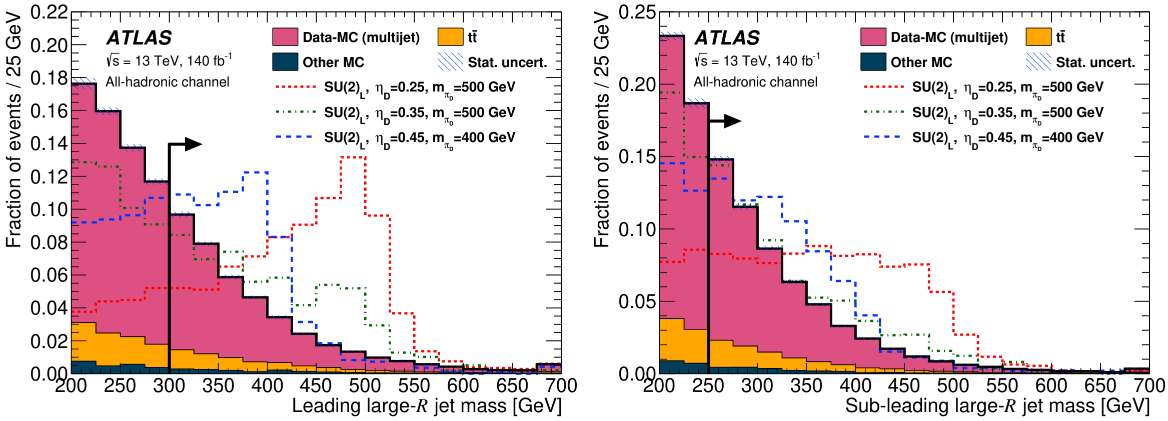

(a) (b)

Figure 4. Mass of the (a) leading and (b) sub-leading large-R jet for all simulated backgrounds overlaid with three example distributions for various signal points after preselection in the all-hadronic channel. Also shown is a simplified data-driven estimate of the multijet background which was created by taking the event yields for data and subtracting all simulated backgrounds from it. Statistical uncertainties stemming from MC are indicated by the shaded region. The SR is to the right of the vertical line in both the subfigures. Individual SR bins select sub-regions of leading and sub-leading large-R jet mass for improved background discrimination. The last bin contains the overflow.

	Tag	Variable	Tag selection	Anti-tag selection
Both large-R jets		$m_{bb}/p_{\mathrm{T},bb}$	> 0.25	> 0.25
Leading large-R jet	bb_1	$\Delta R\,(j, b_2)$	< 1.0	≥ 1.0
Sub-leading large-R jet	bb_2	$\Delta R\,(j, b_2)$	< 1.0	≥ 1.0
Leading large-R jet	$\pi_{D,1}$	$m_{\mathrm{jet,R=1.2}}$	[300–325 GeV, 325–400 GeV, $>$ 400 GeV]	$\leq$ 300 GeV
Sub-leading large-R jet	$\pi_{D,2}$	$m_{\mathrm{jet,R=1.2}}$	[250–300 GeV, 300–350 GeV, $>$ 350 GeV]	$\leq$ 250 GeV

Table 3. Summary of selection criteria for the SR ("Tag selection"). Nine bins are defined in the leading large-R jet vs. sub-leading large-R jet mass plane. The inverted selection ("Anti-tag selection") is also defined for use in the data-driven multijet extrapolation described in section 6.1.

falls into one of the nine mass bins. The SR requires both large-R jets to satisfy both tagging selections (i.e. both jets must be bb_i and $\pi_{D,i}$ tagged). The events where the two leading large-R jets satisfy only one or two out of the four possible tags form the CRs used for the data-driven multijet extrapolation; events that satisfy three tags allow for a validation of the method and thus form the VRs. The SR selection criteria are summarized in table 3.

JHEP09(2024)005

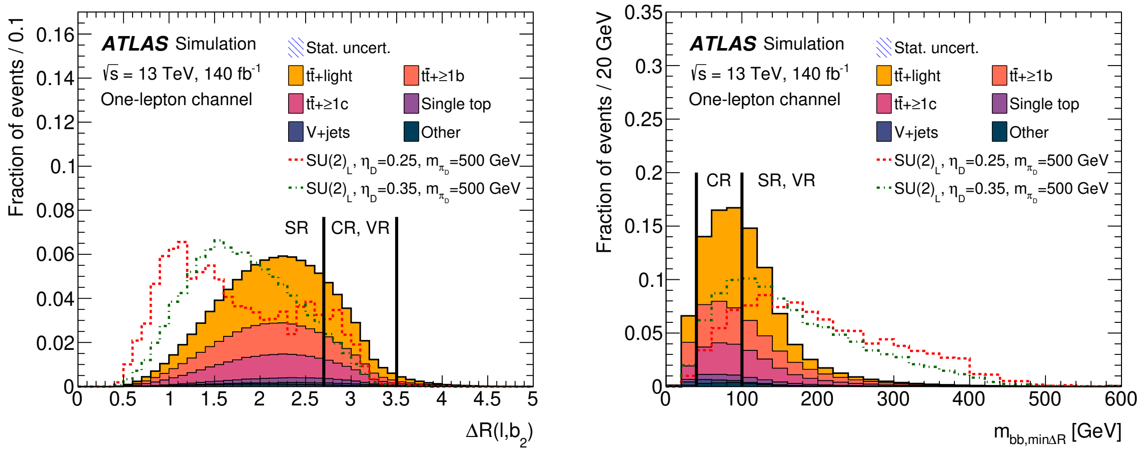

(a) (b)

Figure 5. Normalized distributions of (a) $\Delta R(\ell, b_2)$ and (b) $m_{bb,\min\Delta R}$ for all simulated backgrounds with two example signal distributions overlaid after the one-lepton channel preselection. Statistical uncertainties stemming from MC are indicated by a shaded region, but are not visible on the scale of the y-axis. The vertical dashed lines indicate the selection requirements applied to events in the SR, CR and VR, as indicated by the labels.

5.2 One-lepton channel

Events satisfying the preselection requirements for the one-lepton channel are categorized into SRs, CRs and VRs based on two kinematic variables defined in terms of the properties of the small-R and large-R jets. The first variable, $\Delta R(\ell, b_2)$, is defined as the angle between the lepton in the event and the second closest b-jet to this lepton and aims to suppress $t\bar{t}$ background similar to $\Delta R\,(j, b_2)$ in the all-hadronic channel. The kinematics of the second b-jet as distinguishing characteristic of signal events is also utilized for the second variable, $m_{bb,\min\Delta R}$, defined as the invariant mass of the two b-jets in the event that are closest to each other. This is effective for discriminating high dark pion mass signal points against background in which the two b-quarks closest to each other come e.g. from gluon splitting. The distributions of these variables in signal and background MC simulations are shown in figure 5 for preselected events.

The SR is defined by requiring $\Delta R(\ell, b_2) < 2.7$ and $m_{bb,\min\Delta R} > 100\,\text{GeV}$. A CR for the $t\bar{t}$ +HF background is defined by the requirements $2.7 < \Delta R(\ell, b_2) < 3.5$, and $40\,\text{GeV} < m_{bb,\min\Delta R} < 100\,\text{GeV}$, thus ensuring orthogonality to the SR. This region is used to correct for mismodeling in $t\bar{t}$ +HF events and has a background composition similar to that in the SR. Typical signal contamination in the CR, from signal points that are not already excluded through re-interpretation of other collider searches [2], is below 1%. The $t\bar{t}$ +HF background estimate is validated in a VR defined by the requirements $2.7 < \Delta R(\ell, b_2) < 3.5$, and $m_{bb,\min\Delta R} > 100\,\text{GeV}$, making it orthogonal to both the SR and the CR while also exhibiting a background composition similar to that of the SR and CR.

The statistical analysis in the one-lepton channel relies on a profile-likelihood fit to the distribution of the sum of the masses of the reclustered jets, described in section 4,

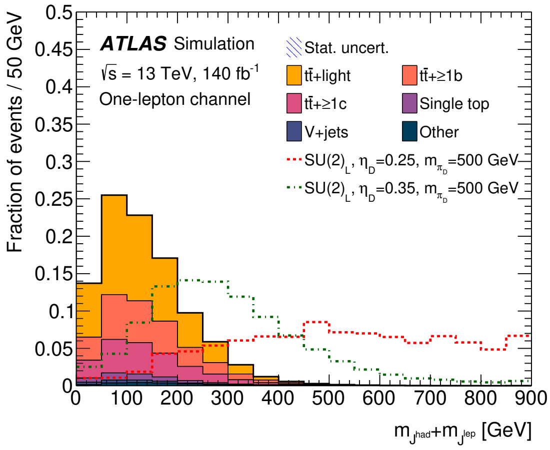

Figure 6. Normalized distributions of $m_{\mathbb{J}\text{had}} + m_{\mathbb{J}\text{lep}}$ for all simulated backgrounds overlaid with two example distributions for various signal points after the one-lepton channel preselection. Statistical uncertainties stemming from MC are indicated by a shaded region, but are not visible on the scale of the y-axis.

$m_{\mathbb{J}\text{had}} + m_{\mathbb{J}\text{lep}}$. This discriminating variable is shown in figure 6 for preselected events. For the fit, all events are further classified into regions split into bins based on the number of jets and b-jets in the event. Six bins are defined labeled XR_5j3b, XR_5j4b, XR_6j3b, XR_6j4b, XR_7j3b and XR_7j4b, where the number before the 'j' indicates the number of jets, the number before the 'b' the number of b-jets and 'X' can take on the values 'S' for an SR, 'C' for a CR and 'V' for a VR bin. In all cases, the highest jet or b-jet multiplicity is inclusive, e.g. the region CR_7j4b is a CR that contains events with ≥ 7 jets and ≥ 4 b-jets.

6 Background estimate

6.1 All-hadronic channel

The dominant background for the analysis in the all-hadronic channel originates from multijet events and constitutes about 75%–85% of the total background in each SR bin. A data-driven method is used to estimate this background, while MC simulation is used to account for the remaining sub-dominant SM processes as described in section 3. Typical ABCD multijet extrapolations are based on two discriminating variables. Here, however, an extended ABCD method is employed that relies on four instead of two discriminating variables, which allows the correction of correlations between pairs of discriminating variables and provide validation regions close to the SR selection.

The multijet background is estimated by extrapolating from regions with small leading and sub-leading $m_{\text{jet,R=1.2}}$ and large $\Delta R\,(j, b_2)$ to SR bins with large leading and sub-leading $m_{\text{jet,R=1.2}}$ and small $\Delta R\,(j, b_2)$. The method is similar to the one detailed in ref. [84]. To this end, two additional anti-tags denoted by a slashed tag label (with orthogonal selections to the already described bb_i and $\pi_{D,i}$ tags) are defined. The tag $\not{b}\not{b}_i$ inverts the bb_i selection, while $\not{\pi}_{\not{D},i}$ places upper requirements on the large-R jet mass, as summarized in table 3. The combinations of possible tags and anti-tags in an event result in 16 separate regions shown

JHEP09(2024)005

Figure 7. Region labels for the 16 regions used in the data-driven multijet estimate in the all-hadronic channel. Region S labels the SR, regions B, C, E and I are used for the ABCD extrapolation, regions D, F, G, H, J and O are used to compute correlation correction factors, and regions K, L, M and N are validation regions. The background estimate is performed independently for all nine SR bins.

in figure 7. The extended ABCD method extrapolates from regions with one tag to each of the nine SR bins. Two-tag regions are used to determine correlation correction factors and three-tag regions are used for validation of the multijet estimate.

The concept of the extended ABCD method is detailed here by explicitly stating the computations for one VR, however, analogous derivations have to be carried out for all SRs and VRs. Considering only region K in figure 7, a 2-variable ABCD estimate for this region would be computed in the standard way through $\hat{K} = \frac{J \cdot D}{B}$, where J, D and B are the number of data events minus the number of simulated events in the respective regions. If $\pi_{D,1}$ and $\pi_{D,2}$ are uncorrelated, $\hat{K}$ would be a valid estimate. However, if $\pi_{D,1}$ and $\pi_{D,2}$ are correlated, then $\hat{K}$ needs to be corrected by a correlation factor (k-factor). As long as there is no significant additional three-tag correlation with the bb_2 tag, this correlation factor, $k_{\pi_{D,1},\pi_{D,2}}$, can be measured from $\frac{F \cdot A}{C \cdot E}$ since $\frac{K \cdot B}{J \cdot D} = \frac{F \cdot A}{C \cdot E}$. Thus,

$$\hat{K} = \frac{J \cdot D}{B} \cdot \frac{F \cdot A}{C \cdot E} = \frac{J \cdot D}{B} \cdot k_{\pi_{D,1},\pi_{D,2}} \,. \tag{6.1}$$

One can also consider the estimate of region K using a three-variable ABCD estimate computed with two correlation correction factors:

$$\hat{K} = \frac{J \cdot C}{A} \cdot k_{\pi_{D,1},\pi_{D,2}} \cdot k_{\pi_{D,1},bb_2} \,, \tag{6.2}$$

where $k_{\pi_{D,1},bb_2} = \frac{D \cdot A}{B \cdot C}$. Substituting this correlation factor into eq. (6.2) yields once again eq. (6.1). All other k-factors can be defined according to the same principle as $k_{\pi_{D,1},\pi_{D,2}}$ and $k_{\pi_{D,1},bb_2}$.

The final multijet background estimate requires a four-variable ABCD estimate $\hat{S}'$ that is computed from data minus event counts from MC simulated backgrounds in the regions B, C, E, and I where exactly one tag is applied and region A with no applied tags according to

$$\hat{S}' = \frac{B \cdot C \cdot E \cdot I}{A^3} \,. \tag{6.3}$$

This estimate is then multiplied by six k-factors to correct for correlations between tags,

$$\hat{S} = \hat{S}' \cdot k_{\pi_{D,1},bb_1} \cdot k_{\pi_{D,2},bb_2} \cdot k_{\pi_{D,1},bb_2} \cdot k_{\pi_{D,2},bb_1} \cdot k_{\pi_{D,1},\pi_{D,2}} \cdot k_{bb_1,bb_2} \,. \tag{6.4}$$

If the selection criteria defined by these tags are independent from each other then the expectation value of the corresponding k-factor will be 1. Correlation factors around 1.5

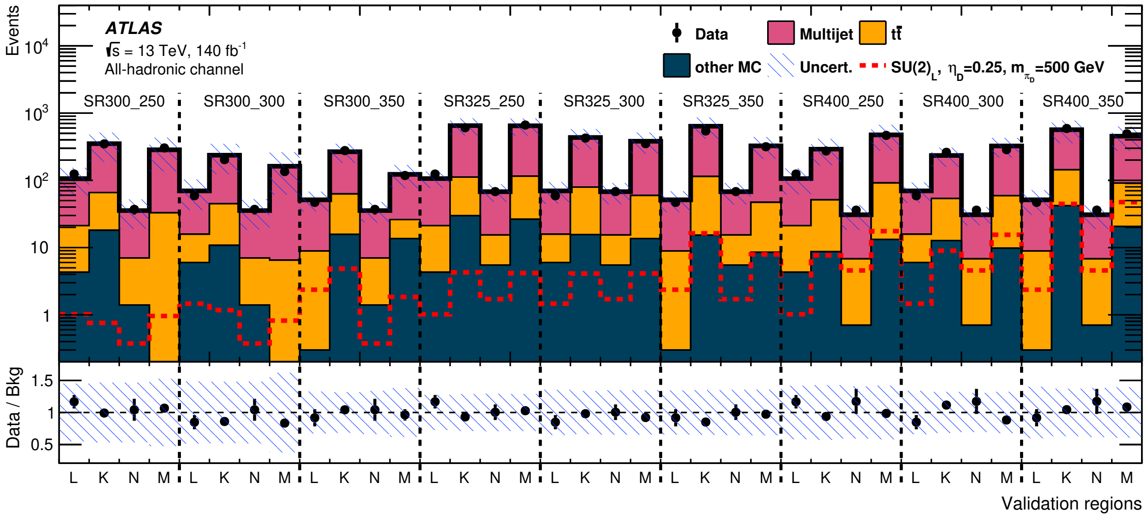

Figure 8. The four all-hadronic channel validation regions K, L, M and N from figure 7 for each of the nine SR mass bins with the following naming convention: the leading large-R jet lower mass boundary in GeV is followed by the sub-leading large-R jet lower mass boundary. The shaded region indicates the uncertainty on the background estimate in each bin that includes the statistical uncertainties from the limited sample sizes in data and simulation as well as a multijet non-closure systematic uncertainty, as detailed in section 7.

are observed between the $\pi_{D,1}$ and bb_1 tags as well as the $\pi_{D,2}$ and bb_2 tags. The bb_1 and bb_2 tags are highly correlated with a k-factor of 0.1 due to the preselection requirement of three b-tagged jets. This could be mitigated by requiring four b-tagged jets, however, this would result in low statistics and high signal contamination for the four-variable ABCD extrapolation regions.

Typical signal contaminations in the extrapolation regions are less than 5% and small compared to the uncertainty applied to the multijet background discussed in section 7. The method is validated through the closure of the estimate in the four 3-tag validation regions K, L, M and N. Figure 8 compares data to estimated background yields for each validation region in each bin of the SR. If significant 3-tag correlations occurred, a discrepancy between multijet estimate and data yields should be visible in the validation regions. However, all data yields are compatible with the background estimate within the uncertainty bands for all validation regions. The uncertainty includes a non-closure systematic uncertainty, which by design covers non-linear correlations and the impact of multijet estimation regions with low statistics. It ranges between 33% and 57% and is derived and discussed in section 7. The procedure was further validated by performing signal injection tests as well as stability tests over time, under variation of the selection criteria and with scaled simulated background contributions. In all cases the resulting background estimates where stable and thus consistent with the nominal estimate.

6.2 One-lepton channel

The background in the one-lepton channel is estimated from MC simulations using the samples described in section 3 and is dominated by $t\bar{t}$ production in association with light-

JHEP09(2024)005

flavor or heavy-flavor quarks. This background is estimated by using the inclusive $t\bar{t}$ sample complemented by the dedicated $t\bar{t}b\bar{b}$ sample, with events categorized into $t\bar{t}+\geq 1b$, $t\bar{t}+\geq 1c$ and $t\bar{t}+$light as described in section 3. The $t\bar{t}$ +HF background that populates the SR is known from previous studies to be underestimated by the current MC predictions [85]. This mismodeling is corrected by keeping the normalization of these backgrounds unconstrained in the profile-likelihood fit to the $m_{\mathbb{J}\mathrm{had}} + m_{\mathbb{J}\mathrm{lep}}$ distribution. To this end, the $t\bar{t}+\geq 1c$ and $t\bar{t}+$light contributions are combined and two normalization factors are fit depending on whether in addition to $t\bar{t}$ any b-quarks are present in the event. In this categorization, the combination of the $t\bar{t}+\geq 1c$ and $t\bar{t}+$light backgrounds is referred to as $t\bar{t}+0b$. The resulting background estimates for the SR, CR and VR are presented in section 8.2.

7 Systematic uncertainties

The predicted signal and background event yields in the SR bins are affected by various sources of systematic uncertainties stemming from instrumentation, the data-driven multijet estimation and theoretical considerations. For the all-hadronic channel, the total uncertainty is dominated by the uncertainty on the multijet background estimate. In the one-lepton channel, the theoretical sources of uncertainty on the background modeling dominate the total uncertainty.

7.1 Experimental uncertainties

The uncertainty in the combined 2015–2018 integrated luminosity is 0.83% [14], obtained using the LUCID-2 detector [11] for the primary luminosity measurements, complemented by measurements using the ID and calorimeters. A systematic variation that might be introduced by the reweighting of simulated samples to match the pileup profile observed in data is estimated by varying the scale factor applied to the pileup distributions. The onset of the H_{T} trigger used in the all-hadronic channel was studied and potential effects of mismodeling were evaluated. All three of these uncertainties were found to have a negligible impact on the analysis ($< 1\%$ in the all-hadronic channel, and ranking from $< 1\%$ to a few percent depending on the signal in the one-lepton channel).

Slight performance differences between data and simulation in lepton reconstruction, identification and isolation are corrected by the application of scale factors that are estimated from tag-and-probe experiments in data and simulation [64, 66]. The impact of lepton momentum scale corrections is evaluated by $\pm 1\sigma$ scale variations. For resolution uncertainties the lepton energy or momentum is smeared. In total seven (twelve) separate variations for electrons (muons) are considered. The impact of lepton uncertainties is less than 1% in both channels.

The determination of the jet energy scale and resolution is done by combining information from collision data, test beam data and simulation as described in ref. [70]. Effects from jet flavor composition, single-particle response and pileup are considered. In the one-lepton channel, 29 parameters are evaluated for scale variations, while 13 parameters are evaluated for jet p_{T} resolution systematic uncertainties. In the all-hadronic channel the variations are simplified since the data-driven background estimation method largely compensates yield changes by different systematic variations and causes most of the systematic uncertainties to be negligibly small. As such, 23 parameters arise from scale variations, while for jet p_T resolution systematic uncertainties 8 parameters are evaluated. The impact of these uncertainties on the final result is small, ranging between < 1% to about 4% in the all-hadronic channel, and remaining < 10% in the one-lepton channel.

Uncertainties on the corrections of b-tagging efficiency differences between data and simulation are derived from dedicated flavor-enriched subsets of the data [75]. Also considered are uncertainties due to the mis-tagging of c-jets [77] and light-flavor jets [76]. Additionally, variations to extrapolate the measured uncertainties to the high-p_T region are considered for both channels [86]. The impact of flavor-tagging systematic uncertainties is less than 1% on the final result in the all-hadronic channel, while a larger contribution is observed in the one-lepton channel, reaching values of the order of 10%.

7.2 Modeling uncertainties in background simulations

For the all-hadronic channel, uncertainties in modeling of the $t\bar{t}$ background are included. For the one-lepton channel, uncertainties in modeling the $t\bar{t}$, $t\bar{t}b\bar{b}$, and single top-quark backgrounds are included. All other simulated backgrounds are negligible in both channels and no systematic uncertainties are assigned to them. For the single top-quark background, a 30% normalization uncertainty is applied [87] with an impact ranging between < 1% and a few percent. Details on the $t\bar{t}$ and $t\bar{t}b\bar{b}$ uncertainties are described below.

7.2.1 $t\bar{t}$ uncertainties

Several uncertainties in the theoretical modeling of the $t\bar{t}$ background samples are considered. In the one-lepton channel the $t\bar{t}$ theory systematic uncertainties apply only on the $t\bar{t}$ + light and $t\bar{t}+\geq 1c$ background components as they are estimated from the five-flavor scheme $t\bar{t}$ sample, while the $t\bar{t}+\geq 1b$ background has dedicated systematic uncertainties.

Missing higher order contributions in perturbative expansion of the $t\bar{t}$ production cross-section are estimated by adding in quadrature contributions from renormalization and factorization scale variations, which are obtained by independently varying the parameters μ_R and μ_F by a factor 0.5 and 2.0 and taking the envelope. Uncertainties on the choice of PDF set used for event simulation are estimated by using the PDF4LHC and NNPDF error sets following the PDF4LHC prescription [88] and taking the envelope. The initial-state radiation (ISR) modeling is estimated by variations of the strong coupling constant α_S through the Var3c tune variation. The amount of final-state radiation (FSR) in an event is estimated by varying the factorization scale by factors 0.5 and 2.0 inside Pythia8. To assess the uncertainty in the matching of NLO matrix elements to the parton shower, the nominal sample is compared to an alternative sample obtained setting the `pthard` Pythia8 parameter to 1 (the default is 0). This parameter regulates the definition of the vetoed region of the showering, important to avoid holes and overlaps in the phase space filled by Powheg and Pythia8. This recommendation follows the description included in ref. [89]. The alternative sample was produced using Powheg interfaced with Pythia8.306 using the NNPDF2.3lo PDF set and the A14 set of tuned parameters. The impacts of using a different parton shower and hadronization model were evaluated by comparing the nominal $t\bar{t}$ sample with another event sample produced with the PowhegBox v2 generator. For the parton shower variation the NNPDF3.0NLO PDF set was used, while events in the sample used to estimate the impact of the hadronization model were interfaced with HERWIG 7.04 [90, 91], using the H7UE set of tuned parameters [91] and the MMHT2014LO PDF set [92]. The impact of a variation of the h_{damp} parameter is assessed by comparing the nominal samples to an alternative set of samples for which h_{damp} is set to $3m_{\text{top}}$.

All alternative samples used to derive the systematic uncertainties are corrected to match the NNLO in QCD and NLO in EW predictions of the top/antitop-quark p_{T} and the top-quark mass distribution using the procedure outlined in section 3.2.1. A systematic uncertainty associated with this reweighting itself is derived from the maximum and minimum 7-point scale variations, independently for the top/antitop-quark p_{T} and the top-quark mass. The variations are taken into account in the final statistical fit by including them as scale variations on the $t\bar{t}$ background.

To avoid over-constraining the $t\bar{t}$ modeling nuisance parameters in the one-lepton channel, the theoretical systematic uncertainties are treated as uncorrelated among $t\bar{t}$ + light and $t\bar{t}+\geq 1c$, jet and b-jet multiplicity bins, and between their shape and acceptance components.

The impact of $t\bar{t}$ modeling uncertainties on the final result is found to range between $< 1\%$ and 10%.

7.2.2 $t\bar{t}b\bar{b}$ uncertainties

Theory uncertainties on the $t\bar{t}b\bar{b}$ sample are only applied to the $t\bar{t}+\geq 1b$ component in the one-lepton channel, as all other $t\bar{t}$ components are estimated from the bulk $t\bar{t}$ sample.

The scale, PDF, ISR, and FSR uncertainties for the $t\bar{t}b\bar{b}$ sample are derived in the same way as the bulk $t\bar{t}$ sample. The impacts of using a different parton shower and hadronization model are evaluated by comparing the nominal $t\bar{t}$ sample to another sample produced with the POWHEGBOX v2 generator. For the parton shower variation the NNPDF3.0NLO PDF set was used, while events in the sample estimating the impact of the hadronization model were interfaced with HERWIG 7.1, using the H7.1-DEFAULT set of tuned parameters and the MMHT2014LO PDF set [92].

The matching uncertainty is evaluated by comparing the nominal sample with an alternative sample obtained by setting the `pthard` PYTHIA8 parameter to 1. The alternative sample was produced using POWHEG interfaced with PYTHIA8.307 using the NNPDF2.3LO PDF set and the A14 set of tuned parameters.

The $t\bar{t}b\bar{b}$ uncertainty nuisance parameters are treated as uncorrelated between the different regions of jet and b-jet multiplicities and are further split up into their shape and acceptance components to avoid over-constraining them in the fit. They constitute the dominant systematic contribution in the one-lepton channel, with an impact on the final results ranging from 1% to about 30%.

7.3 Data-driven background estimation uncertainties

In the all-hadronic channel, the dominant systematic uncertainty originates from the multijet estimation method. Deviations of the ratio between data and SM estimate from unity in the VRs, denoted by $k_{VR} = (\text{data} - \text{MC})/\text{multijet}$, are used to estimate a non-closure systematic uncertainty. These k-factors are a measure of the remaining correlations between 3-tags in the multijet estimation method and are expected to be close to unity. The statistical uncertainties on the k-factors $\sigma_{k_{VR}}$ are added in quadrature so that the final multijet uncertainty is calculated according to:

$$\sigma_{ABCD} = \sqrt{\left(1 - \prod_{VR} k_{VR}\right)^2 + \sum_{VR} \sigma^2_{k_{VR}}}\,, \tag{7.1}$$

where the first term under the square root describes the non-closure component of the systematic uncertainty calculated from the k-factors and the second term the statistical uncertainty summed up in quadrature over all four VRs. The statistical component dominates in most regions and is driven by region H in figure 7 which has the lowest number of events. The computation is done separately for each bin of the SR producing values ranging from 33% to 57%. The uncertainty in each SR mass bin is treated as fully uncorrelated with the other SR mass bins thus yielding a conservative estimate.

8 Statistical analysis and results

Signal hypotheses are evaluated against the data by performing profile-likelihood fits in each analysis channel. The set of nuisance parameters θ that corresponds to the systematic uncertainties is scaled in such a fashion that, before the fit, all individual uncertainties j have $\theta_j = 0$. In addition, the uncertainties of these nuisance parameters σ are scaled to fulfill $\sigma_j = 1$ before fitting. Defining γ as the set of statistical uncertainties with γ_i the uncertainty on the number of predicted events of a specific bin i, the set is scaled to be a factor around 1. The profile-likelihood fit is then performed by minimizing the quantity $q(\mu) = -2\log\mathcal{L}$, where the likelihood $\mathcal{L}$ is defined as

$$\mathcal{L}(\mu, \theta|S, B, N) = \prod_{i\in\text{bins}} \mathcal{P}\left(N_i|\mu S_i + B_i\right) \times \mathcal{P}\left(S_i + B_i|\gamma_i\right) \prod_{j\in\text{syst.}} \mathcal{G}\left(\theta_j, \sigma_j\right) \tag{8.1}$$

with N being the number of data events, S the predicted number of signal events and B the expected number of background events. Statistical and systematic uncertainties are taken to be Poissonian ($\mathcal{P}$) and Gaussian ($\mathcal{G}$) distributed parameters, respectively. The fit is evaluated using the RooFit [93] package with the minimization conducted with the Minuit2 package [94], which yields the optimal values for μ and the set of parameters θ_i, γ_i and σ_i in a signal plus background fit.

8.1 All-hadronic channel

The fit in the all-hadronic channel is performed over all nine SR bins simultaneously. Since the multijet estimate constrains background to the data, most systematic uncertainties (other than from the multijet estimate) have limited impact on the final result and all systematic uncertainties below 1% are ignored. Surviving uncertainties are kept as nuisance parameters in the fit. Because simulated backgrounds constitute less than 20% of the total SM background in the SR, no CRs are used to scale the simulated estimates.

Figure 9 shows the distributions in all SR bins after fitting. No significant pulls or constraints are observed for the fitted nuisance parameters. The results are also summarized in table 4. As can be seen the data are very well described by the background-only hypothesis with no significant excess of events above the SM prediction.

JHEP09(2024)005

	SR300_250	SR300_300	SR300_350
V+jets	< 0.01	1.97 ± 0.89	0.28 ± 0.06
Single top	0.12 ± 0.07	0.00 ± 0.03	< 0.01
$t\bar{t} + X$	0.30 ± 0.04	0.21 ± 0.09	0.17 ± 0.04
$t\bar{t}$	2.9 ± 1.9	1.6 ± 1.1	1.78 ± 0.76
Multijet	16.5 ± 4.3	10.5 ± 3.6	11.1 ± 3.1
Total SM	19.8 ± 4.0	14.2 ± 3.3	13.4 ± 2.9
Data	20	14	16

	SR325_250	SR325_300	SR325_350
V+jets	0.74 ± 0.64	0.12 ± 0.18	0.19 ± 0.16
Single top	0.36 ± 0.06	0.12 ± 0.13	0.27 ± 0.15
$t\bar{t} + X$	0.35 ± 0.06	0.44 ± 0.11	0.50 ± 0.07
$t\bar{t}$	6.4 ± 3.6	4.0 ± 2.0	4.4 ± 2.1
Multijet	33.4 ± 6.7	23.3 ± 5.2	18.1 ± 5.0
Total SM	41.2 ± 5.6	28.0 ± 4.8	23.5 ± 4.6
Data	41	28	23

	SR400_250	SR400_300	SR400_350
V+jets	0.71 ± 0.55	< 0.01	1.19 ± 0.30
Single top	< 0.01	0.47 ± 0.08	0.11 ± 0.02
$t\bar{t} + X$	0.34 ± 0.07	0.40 ± 0.07	0.73 ± 0.10
$t\bar{t}$	3.7 ± 1.8	3.1 ± 2.5	6.1 ± 3.9
Multijet	20.2 ± 5.3	14.7 ± 4.6	28 ± 12
Total SM	25.0 ± 4.8	18.6 ± 4.0	36 ± 11
Data	27	20	45

Table 4. Observed and predicted event yields after the fit under the background-only hypothesis in all nine all-hadronic SR mass bins. The name of each column corresponds to the SR bins: the leading large-R jet lower mass boundary in GeV is followed by the sub-leading large-R jet lower mass boundary; the same convention is used in figure 9. The quoted uncertainties contain statistical and systematic components. The total post-fit uncertainty can be smaller than the sum in quadrature of the different components due to correlations resulting from the fit to data.

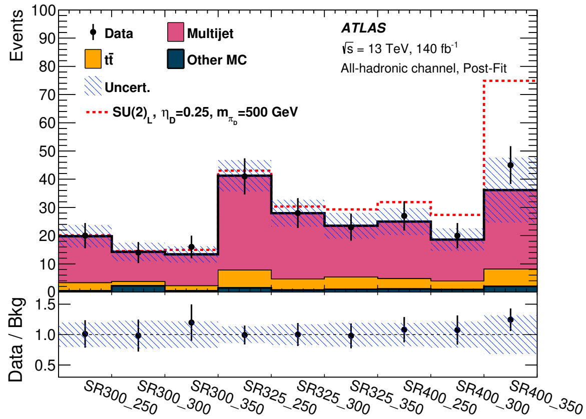

Figure 9. Comparison of the events yields in data and the background prediction after the fit under the background-only hypothesis in all bins of the all-hadronic SR. The dashed line is stacked onto the SM background and shows an example SU(2)$_L$ signal with $\eta_D = 0.25$ and $m_{\pi_D} = 500\,\text{GeV}$. The uncertainty bands contain all statistical and systematic uncertainties. The horizontal axis labels reflect the different SR bins, with the first number indicating the lower boundary of the leading large-R jet mass bin and the second number the lower boundary of the sub-leading large-R jet mass bin.

8.2 One-lepton channel

In the one-lepton channel, a profile-likelihood fit is performed to the binned $m_{\mathbb{J}\text{had}} + m_{\mathbb{J}\text{lep}}$ spectrum in the six SRs and the six CRs defined based on jet and b-jet multiplicity requirements, simultaneously. As already indicated in section 6.2, two independent normalization factors are used for the $t\bar{t}$ background depending on whether in addition to $t\bar{t}$ any b-quarks are present in the event. These two normalization factors are denoted by $k(t\bar{t}+ \geq 1b)$ and $k(t\bar{t} + 0b)$. To avoid over-constraining the background modeling nuisance parameters, the theoretical systematic uncertainties are treated as uncorrelated among different $t\bar{t}$ flavors, jet and b-jet multiplicity bins, and between their shape and acceptance components.

The event yields for all SRs, CRs and VRs are shown after a fit to the data under the background-only hypothesis in figure 10. The corresponding distributions of $m_{\mathbb{J}\text{had}} + m_{\mathbb{J}\text{lep}}$ are shown in figure 11 for all jet and b-jet multiplicity bins of the SR. The SM background estimate is in good agreement with data after the background-only fit. The post-fit normalization factors for the $t\bar{t}$ background components are $k(t\bar{t} + 0b) = 0.92^{+0.09}_{-0.08}$ and $k(t\bar{t}+ \geq 1b) = 1.60^{+0.19}_{-0.17}$. No pulls greater than 1σ are observed for the fitted nuisance parameters, with only some constraints in the nuisance parameters describing the theoretical modeling. Data and post-fit background event yields are shown in table 5. Good agreement between the background prediction and data is observed in all regions.

9 Interpretation

The results are used to set 95% confidence level (CL) upper limits on the dark pion pair production cross-sections following the CL$_S$ technique [95]. Upper limits on the dark pion production cross-sections are shown in figure 12 for four slices of η_D. The impacts of the different systematic uncertainties, described in section 7, on the signal strength, defined as the signal cross-section normalized to the theoretical prediction, of two benchmark signals are

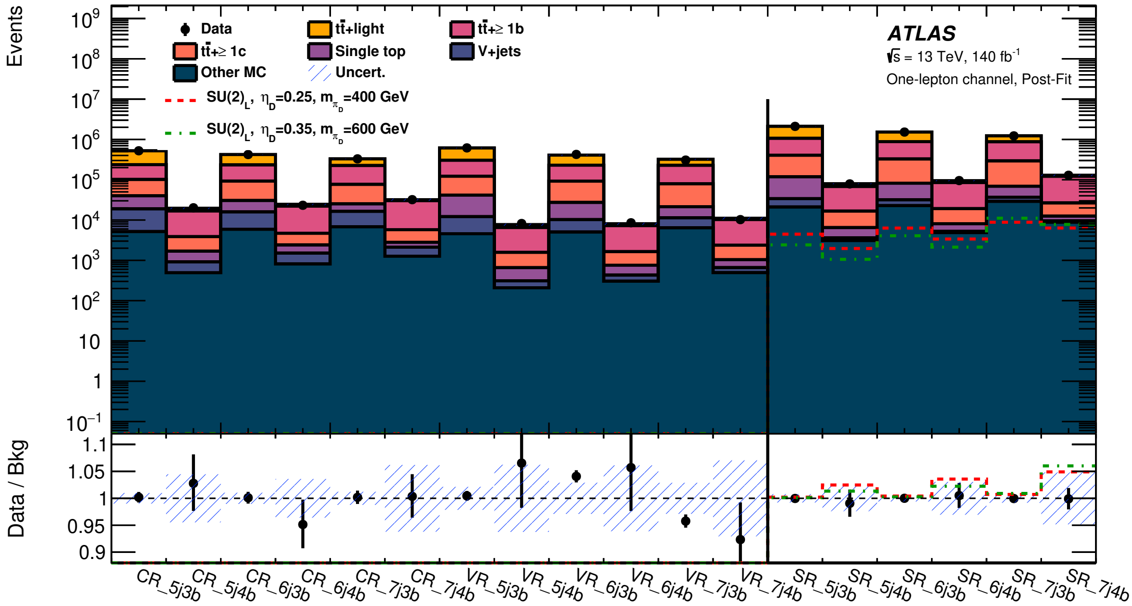

Figure 10. Comparison of the events yields in data and the background prediction in the SRs, CRs, and VRs in the one-lepton channel, after the fit to data in all CRs and SRs under the background-only hypothesis. The uncertainty bands contain all statistical and systematic uncertainties. Two example $\mathrm{SU}(2)_L$ signal points are overlaid in the SRs.

summarized in table 6: the analysis is limited by the systematic uncertainty, with dominant contribution from the theoretical sources of uncertainty on the background modeling.

Using the predicted dark pion pair production cross-sections, the limits can be translated into limits on dark pion masses in the two-dimensional η_D–m_{π_D} plane. The exclusion contour obtained from the all-hadronic channel for the $\mathrm{SU}(2)_L$ model is shown in figure 13(a). No dark pion masses can be excluded for $\eta_D = 0.15$. For $\eta_D = 0.25$ the exclusion covers the mass range $280\,\mathrm{GeV} < m_{\pi_D} < 520\,\mathrm{GeV}$ (expected $280\,\mathrm{GeV} < m_{\pi_D} < 540\,\mathrm{GeV}$), while for $\eta_D = 0.35$, dark pions with masses $m_{\pi_D} < 430\,\mathrm{GeV}$ are excluded (expected $m_{\pi_D} < 450\,\mathrm{GeV}$). The exclusion contour obtained from the one-lepton channel for $\mathrm{SU}(2)_L$ is shown in figure 13(b) and is observed to fully cover the all-hadronic limit and significantly extend the probed phase space for this dark meson model. Since the all-hadronic limit is completely contained within the one-lepton limit, there is no expected gain from a combination of the two channels. Dark pion masses with $m_{\pi_D} < 940\,\mathrm{GeV}$ can be excluded for $\eta_D = 0.45$, $m_{\pi_D} < 720\,\mathrm{GeV}$ are excluded for $\eta_D = 0.35$ and for $\eta_D = 0.25$ the mass region $m_{\pi_D} < 740\,\mathrm{GeV}$ is excluded. The results significantly extend the phase space previously excluded through re-interpretation of other collider searches [2]. In the $\mathrm{SU}(2)_R$ model, cross sections are significantly smaller than for $\mathrm{SU}(2)_L$ and therefore none of the channels have sensitivity to this model with the current data sample.

10 Conclusion

Results from a search for dark mesons originating from strongly-coupled, SU(2) dark flavor symmetry conserving models and decaying to top and bottom quarks are reported. The

JHEP09(2024)005

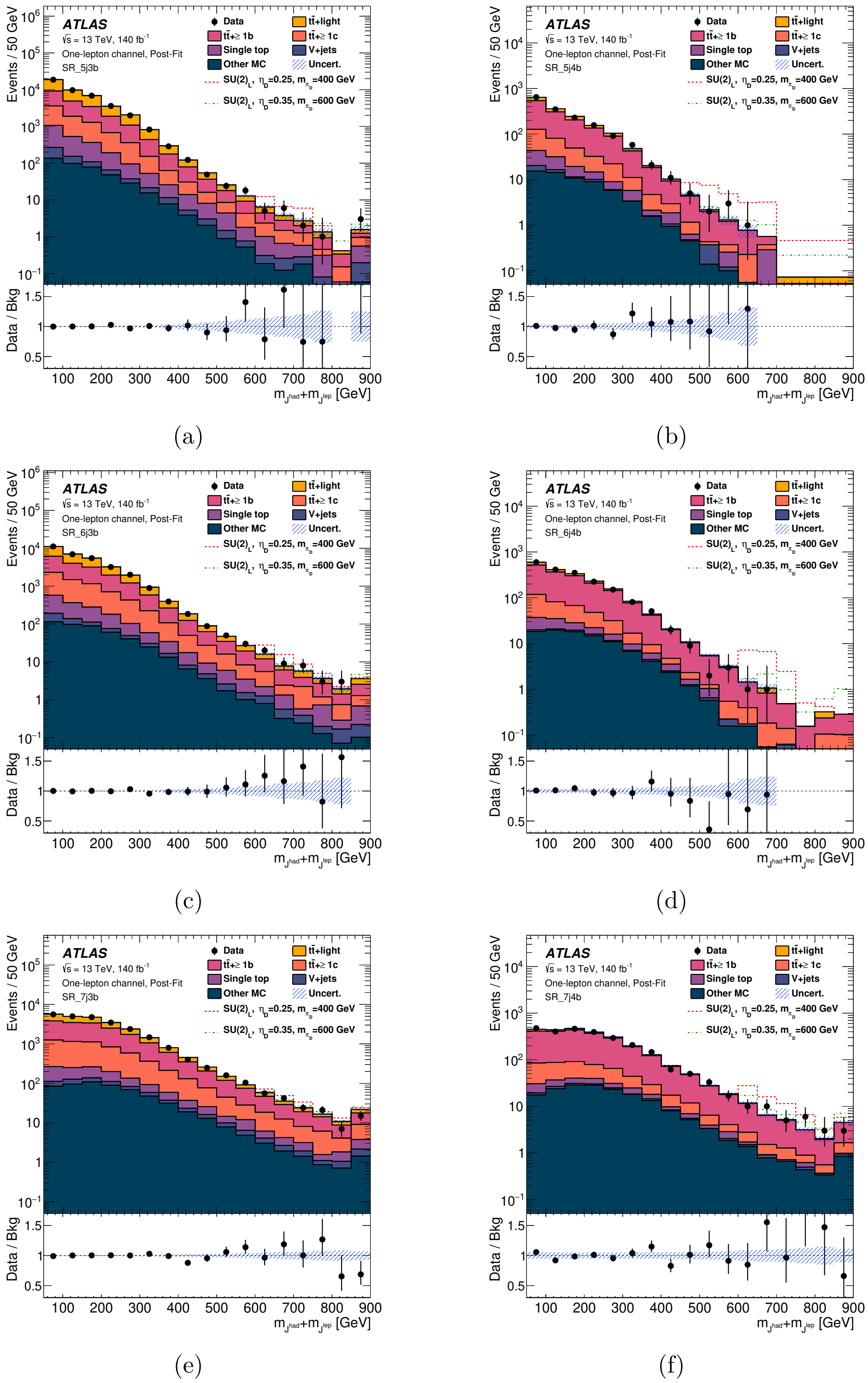

Figure 11. Distributions of $m_{\mathbb{J}\text{had}} + m_{\mathbb{J}\text{lep}}$ in (a) SR_5j3b, (b) SR_5j4b, (c) SR_6j3b, (d) SR_6j4b, (e) SR_7j3b, and (f) SR_7j4b, after the fit to data in all CRs and SRs under the background-only hypothesis. Two example $\mathrm{SU}(2)_L$ signal point with $\eta_D = 0.25$ and $m_{\pi_D} = 400\,\mathrm{GeV}$ is stacked on top of the background. The uncertainty bands contain all statistical and systematic uncertainties. The dashed line in the ratio panel shows the ratio of signal plus background event yields over just background event yields.

JHEP09(2024)005

	SR_5j3b	SR_5j4b	SR_6j3b
$t\bar{t}+\geq 1b$	12400 ± 2600	1150 ± 180	9400 ± 1800
$t\bar{t}+\geq 1c$	5900 ± 500	230 ± 40	5400 ± 600
$t\bar{t}$ + light	23100 ± 1900	270 ± 70	14300 ± 1200
Single top	1800 ± 500	59 ± 18	1080 ± 330
V+jets	274 ± 30	10.2 ± 1.5	192 ± 22
Other MC	416 ± 15	61 ± 4	465 ± 17
Total SM	10500 ± 100	402 ± 20	8430 ± 110
Data	10462	403	8438

	SR_6j4b	SR_7j3b	SR_7j4b
$t\bar{t}+\geq 1b$	1210 ± 120	9900 ± 2500	1900 ± 400
$t\bar{t}+\geq 1c$	247 ± 45	5400 ± 800	350 ± 90
$t\bar{t}$ + light	220 ± 50	8500 ± 1500	180 ± 50
Single top	59 ± 18	710 ± 220	66 ± 21
V+jets	7.7 ± 1.2	170 ± 20	14.9 ± 1.9
Other MC	99 ± 6	620 ± 40	187 ± 14
Total SM	477 ± 22	6600 ± 120	640 ± 40
Data	465	6598	641

Table 5. Observed and predicted event yields after the fit under the background-only hypothesis in the six SR bins in the one-lepton channel. The name of each column corresponds to the bins described in section 5.2, identified with the number of jets followed by the number of b-jets. The quoted uncertainties contain statistical and systematic components. The total post-fit uncertainty can be smaller than the sum in quadrature of the different components due to correlations resulting from the fit to data.

analysis is based on the full Run 2 data sample of proton-proton collisions at $\sqrt{s} = 13$ TeV recorded by the ATLAS detector at the LHC, corresponding to an integrated luminosity of 140 fb^{-1}. The search is performed in the all-hadronic channel, where the event signature results in eight to ten jets of which at least four originate from bottom quarks, and in the one-lepton channel, corresponding to final states with one electron or muon in addition to jets. In the all-hadronic channel, a data-driven technique is used to estimate the predominant multijet background. In the one-lepton channel, the dominant background comes from $t\bar{t}$ production and is estimated from MC simulations.

No excess above the SM background expectation is observed. The strongest exclusion limits are obtained from the one-lepton channel. For SU(2)$_L$ signals with $m_{\pi_D}/m_{\rho_D} = 0.45$, dark pions with masses $m_{\pi_D} < 940$ GeV are excluded, while for $m_{\pi_D}/m_{\rho_D} = 0.25$ the exclusion covers the mass range $m_{\pi_D} < 740$ GeV. These results constitute the first direct collider constraints on this type of model, and significantly extend the phase space previously excluded through re-interpretation of other collider searches.

JHEP09(2024)005

Category	$SU(2)_L$, $\eta_D = 0.25$, $m_{\pi_D} = 400\,\text{GeV}$	$SU(2)_L$, $\eta_D = 0.35$, $m_{\pi_D} = 700\,\text{GeV}$
Luminosity	0.03	0.05
Pileup	0.05	0.09
Flavor tagging	0.28	0.26
Leptons	0.01	0.04
Jets	0.08	0.14
$t\bar{t}+\geq 1b$	0.26	0.53
$t\bar{t}+\geq 1c$	0.12	0.18
$t\bar{t}+$ light	0.13	0.17
Top p_{T} NNLO reweighting	0.08	0.09
Single top	0.06	0.06
Statistical	0.28	0.24
Instrumental	0.30	0.30
Theory	0.38	0.63

Table 6. Impact of different categories of systematic uncertainty in the one-lepton channel, for two signal benchmarks, relative to the total uncertainty on the fitted signal strength. For each category, the fit is repeated with the corresponding group of nuisance parameters fixed to their best-fit values and the impact for each category is evaluated as the quadrature difference between the signal strength uncertainty in the new fit and in the nominal one, divided by the uncertainty in the nominal fit. The contribution from the statistical uncertainty and the systematic one, further separated into the global instrumental and theoretical uncertainties, are shown. The total systematic uncertainty is different from the sum in quadrature of the different groups due to the correlations among the nuisance parameters in the fit.

Acknowledgments

We thank CERN for the very successful operation of the LHC and its injectors, as well as the support staff at CERN and at our institutions worldwide without whom ATLAS could not be operated efficiently.

The crucial computing support from all WLCG partners is acknowledged gratefully, in particular from CERN, the ATLAS Tier-1 facilities at TRIUMF/SFU (Canada), NDGF (Denmark, Norway, Sweden), CC-IN2P3 (France), KIT/GridKA (Germany), INFN-CNAF (Italy), NL-T1 (The Netherlands), PIC (Spain), RAL (U.K.) and BNL (U.S.A.), the Tier-2 facilities worldwide and large non-WLCG resource providers. Major contributors of computing resources are listed in ref. [96].

We gratefully acknowledge the support of ANPCyT, Argentina; YerPhI, Armenia; ARC, Australia; BMWFW and FWF, Austria; ANAS, Azerbaijan; CNPq and FAPESP, Brazil; NSERC, NRC and CFI, Canada; CERN; ANID, Chile; CAS, MOST and NSFC, China; Minciencias, Colombia; MEYS CR, Czech Republic; DNRF and DNSRC, Denmark; IN2P3-CNRS and CEA-DRF/IRFU, France; SRNSFG, Georgia; BMBF, HGF and MPG, Germany;

JHEP09(2024)005

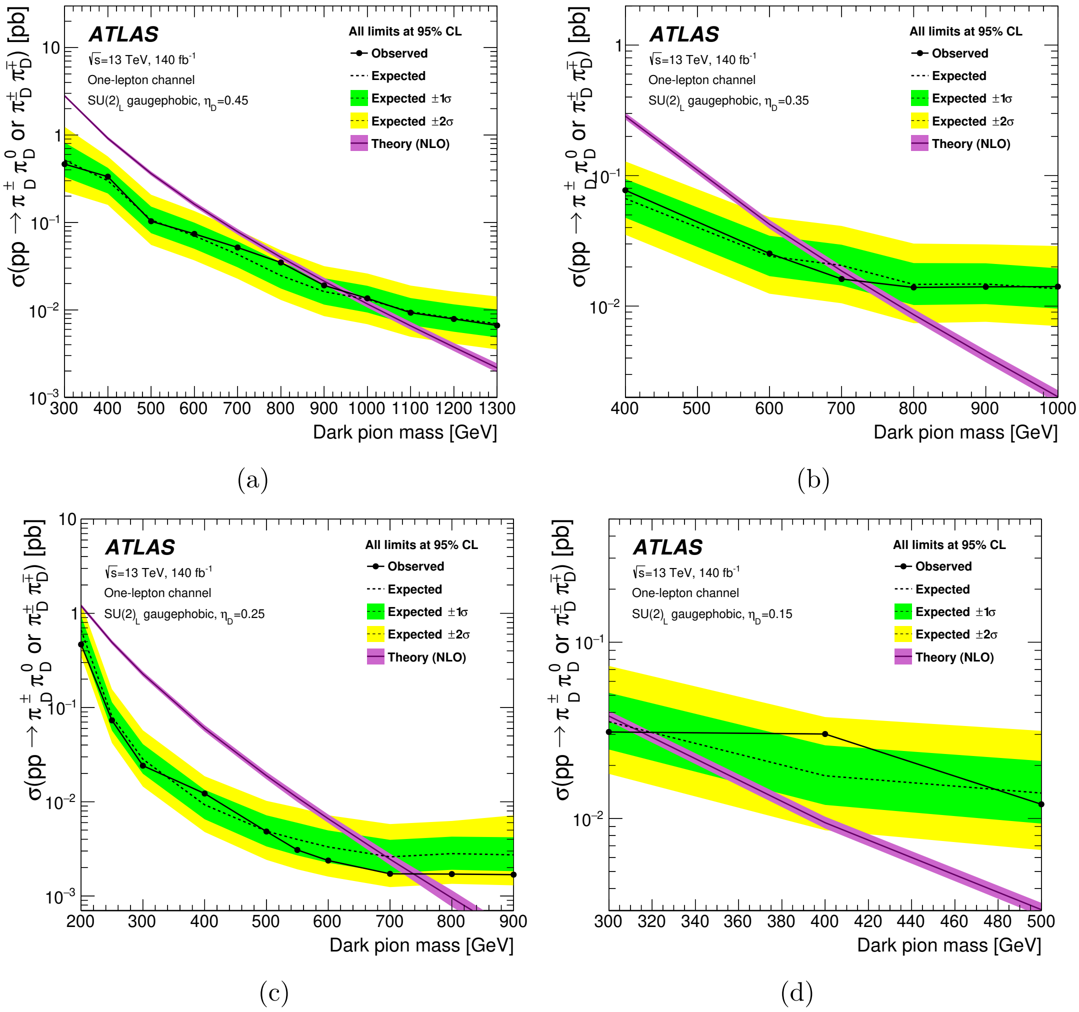

Figure 12. Observed (solid line) and expected (dashed line) limits on the dark pion production cross-section as a function of dark pion mass using the CL_S method for all $\mathrm{SU}(2)_L$ models in four slices of η_D: (a) $\eta_D = 0.45$, (b) $\eta_D = 0.35$, (c) $\eta_D = 0.25$, and (d) $\eta_D = 0.15$. The surrounding shaded bands correspond to one and two standard deviations around the expected limit. The overlaid theory line shows the theoretical dark pion cross-section prediction [4].

GSRI, Greece; RGC and Hong Kong SAR, China; ISF and Benoziyo Center, Israel; INFN, Italy; MEXT and JSPS, Japan; CNRST, Morocco; NWO, The Netherlands; RCN, Norway; MNiSW, Poland; FCT, Portugal; MNE/IFA, Romania; MESTD, Serbia; MSSR, Slovakia; ARIS and MVZI, Slovenia; DSI/NRF, South Africa; MICIU/AEI, Spain; SRC and Wallenberg Foundation, Sweden; SERI, SNSF and Cantons of Bern and Geneva, Switzerland; NSTC, Taipei; TENMAK, Türkiye; STFC/UKRI, United Kingdom; DOE and NSF, United States of America.

Individual groups and members have received support from BCKDF, CANARIE, CRC and DRAC, Canada; CERN-CZ, FORTE and PRIMUS, Czech Republic; COST, ERC, ERDF, Horizon 2020, ICSC-NextGenerationEU and Marie Skłodowska-Curie Actions, European Union; Investissements d'Avenir Labex, Investissements d'Avenir Idex and ANR, France; DFG and AvH Foundation, Germany; Herakleitos, Thales and Aristeia programmes co-financed by

JHEP09(2024)005

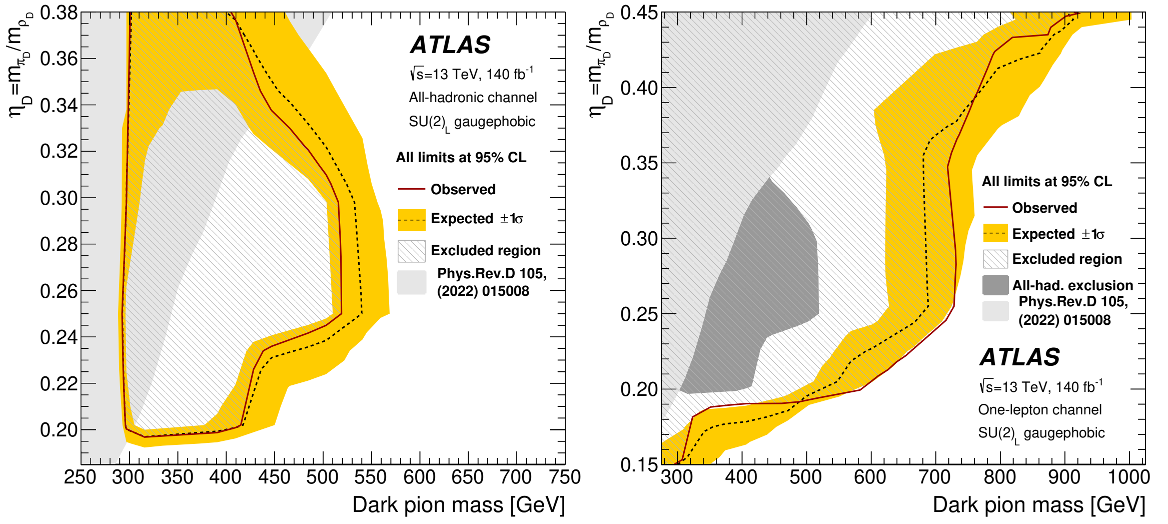

(a) (b)

Figure 13. Observed (solid line) and expected (dashed line) exclusion contours at 95% CL in the η_D–m_{π_D} plane for SU(2)$_L$ signal models in the (a) all-hadronic and (b) one-lepton channel. Masses that are within the contours are excluded, as indicated by the hatched area. An uncertainty band corresponding to the $\pm 1\sigma$ variation on the expected limit is also indicated. The shaded area in (a) and the innermost shaded area in (b) indicates the phase space previously excluded through re-interpretation of other collider searches presented in ref. [2]. The outermost shaded area in (b) indicates the phase space excluded by the analysis in the all-hadronic channel and is identical to the observed limit shown in (a).

EU-ESF and the Greek NSRF, Greece; BSF-NSF and MINERVA, Israel; NCN and NAWA, Poland; La Caixa Banking Foundation, CERCA Programme Generalitat de Catalunya and PROMETEO and GenT Programmes Generalitat Valenciana, Spain; Göran Gustafssons Stiftelse, Sweden; The Royal Society and Leverhulme Trust, United Kingdom.

In addition, individual members wish to acknowledge support from Armenia: Yerevan Physics Institute (FAPERJ); CERN: European Organization for Nuclear Research (CERN PJAS); Chile: Agencia Nacional de Investigación y Desarrollo (FONDECYT 1230812, FONDECYT 1230987, FONDECYT 1240864); China: Chinese Ministry of Science and Technology (MOST-2023YFA1605700), National Natural Science Foundation of China (NSFC — 12175119, NSFC 12275265, NSFC-12075060); Czech Republic: Czech Science Foundation (GACR — 24-11373S), Ministry of Education Youth and Sports (FORTE CZ.02.01.01/00/22_008/0004632), PRIMUS Research Programme (PRIMUS/21/SCI/017); EU: H2020 European Research Council (ERC — 101002463); European Union: European Research Council (ERC — 948254, ERC 101089007), Horizon 2020 Framework Programme (MUCCA — CHIST-ERA-19-XAI-00), European Union, Future Artificial Intelligence Research (FAIR-NextGenerationEU PE00000013), Italian Center for High Performance Computing, Big Data and Quantum Computing (ICSC, NextGenerationEU); France: Agence Nationale de la Recherche (ANR-20-CE31-0013, ANR-21-CE31-0013, ANR-21-CE31-0022, ANR-22-EDIR-0002), Investissements d'Avenir Labex (ANR-11-LABX-0012); Germany: Baden-Württemberg Stiftung (BW Stiftung-Postdoc Eliteprogramme), Deutsche Forschungsgemeinschaft (DFG — 469666862,

JHEP09(2024)005

DFG — CR 312/5-2); Italy: Istituto Nazionale di Fisica Nucleare (ICSC, NextGenerationEU), Ministero dell'Università e della Ricerca (PRIN — 20223N7F8K — PNRR M4.C2.1.1); Japan: Japan Society for the Promotion of Science (JSPS KAKENHI JP22H01227, JSPS KAKENHI JP22H04944, JSPS KAKENHI JP22KK0227, JSPS KAKENHI JP23KK0245); The Netherlands: Netherlands Organisation for Scientific Research (NWO Veni 2020 — VI.Veni.202.179); Norway: Research Council of Norway (RCN-314472); Poland: Ministry of Science and Higher Education (IDUB AGH, POB8, D4 no 9722), Polish National Agency for Academic Exchange (PPN/PPO/2020/1/00002/U/00001), Polish National Science Centre (NCN 2021/42/E/ST2/00350, NCN OPUS nr 2022/47/B/ST2/03059, NCN UMO-2019/34/E/ST2/00393, UMO-2020/37/B/ST2/01043, UMO-2021/40/C/ST2/00187, UMO-2022/47/O/ST2/00148, UMO-2023/49/B/ST2/04085); Slovenia: Slovenian Research Agency (ARIS grant J1-3010); Spain: Generalitat Valenciana (Artemisa, FEDER, IDIFEDER/2018/048), Ministry of Science and Innovation (MCIN & NextGenEU PCI2022-135018-2, MICIN & FEDER PID2021-125273NB, RYC2019-028510-I, RYC2020-030254-I, RYC2021-031273-I, RYC2022-038164-I), PROMETEO and GenT Programmes Generalitat Valenciana (CIDEGENT/2019/027); Sweden: Swedish Research Council (Swedish Research Council 2023-04654, VR 2018-00482, VR 2022-03845, VR 2022-04683, VR 2023-03403, VR grant 2021-03651), Knut and Alice Wallenberg Foundation (KAW 2018.0157, KAW 2018.0458, KAW 2019.0447, KAW 2022.0358); Switzerland: Swiss National Science Foundation (SNSF — PCEFP2_194658); United Kingdom: Leverhulme Trust (Leverhulme Trust RPG-2020-004), Royal Society (NIF-R1-231091); United States of America: U.S. Department of Energy (ECA DE-AC02-76SF00515), Neubauer Family Foundation.

References

[1] G.D. Kribs and E.T. Neil, *Review of strongly-coupled composite dark matter models and lattice simulations*, *Int. J. Mod. Phys. A* **31** (2016) 1643004 [arXiv:1604.04627] [INSPIRE].

[2] J.M. Butterworth, L. Corpe, X. Kong, S. Kulkarni and M. Thomas, *New sensitivity of LHC measurements to composite dark matter models*, *Phys. Rev. D* **105** (2022) 015008 [arXiv:2105.08494] [INSPIRE].

[3] T. Appelquist et al., *Stealth Dark Matter: Dark scalar baryons through the Higgs portal*, *Phys. Rev. D* **92** (2015) 075030 [arXiv:1503.04203] [INSPIRE].

[4] G.D. Kribs, A. Martin, B. Ostdiek and T. Tong, *Dark Mesons at the LHC*, *JHEP* **07** (2019) 133 [arXiv:1809.10184] [INSPIRE].

[5] G.D. Kribs, A. Martin and T. Tong, *Effective Theories of Dark Mesons with Custodial Symmetry*, *JHEP* **08** (2019) 020 [arXiv:1809.10183] [INSPIRE].

[6] ATLAS collaboration, *Search for new high-mass phenomena in the dilepton final state using* $36\,fb^{-1}$ *of proton-proton collision data at* $\sqrt{s} = 13$ *TeV with the ATLAS detector*, *JHEP* **10** (2017) 182 [arXiv:1707.02424] [INSPIRE].

[7] CMS collaboration, *Search for high-mass resonances in dilepton final states in proton-proton collisions at* $\sqrt{s} = 13$ *TeV*, *JHEP* **06** (2018) 120 [arXiv:1803.06292] [INSPIRE].

[8] ATLAS collaboration, *The ATLAS Experiment at the CERN Large Hadron Collider*, 2008 *JINST* **3** S08003 [INSPIRE].

[9] ATLAS collaboration, *ATLAS Insertable B-Layer Technical Design Report*, ATLAS-TDR-19 (2010).

[10] B. Abbott et al., *Production and Integration of the ATLAS Insertable B-Layer*, 2018 *JINST* **13** T05008 [arXiv:1803.00844] [INSPIRE].

[11] G. Avoni et al., *The new LUCID-2 detector for luminosity measurement and monitoring in ATLAS*, 2018 *JINST* **13** P07017 [INSPIRE].

[12] ATLAS collaboration, *Performance of the ATLAS Trigger System in 2015*, *Eur. Phys. J. C* **77** (2017) 317 [arXiv:1611.09661] [INSPIRE].

[13] ATLAS collaboration, *Software and computing for Run 3 of the ATLAS experiment at the LHC*, arXiv:2404.06335 [INSPIRE].

[14] ATLAS collaboration, *Luminosity determination in pp collisions at* $\sqrt{s} = 13$ *TeV using the ATLAS detector at the LHC*, *Eur. Phys. J. C* **83** (2023) 982 [arXiv:2212.09379] [INSPIRE].

[15] GEANT4 collaboration, *GEANT4 — a simulation toolkit*, *Nucl. Instrum. Meth. A* **506** (2003) 250 [INSPIRE].

[16] ATLAS collaboration, *The ATLAS Simulation Infrastructure*, *Eur. Phys. J. C* **70** (2010) 823 [arXiv:1005.4568] [INSPIRE].

[17] J. Alwall et al., *The automated computation of tree-level and next-to-leading order differential cross sections, and their matching to parton shower simulations*, *JHEP* **07** (2014) 079 [arXiv:1405.0301] [INSPIRE].

[18] T. Sjöstrand et al., *An introduction to PYTHIA 8.2*, *Comput. Phys. Commun.* **191** (2015) 159 [arXiv:1410.3012] [INSPIRE].

[19] ATLAS collaboration, *ATLAS Pythia 8 tunes to* 7 *TeV data*, ATL-PHYS-PUB-2014-021 (2014).

[20] NNPDF collaboration, *Parton distributions with LHC data*, *Nucl. Phys. B* **867** (2013) 244 [arXiv:1207.1303] [INSPIRE].

[21] D.J. Lange, *The EvtGen particle decay simulation package*, *Nucl. Instrum. Meth. A* **462** (2001) 152 [INSPIRE].

[22] C. Bierlich et al., *A comprehensive guide to the physics and usage of PYTHIA 8.3*, *SciPost Phys. Codebases* **2022** (2022) 8 [arXiv:2203.11601] [INSPIRE].

[23] S. Frixione, P. Nason and G. Ridolfi, *A Positive-weight next-to-leading-order Monte Carlo for heavy flavour hadroproduction*, *JHEP* **09** (2007) 126 [arXiv:0707.3088] [INSPIRE].

[24] P. Nason, *A New method for combining NLO QCD with shower Monte Carlo algorithms*, *JHEP* **11** (2004) 040 [hep-ph/0409146] [INSPIRE].

[25] S. Frixione, P. Nason and C. Oleari, *Matching NLO QCD computations with Parton Shower simulations: the POWHEG method*, *JHEP* **11** (2007) 070 [arXiv:0709.2092] [INSPIRE].

[26] S. Alioli, P. Nason, C. Oleari and E. Re, *A general framework for implementing NLO calculations in shower Monte Carlo programs: the POWHEG BOX*, *JHEP* **06** (2010) 043 [arXiv:1002.2581] [INSPIRE].

JHEP09(2024)005

[27] NNPDF collaboration, *Parton distributions for the LHC Run II*, *JHEP* **04** (2015) 040 [arXiv:1410.8849] [INSPIRE].

[28] S. Carrazza, S. Forte, Z. Kassabov, J.I. Latorre and J. Rojo, *An Unbiased Hessian Representation for Monte Carlo PDFs*, *Eur. Phys. J. C* **75** (2015) 369 [arXiv:1505.06736] [INSPIRE].

[29] ATLAS collaboration, *Studies on top-quark Monte Carlo modelling for Top2016*, ATL-PHYS-PUB-2016-020 (2016).

[30] M. Beneke, P. Falgari, S. Klein and C. Schwinn, *Hadronic top-quark pair production with NNLL threshold resummation*, *Nucl. Phys. B* **855** (2012) 695 [arXiv:1109.1536] [INSPIRE].

[31] M. Cacciari, M. Czakon, M. Mangano, A. Mitov and P. Nason, *Top-pair production at hadron colliders with next-to-next-to-leading logarithmic soft-gluon resummation*, *Phys. Lett. B* **710** (2012) 612 [arXiv:1111.5869] [INSPIRE].

[32] P. Bärnreuther, M. Czakon and A. Mitov, *Percent Level Precision Physics at the Tevatron: First Genuine NNLO QCD Corrections to $q\bar{q} \to t\bar{t} + X$*, *Phys. Rev. Lett.* **109** (2012) 132001 [arXiv:1204.5201] [INSPIRE].

[33] M. Czakon and A. Mitov, *NNLO corrections to top-pair production at hadron colliders: the all-fermionic scattering channels*, *JHEP* **12** (2012) 054 [arXiv:1207.0236] [INSPIRE].

[34] M. Czakon and A. Mitov, *NNLO corrections to top pair production at hadron colliders: the quark-gluon reaction*, *JHEP* **01** (2013) 080 [arXiv:1210.6832] [INSPIRE].

[35] M. Czakon, P. Fiedler and A. Mitov, *Total Top-Quark Pair-Production Cross Section at Hadron Colliders Through $O(\alpha_S^4)$*, *Phys. Rev. Lett.* **110** (2013) 252004 [arXiv:1303.6254] [INSPIRE].

[36] M. Czakon and A. Mitov, *Top++: A Program for the Calculation of the Top-Pair Cross-Section at Hadron Colliders*, *Comput. Phys. Commun.* **185** (2014) 2930 [arXiv:1112.5675] [INSPIRE].

[37] T. Ježo, J.M. Lindert, N. Moretti and S. Pozzorini, *New NLOPS predictions for $t\bar{t} + b$-jet production at the LHC*, *Eur. Phys. J. C* **78** (2018) 502 [arXiv:1802.00426] [INSPIRE].

[38] F. Buccioni et al., *OpenLoops 2*, *Eur. Phys. J. C* **79** (2019) 866 [arXiv:1907.13071] [INSPIRE].

[39] F. Cascioli, P. Maierhöfer and S. Pozzorini, *Scattering Amplitudes with Open Loops*, *Phys. Rev. Lett.* **108** (2012) 111601 [arXiv:1111.5206] [INSPIRE].

[40] A. Denner, S. Dittmaier and L. Hofer, *Collier: a fortran-based Complex One-Loop LIbrary in Extended Regularizations*, *Comput. Phys. Commun.* **212** (2017) 220 [arXiv:1604.06792] [INSPIRE].

[41] T. Ježo, *Powheg-box-res ttbb source code*, (2019), https://gitlab.cern.ch/tjezo/powheg-box-res_ttbb/.

[42] ATLAS collaboration, *Measurements of top-quark pair differential cross-sections in the lepton+jets channel in pp collisions at $\sqrt{s} = 8$ TeV using the ATLAS detector*, *Eur. Phys. J. C* **76** (2016) 538 [arXiv:1511.04716] [INSPIRE].

[43] M. Czakon, D. Heymes, A. Mitov, D. Pagani, I. Tsinikos and M. Zaro, *Top-pair production at the LHC through NNLO QCD and NLO EW*, *JHEP* **10** (2017) 186 [arXiv:1705.04105] [INSPIRE].

[44] M. Cacciari, G.P. Salam and G. Soyez, *The anti-k_t jet clustering algorithm*, *JHEP* **04** (2008) 063 [arXiv:0802.1189] [INSPIRE].

[45] M. Cacciari, G.P. Salam and G. Soyez, *FastJet User Manual*, *Eur. Phys. J. C* **72** (2012) 1896 [arXiv:1111.6097] [INSPIRE].

[46] E. Bothmann et al., *Event Generation with Sherpa 2.2*, *SciPost Phys.* **7** (2019) 034 [arXiv:1905.09127] [INSPIRE].

[47] T. Gleisberg and S. Höche, *Comix, a new matrix element generator*, *JHEP* **12** (2008) 039 [arXiv:0808.3674] [INSPIRE].

[48] S. Schumann and F. Krauss, *A Parton shower algorithm based on Catani-Seymour dipole factorisation*, *JHEP* **03** (2008) 038 [arXiv:0709.1027] [INSPIRE].

[49] S. Höche, F. Krauss, M. Schönherr and F. Siegert, *A critical appraisal of NLO+PS matching methods*, *JHEP* **09** (2012) 049 [arXiv:1111.1220] [INSPIRE].

[50] S. Höche, F. Krauss, M. Schönherr and F. Siegert, *QCD matrix elements + parton showers: The NLO case*, *JHEP* **04** (2013) 027 [arXiv:1207.5030] [INSPIRE].

[51] S. Catani, F. Krauss, B.R. Webber and R. Kuhn, *QCD matrix elements + parton showers*, *JHEP* **11** (2001) 063 [hep-ph/0109231] [INSPIRE].

[52] S. Höche, F. Krauss, S. Schumann and F. Siegert, *QCD matrix elements and truncated showers*, *JHEP* **05** (2009) 053 [arXiv:0903.1219] [INSPIRE].

[53] C. Anastasiou, L.J. Dixon, K. Melnikov and F. Petriello, *High precision QCD at hadron colliders: Electroweak gauge boson rapidity distributions at NNLO*, *Phys. Rev. D* **69** (2004) 094008 [hep-ph/0312266] [INSPIRE].

[54] E. Re, *Single-top Wt-channel production matched with parton showers using the POWHEG method*, *Eur. Phys. J. C* **71** (2011) 1547 [arXiv:1009.2450] [INSPIRE].

[55] S. Frixione, E. Laenen, P. Motylinski, C. White and B.R. Webber, *Single-top hadroproduction in association with a W boson*, *JHEP* **07** (2008) 029 [arXiv:0805.3067] [INSPIRE].

[56] R. Frederix, E. Re and P. Torrielli, *Single-top t-channel hadroproduction in the four-flavour scheme with POWHEG and aMC@NLO*, *JHEP* **09** (2012) 130 [arXiv:1207.5391] [INSPIRE].

[57] S. Alioli, P. Nason, C. Oleari and E. Re, *NLO single-top production matched with shower in POWHEG: s- and t-channel contributions*, *JHEP* **09** (2009) 111 [*Erratum ibid.* **02** (2010) 011] [arXiv:0907.4076] [INSPIRE].

[58] R. Frederix, D. Pagani and M. Zaro, *Large NLO corrections in* $t\bar{t}W^{\pm}$ *and* $t\bar{t}t\bar{t}$ *hadroproduction from supposedly subleading EW contributions*, *JHEP* **02** (2018) 031 [arXiv:1711.02116] [INSPIRE].

[59] S. Frixione, E. Laenen, P. Motylinski and B.R. Webber, *Angular correlations of lepton pairs from vector boson and top quark decays in Monte Carlo simulations*, *JHEP* **04** (2007) 081 [hep-ph/0702198] [INSPIRE].

[60] P. Artoisenet, R. Frederix, O. Mattelaer and R. Rietkerk, *Automatic spin-entangled decays of heavy resonances in Monte Carlo simulations*, *JHEP* **03** (2013) 015 [arXiv:1212.3460] [INSPIRE].

[61] H.B. Hartanto, B. Jäger, L. Reina and D. Wackeroth, *Higgs boson production in association with top quarks in the POWHEG BOX*, *Phys. Rev. D* **91** (2015) 094003 [arXiv:1501.04498] [INSPIRE].

[62] LHC Higgs Cross Section Working Group, *Handbook of LHC Higgs Cross Sections. Part 4. Deciphering the Nature of the Higgs Sector*, arXiv:1610.07922 [DOI:10.23731/CYRM-2017-002] [INSPIRE].

[63] ATLAS collaboration, *Vertex Reconstruction Performance of the ATLAS Detector at* $\sqrt{s} = 13$ *TeV*, ATL-PHYS-PUB-2015-026 (2015).

JHEP09(2024)005

[64] ATLAS collaboration, *Electron and photon performance measurements with the ATLAS detector using the 2015–2017 LHC proton-proton collision data*, 2019 *JINST* **14** P12006 [arXiv:1908.00005] [INSPIRE].

[65] ATLAS collaboration, *Electron reconstruction and identification in the ATLAS experiment using the 2015 and 2016 LHC proton-proton collision data at* $\sqrt{s} = 13$ *TeV*, *Eur. Phys. J. C* **79** (2019) 639 [arXiv:1902.04655] [INSPIRE].

[66] ATLAS collaboration, *Muon reconstruction and identification efficiency in ATLAS using the full Run 2 pp collision data set at* $\sqrt{s} = 13$ *TeV*, *Eur. Phys. J. C* **81** (2021) 578 [arXiv:2012.00578] [INSPIRE].

[67] ATLAS collaboration, *Jet reconstruction and performance using particle flow with the ATLAS Detector*, *Eur. Phys. J. C* **77** (2017) 466 [arXiv:1703.10485] [INSPIRE].

[68] ATLAS collaboration, *Topological cell clustering in the ATLAS calorimeters and its performance in LHC Run 1*, *Eur. Phys. J. C* **77** (2017) 490 [arXiv:1603.02934] [INSPIRE].

[69] ATLAS collaboration, *Performance of pile-up mitigation techniques for jets in pp collisions at* $\sqrt{s} = 8$ *TeV using the ATLAS detector*, *Eur. Phys. J. C* **76** (2016) 581 [arXiv:1510.03823] [INSPIRE].

[70] ATLAS collaboration, *Jet energy scale and resolution measured in proton-proton collisions at* $\sqrt{s} = 13$ *TeV with the ATLAS detector*, *Eur. Phys. J. C* **81** (2021) 689 [arXiv:2007.02645] [INSPIRE].

[71] ATLAS collaboration, *Characterisation and mitigation of beam-induced backgrounds observed in the ATLAS detector during the 2011 proton-proton run*, 2013 *JINST* **8** P07004 [arXiv:1303.0223] [INSPIRE].

[72] ATLAS collaboration, *Selection of jets produced in* 13 *TeV proton-proton collisions with the ATLAS detector*, ATLAS-CONF-2015-029 (2015).

[73] ATLAS collaboration, *ATLAS flavour-tagging algorithms for the LHC Run 2 pp collision dataset*, *Eur. Phys. J. C* **83** (2023) 681 [arXiv:2211.16345] [INSPIRE].

[74] ATLAS collaboration, *Optimisation and performance studies of the ATLAS b-tagging algorithms for the 2017–18 LHC run*, ATL-PHYS-PUB-2017-013 (2017).

[75] ATLAS collaboration, *ATLAS b-jet identification performance and efficiency measurement with* $t\bar{t}$ *events in pp collisions at* $\sqrt{s} = 13$ *TeV*, *Eur. Phys. J. C* **79** (2019) 970 [arXiv:1907.05120] [INSPIRE].

[76] ATLAS collaboration, *Calibration of the light-flavour jet mistagging efficiency of the b-tagging algorithms with Z+jets events using* 139 fb^{-1} *of ATLAS proton-proton collision data at* $\sqrt{s} = 13$ *TeV*, *Eur. Phys. J. C* **83** (2023) 728 [arXiv:2301.06319] [INSPIRE].

[77] ATLAS collaboration, *Measurement of the c-jet mistagging efficiency in* $t\bar{t}$ *events using pp collision data at* $\sqrt{s} = 13$ *TeV collected with the ATLAS detector*, *Eur. Phys. J. C* **82** (2022) 95 [arXiv:2109.10627] [INSPIRE].

[78] B. Nachman, P. Nef, A. Schwartzman, M. Swiatlowski and C. Wanotayaroj, *Jets from Jets: Re-clustering as a tool for large radius jet reconstruction and grooming at the LHC*, *JHEP* **02** (2015) 075 [arXiv:1407.2922] [INSPIRE].

[79] ATLAS collaboration, *The performance of the jet trigger for the ATLAS detector during 2011 data taking*, *Eur. Phys. J. C* **76** (2016) 526 [arXiv:1606.07759] [INSPIRE].

[80] ATLAS collaboration, *Performance of the ATLAS muon triggers in Run 2*, 2020 *JINST* **15** P09015 [arXiv:2004.13447] [INSPIRE].

[81] ATLAS collaboration, *Performance of electron and photon triggers in ATLAS during LHC Run 2*, *Eur. Phys. J. C* **80** (2020) 47 [arXiv:1909.00761] [INSPIRE].

[82] ATLAS collaboration, *Operation of the ATLAS trigger system in Run 2*, 2020 *JINST* **15** P10004 [arXiv:2007.12539] [INSPIRE].

[83] ATLAS collaboration, *The ATLAS inner detector trigger performance in pp collisions at* 13 *TeV during LHC Run 2*, *Eur. Phys. J. C* **82** (2022) 206 [arXiv:2107.02485] [INSPIRE].

[84] ATLAS collaboration, *Measurements of $t\bar{t}$ differential cross-sections of highly boosted top quarks decaying to all-hadronic final states in pp collisions at $\sqrt{s} = 13$ TeV using the ATLAS detector*, *Phys. Rev. D* **98** (2018) 012003 [arXiv:1801.02052] [INSPIRE].

[85] ATLAS collaboration, *Measurements of inclusive and differential fiducial cross-sections of $t\bar{t}$ production with additional heavy-flavour jets in proton-proton collisions at $\sqrt{s} = 13$ TeV with the ATLAS detector*, *JHEP* **04** (2019) 046 [arXiv:1811.12113] [INSPIRE].

[86] ATLAS collaboration, *Simulation-based extrapolation of b-tagging calibrations towards high transverse momenta in the ATLAS experiment*, ATL-PHYS-PUB-2021-003 (2021).

[87] ATLAS collaboration, *Search for top-philic heavy resonances in pp collisions at $\sqrt{s} = 13$ TeV with the ATLAS detector*, *Eur. Phys. J. C* **84** (2024) 157 [arXiv:2304.01678] [INSPIRE].

[88] M. Botje et al., *The PDF4LHC Working Group Interim Recommendations*, arXiv:1101.0538 [INSPIRE].

[89] S. Höche, S. Mrenna, S. Payne, C.T. Preuss and P. Skands, *A Study of QCD Radiation in VBF Higgs Production with Vincia and Pythia*, *SciPost Phys.* **12** (2022) 010 [arXiv:2106.10987] [INSPIRE].

[90] M. Bähr et al., *Herwig++ Physics and Manual*, *Eur. Phys. J. C* **58** (2008) 639 [arXiv:0803.0883] [INSPIRE].

[91] J. Bellm et al., *Herwig 7.0/Herwig++ 3.0 release note*, *Eur. Phys. J. C* **76** (2016) 196 [arXiv:1512.01178] [INSPIRE].

[92] L.A. Harland-Lang, A.D. Martin, P. Motylinski and R.S. Thorne, *Parton distributions in the LHC era: MMHT 2014 PDFs*, *Eur. Phys. J. C* **75** (2015) 204 [arXiv:1412.3989] [INSPIRE].

[93] W. Verkerke and D.P. Kirkby, *The RooFit toolkit for data modeling*, *eConf C* **0303241** (2003) MOLT007 [physics/0306116] [INSPIRE].

[94] M. Hatlo, F. James, P. Mato, L. Moneta, M. Winkler and A. Zsenei, *Developments of mathematical software libraries for the LHC experiments*, *IEEE Trans. Nucl. Sci.* **52** (2005) 2818 [INSPIRE].

[95] A.L. Read, *Presentation of search results: The CL_s technique*, *J. Phys. G* **28** (2002) 2693 [INSPIRE].

[96] ATLAS collaboration, *ATLAS Computing Acknowledgements*, ATL-SOFT-PUB-2023-001 (2023).

The ATLAS collaboration

G. Aad[104], E. Aakvaag[17], B. Abbott[123], S. Abdelhameed[119a], K. Abeling[56], N.J. Abicht[50], S.H. Abidi[30], M. Aboelela[45], A. Aboulhorma[36e], H. Abramowicz[154], H. Abreu[153], Y. Abulaiti[120], B.S. Acharya[70a,70b,k], A. Ackermann[64a], C. Adam Bourdarios[4], L. Adamczyk[87a], S.V. Addepalli[27], M.J. Addison[103], J. Adelman[118], A. Adiguzel[22c], T. Adye[137], A.A. Affolder[139], Y. Afik[40], M.N. Agaras[13], J. Agarwala[74a,74b], A. Aggarwal[102], C. Agheorghiesei[28c], F. Ahmadov[39,y], W.S. Ahmed[106], S. Ahuja[97], X. Ai[63e], G. Aielli[77a,77b], A. Aikot[166], M. Ait Tamlihat[36e], B. Aitbenchikh[36a], M. Akbiyik[102], T.P.A. Åkesson[100], A.V. Akimov[38], D. Akiyama[171], N.N. Akolkar[25], S. Aktas[22a], K. Al Khoury[42], G.L. Alberghi[24b], J. Albert[168], P. Albicocco[54], G.L. Albouy[61], S. Alderweireldt[53], Z.L. Alegria[124], M. Aleksa[37], I.N. Aleksandrov[39], C. Alexa[28b], T. Alexopoulos[10], F. Alfonsi[24b], M. Algren[57], M. Alhroob[170], B. Ali[135], H.M.J. Ali[93,s], S. Ali[32], S.W. Alibocus[94], M. Aliev[34c], G. Alimonti[72a], W. Alkakhi[56], C. Allaire[67], B.M.M. Allbrooke[149], J.F. Allen[53], C.A. Allendes Flores[140f], P.P. Allport[21], A. Aloisio[73a,73b], F. Alonso[92], C. Alpigiani[141], Z.M.K. Alsolami[93], M. Alvarez Estevez[101], A. Alvarez Fernandez[102], M. Alves Cardoso[57], M.G. Alviggi[73a,73b], M. Aly[103], Y. Amaral Coutinho[84b], A. Ambler[106], C. Amelung[37], M. Amerl[103], C.G. Ames[111], D. Amidei[108], B. Amini[55], K.J. Amirie[158], S.P. Amor Dos Santos[133a], K.R. Amos[166], D. Amperiadou[155], S. An[85], V. Ananiev[128], C. Anastopoulos[142], T. Andeen[11], J.K. Anders[37], A.C. Anderson[60], S.Y. Andrean[48a,48b], A. Andreazza[72a,72b], S. Angelidakis[9], A. Angerami[42], A.V. Anisenkov[38], A. Annovi[75a], C. Antel[57], E. Antipov[148], M. Antonelli[54], F. Anulli[76a], M. Aoki[85], T. Aoki[156], M.A. Aparo[149], L. Aperio Bella[49], C. Appelt[19], A. Apyan[27], S.J. Arbiol Val[88], C. Arcangeletti[54], A.T.H. Arce[52], J-F. Arguin[110], S. Argyropoulos[55], J.-H. Arling[49], O. Arnaez[4], H. Arnold[148], G. Artoni[76a,76b], H. Asada[113], K. Asai[121], S. Asai[156], N.A. Asbah[37], R.A. Ashby Pickering[170], K. Assamagan[30], R. Astalos[29a], K.S.V. Astrand[100], S. Atashi[162], R.J. Atkin[34a], M. Atkinson[165], H. Atmani[36f], P.A. Atmasiddha[131], K. Augsten[135], S. Auricchio[73a,73b], A.D. Auriol[21], V.A. Austrup[103], G. Avolio[37], K. Axiotis[57], G. Azuelos[110,ad], D. Babal[29b], H. Bachacou[138], K. Bachas[155,o], A. Bachiu[35], F. Backman[48a,48b], A. Badea[40], T.M. Baer[108], P. Bagnaia[76a,76b], M. Bahmani[19], D. Bahner[55], K. Bai[126], J.T. Baines[137], L. Baines[96], O.K. Baker[175], E. Bakos[16], D. Bakshi Gupta[8], L.E. Balabram Filho[84b], V. Balakrishnan[123], R. Balasubramanian[4], E.M. Baldin[38], P. Balek[87a], E. Ballabene[24b,24a], F. Balli[138], L.M. Baltes[64a], W.K. Balunas[33], J. Balz[102], I. Bamwidhi[119b], E. Banas[88], M. Bandieramonte[132], A. Bandyopadhyay[25], S. Bansal[25], L. Barak[154], M. Barakat[49], E.L. Barberio[107], D. Barberis[58b,58a], M. Barbero[104], M.Z. Barel[117], T. Barillari[112], M-S. Barisits[37], T. Barklow[146], P. Baron[125], D.A. Baron Moreno[103], A. Baroncelli[63a], A.J. Barr[129], J.D. Barr[98], F. Barreiro[101], J. Barreiro Guimarães da Costa[14], U. Barron[154], M.G. Barros Teixeira[133a], S. Barsov[38], F. Bartels[64a], R. Bartoldus[146], A.E. Barton[93], P. Bartos[29a], A. Basan[102], M. Baselga[50], A. Bassalat[67,b], M.J. Basso[159a], S. Bataju[45], R. Bate[167], R.L. Bates[60], S. Batlamous[101], B. Batool[144], M. Battaglia[139], D. Battulga[19], M. Bauce[76a,76b], M. Bauer[80], P. Bauer[25], L.T. Bazzano Hurrell[31], J.B. Beacham[52], T. Beau[130], J.Y. Beaucamp[92], P.H. Beauchemin[161], P. Bechtle[25], H.P. Beck[20,n],

K. Becker[170], A.J. Beddall[83], V.A. Bednyakov[39], C.P. Bee[148], L.J. Beemster[16], T.A. Beermann[37], M. Begalli[84d], M. Begel[30], A. Behera[148], J.K. Behr[49], J.F. Beirer[37], F. Beisiegel[25], M. Belfkir[119b], G. Bella[154], L. Bellagamba[24b], A. Bellerive[35], P. Bellos[21], K. Beloborodov[38], D. Benchekroun[36a], F. Bendebba[36a], Y. Benhammou[154], K.C. Benkendorfer[62], L. Beresford[49], M. Beretta[54], E. Bergeaas Kuutmann[164], N. Berger[4], B. Bergmann[135], J. Beringer[18a], G. Bernardi[5], C. Bernius[146], F.U. Bernlochner[25], F. Bernon[37,104], A. Berrocal Guardia[13], T. Berry[97], P. Berta[136], A. Berthold[51], S. Bethke[112], A. Betti[76a,76b], A.J. Bevan[96], N.K. Bhalla[55], S. Bhatta[148], D.S. Bhattacharya[169], P. Bhattarai[146], K.D. Bhide[55], V.S. Bhopatkar[124], R.M. Bianchi[132], G. Bianco[24b,24a], O. Biebel[111], R. Bielski[126], M. Biglietti[78a], C.S. Billingsley[45], Y. Bimgdi[36f], M. Bindi[56], A. Bingul[22b], C. Bini[76a,76b], G.A. Bird[33], M. Birman[172], M. Biros[136], S. Biryukov[149], T. Bisanz[50], E. Bisceglie[44b,44a], J.P. Biswal[137], D. Biswas[144], I. Bloch[49], A. Blue[60], U. Blumenschein[96], J. Blumenthal[102], V.S. Bobrovnikov[38], M. Boehler[55], B. Boehm[169], D. Bogavac[37], A.G. Bogdanchikov[38], L.S. Boggia[130], C. Bohm[48a], V. Boisvert[97], P. Bokan[37], T. Bold[87a], M. Bomben[5], M. Bona[96], M. Boonekamp[138], C.D. Booth[97], A.G. Borbély[60], I.S. Bordulev[38], G. Borissov[93], D. Bortoletto[129], D. Boscherini[24b], M. Bosman[13], J.D. Bossio Sola[37], K. Bouaouda[36a], N. Bouchhar[166], L. Boudet[4], J. Boudreau[132], E.V. Bouhova-Thacker[93], D. Boumediene[41], R. Bouquet[58b,58a], A. Boveia[122], J. Boyd[37], D. Boye[30], I.R. Boyko[39], L. Bozianu[57], J. Bracinik[21], N. Brahimi[4], G. Brandt[174], O. Brandt[33], F. Braren[49], B. Brau[105], J.E. Brau[126], R. Brener[172], L. Brenner[117], R. Brenner[164], S. Bressler[172], G. Brianti[79a,79b], D. Britton[60], D. Britzger[112], I. Brock[25], G. Brooijmans[42], E.M. Brooks[159b], E. Brost[30], L.M. Brown[168], L.E. Bruce[62], T.L. Bruckler[129], P.A. Bruckman de Renstrom[88], B. Brüers[49], A. Bruni[24b], G. Bruni[24b], M. Bruschi[24b], N. Bruscino[76a,76b], T. Buanes[17], Q. Buat[141], D. Buchin[112], A.G. Buckley[60], O. Bulekov[38], B.A. Bullard[146], S. Burdin[94], C.D. Burgard[50], A.M. Burger[37], B. Burghgrave[8], O. Burlayenko[55], J. Burleson[165], J.T.P. Burr[33], J.C. Burzynski[145], E.L. Busch[42], V. Büscher[102], P.J. Bussey[60], J.M. Butler[26], C.M. Buttar[60], J.M. Butterworth[98], W. Buttinger[137], C.J. Buxo Vazquez[109], A.R. Buzykaev[38], S. Cabrera Urbán[166], L. Cadamuro[67], D. Caforio[59], H. Cai[132], Y. Cai[14,114c], Y. Cai[114a], V.M.M. Cairo[37], O. Cakir[3a], N. Calace[37], P. Calafiura[18a], G. Calderini[130], P. Calfayan[69], G. Callea[60], L.P. Caloba[84b], D. Calvet[41], S. Calvet[41], M. Calvetti[75a,75b], R. Camacho Toro[130], S. Camarda[37], D. Camarero Munoz[27], P. Camarri[77a,77b], M.T. Camerlingo[73a,73b], D. Cameron[37], C. Camincher[168], M. Campanelli[98], A. Camplani[43], V. Canale[73a,73b], A.C. Canbay[3a], E. Canonero[97], J. Cantero[166], Y. Cao[165], F. Capocasa[27], M. Capua[44b,44a], A. Carbone[72a,72b], R. Cardarelli[77a], J.C.J. Cardenas[8], G. Carducci[44b,44a], T. Carli[37], G. Carlino[73a], J.I. Carlotto[13], B.T. Carlson[132,p], E.M. Carlson[168,159a], J. Carmignani[94], L. Carminati[72a,72b], A. Carnelli[138], M. Carnesale[76a,76b], S. Caron[116], E. Carquin[140f], I.B. Carr[107], S. Carrá[72a], G. Carratta[24b,24a], A.M. Carroll[126], T.M. Carter[53], M.P. Casado[13,h], M. Caspar[49], F.L. Castillo[4], L. Castillo Garcia[13], V. Castillo Gimenez[166], N.F. Castro[133a,133e], A. Catinaccio[37], J.R. Catmore[128], T. Cavaliere[4], V. Cavaliere[30], N. Cavalli[24b,24a], L.J. Caviedes Betancourt[23b], Y.C. Cekmecelioglu[49], E. Celebi[83], S. Cella[37],

F. Celli[129], M.S. Centonze[71a,71b], V. Cepaitis[57], K. Cerny[125], A.S. Cerqueira[84a], A. Cerri[149], L. Cerrito[77a,77b], F. Cerutti[18a], B. Cervato[144], A. Cervelli[24b], G. Cesarini[54], S.A. Cetin[83], D. Chakraborty[118], J. Chan[18a], W.Y. Chan[156], J.D. Chapman[33], E. Chapon[138], B. Chargeishvili[152b], D.G. Charlton[21], M. Chatterjee[20], C. Chauhan[136], Y. Che[114a], S. Chekanov[6], S.V. Chekulaev[159a], G.A. Chelkov[39,a], A. Chen[108], B. Chen[154], B. Chen[168], H. Chen[114a], H. Chen[30], J. Chen[63c], J. Chen[145], M. Chen[129], S. Chen[89], S.J. Chen[114a], X. Chen[63c], X. Chen[15,ac], Y. Chen[63a], C.L. Cheng[173], H.C. Cheng[65a], S. Cheong[146], A. Cheplakov[39], E. Cheremushkina[49], E. Cherepanova[117], R. Cherkaoui El Moursli[36e], E. Cheu[7], K. Cheung[66], L. Chevalier[138], V. Chiarella[54], G. Chiarelli[75a], N. Chiedde[104], G. Chiodini[71a], A.S. Chisholm[21], A. Chitan[28b], M. Chitishvili[166], M.V. Chizhov[39,q], K. Choi[11], Y. Chou[141], E.Y.S. Chow[116], K.L. Chu[172], M.C. Chu[65a], X. Chu[14,114c], Z. Chubinidze[54], J. Chudoba[134], J.J. Chwastowski[88], D. Cieri[112], K.M. Ciesla[87a], V. Cindro[95], A. Ciocio[18a], F. Cirotto[73a,73b], Z.H. Citron[172], M. Citterio[72a], D.A. Ciubotaru[28b], A. Clark[57], P.J. Clark[53], N. Clarke Hall[98], C. Clarry[158], J.M. Clavijo Columbie[49], S.E. Clawson[49], C. Clement[48a,48b], Y. Coadou[104], M. Cobal[70a,70c], A. Coccaro[58b], R.F. Coelho Barrue[133a], R. Coelho Lopes De Sa[105], S. Coelli[72a], B. Cole[42], J. Collot[61], P. Conde Muiño[133a,133g], M.P. Connell[34c], S.H. Connell[34c], E.I. Conroy[129], F. Conventi[73a,ae], H.G. Cooke[21], A.M. Cooper-Sarkar[129], F.A. Corchia[24b,24a], A. Cordeiro Oudot Choi[130], L.D. Corpe[41], M. Corradi[76a,76b], F. Corriveau[106,x], A. Cortes-Gonzalez[19], M.J. Costa[166], F. Costanza[4], D. Costanzo[142], B.M. Cote[122], J. Couthures[4], G. Cowan[97], K. Cranmer[173], L. Cremer[50], D. Cremonini[24b,24a], S. Crépé-Renaudin[61], F. Crescioli[130], M. Cristinziani[144], M. Cristoforetti[79a,79b], V. Croft[117], J.E. Crosby[124], G. Crosetti[44b,44a], A. Cueto[101], H. Cui[98], Z. Cui[7], W.R. Cunningham[60], F. Curcio[166], J.R. Curran[53], P. Czodrowski[37], M.J. Da Cunha Sargedas De Sousa[58b,58a], J.V. Da Fonseca Pinto[84b], C. Da Via[103], W. Dabrowski[87a], T. Dado[37], S. Dahbi[151], T. Dai[108], D. Dal Santo[20], C. Dallapiccola[105], M. Dam[43], G. D'amen[30], V. D'Amico[111], J. Damp[102], J.R. Dandoy[35], D. Dannheim[37], M. Danninger[145], V. Dao[148], G. Darbo[58b], S.J. Das[30,af], F. Dattola[49], S. D'Auria[72a,72b], A. D'avanzo[73a,73b], C. David[34a], T. Davidek[136], I. Dawson[96], H.A. Day-hall[135], K. De[8], R. De Asmundis[73a], N. De Biase[49], S. De Castro[24b,24a], N. De Groot[116], P. de Jong[117], H. De la Torre[118], A. De Maria[114a], A. De Salvo[76a], U. De Sanctis[77a,77b], F. De Santis[71a,71b], A. De Santo[149], J.B. De Vivie De Regie[61], J. Debevc[95], D.V. Dedovich[39], J. Degens[94], A.M. Deiana[45], F. Del Corso[24b,24a], J. Del Peso[101], L. Delagrange[130], F. Deliot[138], C.M. Delitzsch[50], M. Della Pietra[73a,73b], D. Della Volpe[57], A. Dell'Acqua[37], L. Dell'Asta[72a,72b], M. Delmastro[4], P.A. Delsart[61], S. Demers[175], M. Demichev[39], S.P. Denisov[38], L. D'Eramo[41], D. Derendarz[88], F. Derue[130], P. Dervan[94], K. Desch[25], C. Deutsch[25], F.A. Di Bello[58b,58a], A. Di Ciaccio[77a,77b], L. Di Ciaccio[4], A. Di Domenico[76a,76b], C. Di Donato[73a,73b], A. Di Girolamo[37], G. Di Gregorio[37], A. Di Luca[79a,79b], B. Di Micco[78a,78b], R. Di Nardo[78a,78b], K.F. Di Petrillo[40], M. Diamantopoulou[35], F.A. Dias[117], T. Dias Do Vale[145], M.A. Diaz[140a,140b], F.G. Diaz Capriles[25], A.R. Didenko[39], M. Didenko[166], E.B. Diehl[108], S. Díez Cornell[49], C. Diez Pardos[144], C. Dimitriadi[164], A. Dimitrievska[21], J. Dingfelder[25], T. Dingley[129], I-M. Dinu[28b], S.J. Dittmeier[64b], F. Dittus[37], M. Divisek[136], B. Dixit[94], F. Djama[104],

JHEP09(2024)005

T. Djobava[152b], C. Doglioni[103,100], A. Dohnalova[29a], J. Dolejsi[136], Z. Dolezal[136], K. Domijan[87a], K.M. Dona[40], M. Donadelli[84d], B. Dong[109], J. Donini[41], A. D'Onofrio[73a,73b], M. D'Onofrio[94], J. Dopke[137], A. Doria[73a], N. Dos Santos Fernandes[133a], P. Dougan[103], M.T. Dova[92], A.T. Doyle[60], M.A. Draguet[129], E. Dreyer[172], I. Drivas-koulouris[10], M. Drnevich[120], M. Drozdova[57], D. Du[63a], T.A. du Pree[117], F. Dubinin[38], M. Dubovsky[29a], E. Duchovni[172], G. Duckeck[111], O.A. Ducu[28b], D. Duda[53], A. Dudarev[37], E.R. Duden[27], M. D'uffizi[103], L. Duflot[67], M. Dührssen[37], I. Duminica[28g], A.E. Dumitriu[28b], M. Dunford[64a], S. Dungs[50], K. Dunne[48a,48b], A. Duperrin[104], H. Duran Yildiz[3a], M. Düren[59], A. Durglishvili[152b], B.L. Dwyer[118], G.I. Dyckes[18a], M. Dyndal[87a], B.S. Dziedzic[37], Z.O. Earnshaw[149], G.H. Eberwein[129], B. Eckerova[29a], S. Eggebrecht[56], E. Egidio Purcino De Souza[84e], L.F. Ehrke[57], G. Eigen[17], K. Einsweiler[18a], T. Ekelof[164], P.A. Ekman[100], S. El Farkh[36b], Y. El Ghazali[63a], H. El Jarrari[37], A. El Moussaouy[36a], V. Ellajosyula[164], M. Ellert[164], F. Ellinghaus[174], N. Ellis[37], J. Elmsheuser[30], M. Elsawy[119a], M. Elsing[37], D. Emeliyanov[137], Y. Enari[85], I. Ene[18a], S. Epari[13], P.A. Erland[88], D. Ernani Martins Neto[88], M. Errenst[174], M. Escalier[67], C. Escobar[166], E. Etzion[154], G. Evans[133a], H. Evans[69], L.S. Evans[97], A. Ezhilov[38], S. Ezzarqtouni[36a], F. Fabbri[24b,24a], L. Fabbri[24b,24a], G. Facini[98], V. Fadeyev[139], R.M. Fakhrutdinov[38], D. Fakoudis[102], S. Falciano[76a], L.F. Falda Ulhoa Coelho[37], F. Fallavollita[112], G. Falsetti[44b,44a], J. Faltova[136], C. Fan[165], K.Y. Fan[65b], Y. Fan[14], Y. Fang[14,114c], M. Fanti[72a,72b], M. Faraj[70a,70b], Z. Farazpay[99], A. Farbin[8], A. Farilla[78a], T. Farooque[109], S.M. Farrington[53], F. Fassi[36e], D. Fassouliotis[9], M. Faucci Giannelli[77a,77b], W.J. Fawcett[33], L. Fayard[67], P. Federic[136], P. Federicova[134], O.L. Fedin[38,a], M. Feickert[173], L. Feligioni[104], D.E. Fellers[126], C. Feng[63b], Z. Feng[117], M.J. Fenton[162], L. Ferencz[49], R.A.M. Ferguson[93], S.I. Fernandez Luengo[140f], P. Fernandez Martinez[13], M.J.V. Fernoux[104], J. Ferrando[93], A. Ferrari[164], P. Ferrari[117,116], R. Ferrari[74a], D. Ferrere[57], C. Ferretti[108], D. Fiacco[76a,76b], F. Fiedler[102], P. Fiedler[135], A. Filipčič[95], E.K. Filmer[1], F. Filthaut[116], M.C.N. Fiolhais[133a,133c,c], L. Fiorini[166], W.C. Fisher[109], T. Fitschen[103], P.M. Fitzhugh[138], I. Fleck[144], P. Fleischmann[108], T. Flick[174], M. Flores[34d,aa], L.R. Flores Castillo[65a], L. Flores Sanz De Acedo[37], F.M. Follega[79a,79b], N. Fomin[33], J.H. Foo[158], A. Formica[138], A.C. Forti[103], E. Fortin[37], A.W. Fortman[18a], M.G. Foti[18a], L. Fountas[9,i], D. Fournier[67], H. Fox[93], P. Francavilla[75a,75b], S. Francescato[62], S. Franchellucci[57], M. Franchini[24b,24a], S. Franchino[64a], D. Francis[37], L. Franco[116], V. Franco Lima[37], L. Franconi[49], M. Franklin[62], G. Frattari[27], Y.Y. Frid[154], J. Friend[60], N. Fritzsche[37], A. Froch[55], D. Froidevaux[37], J.A. Frost[129], Y. Fu[63a], S. Fuenzalida Garrido[140f], M. Fujimoto[104], K.Y. Fung[65a], E. Furtado De Simas Filho[84e], M. Furukawa[156], J. Fuster[166], A. Gaa[56], A. Gabrielli[24b,24a], A. Gabrielli[158], P. Gadow[37], G. Gagliardi[58b,58a], L.G. Gagnon[18a], S. Gaid[163], S. Galantzan[154], J. Gallagher[1], E.J. Gallas[129], B.J. Gallop[137], K.K. Gan[122], S. Ganguly[156], Y. Gao[53], F.M. Garay Walls[140a,140b], B. Garcia[30], C. García[166], A. Garcia Alonso[117], A.G. Garcia Caffaro[175], J.E. García Navarro[166], M. Garcia-Sciveres[18a], G.L. Gardner[131], R.W. Gardner[40], N. Garelli[161], D. Garg[81], R.B. Garg[146], J.M. Gargan[53], C.A. Garner[158], C.M. Garvey[34a], V.K. Gassmann[161], G. Gaudio[74a], V. Gautam[13], P. Gauzzi[76a,76b], J. Gavranovic[95], I.L. Gavrilenko[38], A. Gavrilyuk[38], C. Gay[167],

G. Gaycken[126], E.N. Gazis[10], A.A. Geanta[28b], C.M. Gee[139], A. Gekow[122], C. Gemme[58b], M.H. Genest[61], A.D. Gentry[115], S. George[97], W.F. George[21], T. Geralis[47], P. Gessinger-Befurt[37], M.E. Geyik[174], M. Ghani[170], K. Ghorbanian[96], A. Ghosal[144], A. Ghosh[162], A. Ghosh[7], B. Giacobbe[24b], S. Giagu[76a,76b], T. Giani[117], A. Giannini[63a], S.M. Gibson[97], M. Gignac[139], D.T. Gil[87b], A.K. Gilbert[87a], B.J. Gilbert[42], D. Gillberg[35], G. Gilles[117], L. Ginabat[130], D.M. Gingrich[2,ad], M.P. Giordani[70a,70c], P.F. Giraud[138], G. Giugliarelli[70a,70c], D. Giugni[72a], F. Giuli[37], I. Gkialas[9,i], L.K. Gladilin[38], C. Glasman[101], G.R. Gledhill[126], G. Glemža[49], M. Glisic[126], I. Gnesi[44b], Y. Go[30], M. Goblirsch-Kolb[37], B. Gocke[50], D. Godin[110], B. Gokturk[22a], S. Goldfarb[107], T. Golling[57], M.G.D. Gololo[34g], D. Golubkov[38], J.P. Gombas[109], A. Gomes[133a,133b], G. Gomes Da Silva[144], A.J. Gomez Delegido[166], R. Gonçalo[133a], L. Gonella[21], A. Gongadze[152c], F. Gonnella[21], J.L. Gonski[146], R.Y. González Andana[53], S. González de la Hoz[166], R. Gonzalez Lopez[94], C. Gonzalez Renteria[18a], M.V. Gonzalez Rodrigues[49], R. Gonzalez Suarez[164], S. Gonzalez-Sevilla[57], L. Goossens[37], B. Gorini[37], E. Gorini[71a,71b], A. Gorišek[95], T.C. Gosart[131], A.T. Goshaw[52], M.I. Gostkin[39], S. Goswami[124], C.A. Gottardo[37], S.A. Gotz[111], M. Gouighri[36b], V. Goumarre[49], A.G. Goussiou[141], N. Govender[34c], R.P. Grabarczyk[129], I. Grabowska-Bold[87a], K. Graham[35], E. Gramstad[128], S. Grancagnolo[71a,71b], C.M. Grant[1,138], P.M. Gravila[28f], F.G. Gravili[71a,71b], H.M. Gray[18a], M. Greco[71a,71b], M.J. Green[1], C. Grefe[25], A.S. Grefsrud[17], I.M. Gregor[49], K.T. Greif[162], P. Grenier[146], S.G. Grewe[112], A.A. Grillo[139], K. Grimm[32], S. Grinstein[13,t], J.-F. Grivaz[67], E. Gross[172], J. Grosse-Knetter[56], L. Guan[108], J.G.R. Guerrero Rojas[166], G. Guerrieri[37], R. Gugel[102], J.A.M. Guhit[108], A. Guida[19], E. Guilloton[170], S. Guindon[37], F. Guo[14,114c], J. Guo[63c], L. Guo[49], Y. Guo[108], R. Gupta[132], S. Gurbuz[25], S.S. Gurdasani[55], G. Gustavino[76a,76b], P. Gutierrez[123], L.F. Gutierrez Zagazeta[131], M. Gutsche[51], C. Gutschow[98], C. Gwenlan[129], C.B. Gwilliam[94], E.S. Haaland[128], A. Haas[120], M. Habedank[49], C. Haber[18a], H.K. Hadavand[8], A. Hadef[51], S. Hadzic[112], A.I. Hagan[93], J.J. Hahn[144], E.H. Haines[98], M. Haleem[169], J. Haley[124], J.J. Hall[142], G.D. Hallewell[104], L. Halser[20], K. Hamano[168], M. Hamer[25], G.N. Hamity[53], E.J. Hampshire[97], J. Han[63b], K. Han[63a], L. Han[114a], L. Han[63a], S. Han[18a], Y.F. Han[158], K. Hanagaki[85], M. Hance[139], D.A. Hangal[42], H. Hanif[145], M.D. Hank[131], J.B. Hansen[43], P.H. Hansen[43], D. Harada[57], T. Harenberg[174], S. Harkusha[38], M.L. Harris[105], Y.T. Harris[25], J. Harrison[13], N.M. Harrison[122], P.F. Harrison[170], N.M. Hartman[112], N.M. Hartmann[111], R.Z. Hasan[97,137], Y. Hasegawa[143], F. Haslbeck[129], S. Hassan[17], R. Hauser[109], C.M. Hawkes[21], R.J. Hawkings[37], Y. Hayashi[156], D. Hayden[109], C. Hayes[108], R.L. Hayes[117], C.P. Hays[129], J.M. Hays[96], H.S. Hayward[94], F. He[63a], M. He[14,114c], Y. He[49], Y. He[98], N.B. Heatley[96], V. Hedberg[100], A.L. Heggelund[128], N.D. Hehir[96,*], C. Heidegger[55], K.K. Heidegger[55], J. Heilman[35], S. Heim[49], T. Heim[18a], J.G. Heinlein[131], J.J. Heinrich[126], L. Heinrich[112,ab], J. Hejbal[134], A. Held[173], S. Hellesund[17], C.M. Helling[167], S. Hellman[48a,48b], R.C.W. Henderson[93], L. Henkelmann[33], A.M. Henriques Correia[37], H. Herde[100], Y. Hernández Jiménez[148], L.M. Herrmann[25], T. Herrmann[51], G. Herten[55], R. Hertenberger[111], L. Hervas[37], M.E. Hesping[102], N.P. Hessey[159a], M. Hidaoui[36b], N. Hidic[136], E. Hill[158], S.J. Hillier[21], J.R. Hinds[109],

JHEP09(2024)005

F. Hinterkeuser[25], M. Hirose[127], S. Hirose[160], D. Hirschbuehl[174], T.G. Hitchings[103], B. Hiti[95], J. Hobbs[148], R. Hobincu[28e], N. Hod[172], M.C. Hodgkinson[142], B.H. Hodkinson[129], A. Hoecker[37], D.D. Hofer[108], J. Hofer[166], T. Holm[25], M. Holzbock[37], L.B.A.H. Hommels[33], B.P. Honan[103], J.J. Hong[69], J. Hong[63c], T.M. Hong[132], B.H. Hooberman[165], W.H. Hopkins[6], M.C. Hoppesch[165], Y. Horii[113], M.E. Horstmann[112], S. Hou[151], A.S. Howard[95], J. Howarth[60], J. Hoya[6], M. Hrabovsky[125], A. Hrynevich[49], T. Hryn'ova[4], P.J. Hsu[66], S.-C. Hsu[141], T. Hsu[67], M. Hu[18a], Q. Hu[63a], S. Huang[65b], X. Huang[14,114c], Y. Huang[142], Y. Huang[102], Y. Huang[14], Z. Huang[103], Z. Hubacek[135], M. Huebner[25], F. Huegging[25], T.B. Huffman[129], C.A. Hugli[49], M. Huhtinen[37], S.K. Huiberts[17], R. Hulsken[106], N. Huseynov[12,f], J. Huston[109], J. Huth[62], R. Hyneman[146], G. Iacobucci[57], G. Iakovidis[30], L. Iconomidou-Fayard[67], J.P. Iddon[37], P. Iengo[73a,73b], R. Iguchi[156], Y. Iiyama[156], T. Iizawa[129], Y. Ikegami[85], N. Ilic[158], H. Imam[84c], G. Inacio Goncalves[84d], M. Ince Lezki[57], T. Ingebretsen Carlson[48a,48b], J.M. Inglis[96], G. Introzzi[74a,74b], M. Iodice[78a], V. Ippolito[76a,76b], R.K. Irwin[94], M. Ishino[156], W. Islam[173], C. Issever[19,49], S. Istin[22a,ah], H. Ito[171], R. Iuppa[79a,79b], A. Ivina[172], J.M. Izen[46], V. Izzo[73a], P. Jacka[134], P. Jackson[1], C.S. Jagfeld[111], G. Jain[159a], P. Jain[49], K. Jakobs[55], T. Jakoubek[172], J. Jamieson[60], W. Jang[156], M. Javurkova[105], P. Jawahar[103], L. Jeanty[126], J. Jejelava[152a,z], P. Jenni[55,e], C.E. Jessiman[35], C. Jia[63b], J. Jia[148], X. Jia[14,114c], Z. Jia[114a], C. Jiang[53], S. Jiggins[49], J. Jimenez Pena[13], S. Jin[114a], A. Jinaru[28b], O. Jinnouchi[157], P. Johansson[142], K.A. Johns[7], J.W. Johnson[139], F.A. Jolly[49], D.M. Jones[149], E. Jones[49], K.S. Jones[8], P. Jones[33], R.W.L. Jones[93], T.J. Jones[94], H.L. Joos[56,37], R. Joshi[122], J. Jovicevic[16], X. Ju[18a], J.J. Junggeburth[105], T. Junkermann[64a], A. Juste Rozas[13,t], M.K. Juzek[88], S. Kabana[140e], A. Kaczmarska[88], M. Kado[112], H. Kagan[122], M. Kagan[146], A. Kahn[131], C. Kahra[102], T. Kaji[156], E. Kajomovitz[153], N. Kakati[172], I. Kalaitzidou[55], C.W. Kalderon[30], N.J. Kang[139], D. Kar[34g], K. Karava[129], M.J. Kareem[159b], E. Karentzos[55], O. Karkout[117], S.N. Karpov[39], Z.M. Karpova[39], V. Kartvelishvili[93], A.N. Karyukhin[38], E. Kasimi[155], J. Katzy[49], S. Kaur[35], K. Kawade[143], M.P. Kawale[123], C. Kawamoto[89], T. Kawamoto[63a], E.F. Kay[37], F.I. Kaya[161], S. Kazakos[109], V.F. Kazanin[38], Y. Ke[148], J.M. Keaveney[34a], R. Keeler[168], G.V. Kehris[62], J.S. Keller[35], A.S. Kelly[98], J.J. Kempster[149], P.D. Kennedy[102], O. Kepka[134], B.P. Kerridge[137], S. Kersten[174], B.P. Kerševan[95], L. Keszeghova[29a], S. Ketabchi Haghighat[158], R.A. Khan[132], A. Khanov[124], A.G. Kharlamov[38], T. Kharlamova[38], E.E. Khoda[141], M. Kholodenko[133a], T.J. Khoo[19], G. Khoriauli[169], J. Khubua[152b,*], Y.A.R. Khwaira[130], B. Kibirige[34g], D. Kim[6], D.W. Kim[48a,48b], Y.K. Kim[40], N. Kimura[98], M.K. Kingston[56], A. Kirchhoff[56], C. Kirfel[25], F. Kirfel[25], J. Kirk[137], A.E. Kiryunin[112], S. Kita[160], C. Kitsaki[10], O. Kivernyk[25], M. Klassen[161], C. Klein[35], L. Klein[169], M.H. Klein[45], S.B. Klein[57], U. Klein[94], P. Klimek[37], A. Klimentov[30], T. Klioutchnikova[37], P. Kluit[117], S. Kluth[112], E. Kneringer[80], T.M. Knight[158], A. Knue[50], D. Kobylianskii[172], S.F. Koch[129], M. Kocian[146], P. Kodyš[136], D.M. Koeck[126], P.T. Koenig[25], T. Koffas[35], O. Kolay[51], I. Koletsou[4], T. Komarek[88], K. Köneke[55], A.X.Y. Kong[1], T. Kono[121], N. Konstantinidis[98], P. Kontaxakis[57], B. Konya[100], R. Kopeliansky[42], S. Koperny[87a], K. Korcyl[88], K. Kordas[155,d], A. Korn[98], S. Korn[56], I. Korolkov[13], N. Korotkova[38],

JHEP09(2024)005

B. Kortman[117], O. Kortner[112], S. Kortner[112], W.H. Kostecka[118], V.V. Kostyukhin[144], A. Kotsokechagia[37], A. Kotwal[52], A. Koulouris[37], A. Kourkoumeli-Charalampidi[74a,74b], C. Kourkoumelis[9], E. Kourlitis[112,ab], O. Kovanda[126], R. Kowalewski[168], W. Kozanecki[126], A.S. Kozhin[38], V.A. Kramarenko[38], G. Kramberger[95], P. Kramer[102], M.W. Krasny[130], A. Krasznahorkay[37], A.C. Kraus[118], J.W. Kraus[174], J.A. Kremer[49], T. Kresse[51], L. Kretschmann[174], J. Kretzschmar[94], K. Kreul[19], P. Krieger[158], M. Krivos[136], K. Krizka[21], K. Kroeninger[50], H. Kroha[112], J. Kroll[134], J. Kroll[131], K.S. Krowpman[109], U. Kruchonak[39], H. Krüger[25], N. Krumnack[82], M.C. Kruse[52], O. Kuchinskaia[38], S. Kuday[3a], S. Kuehn[37], R. Kuesters[55], T. Kuhl[49], V. Kukhtin[39], Y. Kulchitsky[38,a], S. Kuleshov[140d,140b], M. Kumar[34g], N. Kumari[49], P. Kumari[159b], A. Kupco[134], T. Kupfer[50], A. Kupich[38], O. Kuprash[55], H. Kurashige[86], L.L. Kurchaninov[159a], O. Kurdysh[67], Y.A. Kurochkin[38], A. Kurova[38], M. Kuze[157], A.K. Kvam[105], J. Kvita[125], T. Kwan[106], N.G. Kyriacou[108], L.A.O. Laatu[104], C. Lacasta[166], F. Lacava[76a,76b], H. Lacker[19], D. Lacour[130], N.N. Lad[98], E. Ladygin[39], A. Lafarge[41], B. Laforge[130], T. Lagouri[175], F.Z. Lahbabi[36a], S. Lai[56], J.E. Lambert[168], S. Lammers[69], W. Lampl[7], C. Lampoudis[155,d], G. Lamprinoudis[102], A.N. Lancaster[118], E. Lançon[30], U. Landgraf[55], M.P.J. Landon[96], V.S. Lang[55], O.K.B. Langrekken[128], A.J. Lankford[162], F. Lanni[37], K. Lantzsch[25], A. Lanza[74a], M. Lanzac Berrocal[166], J.F. Laporte[138], T. Lari[72a], F. Lasagni Manghi[24b], M. Lassnig[37], V. Latonova[134], A. Laurier[153], S.D. Lawlor[142], Z. Lawrence[103], R. Lazaridou[170], M. Lazzaroni[72a,72b], B. Le[103], H.D.M. Le[109], E.M. Le Boulicaut[175], L.T. Le Pottier[18a], B. Leban[24b,24a], A. Lebedev[82], M. LeBlanc[103], F. Ledroit-Guillon[61], S.C. Lee[151], S. Lee[48a,48b], T.F. Lee[94], L.L. Leeuw[34c], H.P. Lefebvre[97], M. Lefebvre[168], C. Leggett[18a], G. Lehmann Miotto[37], M. Leigh[57], W.A. Leight[105], W. Leinonen[116], A. Leisos[155,r], M.A.L. Leite[84c], C.E. Leitgeb[19], R. Leitner[136], K.J.C. Leney[45], T. Lenz[25], S. Leone[75a], C. Leonidopoulos[53], A. Leopold[147], R. Les[109], C.G. Lester[33], M. Levchenko[38], J. Levêque[4], L.J. Levinson[172], G. Levrini[24b,24a], M.P. Lewicki[88], C. Lewis[141], D.J. Lewis[4], L. Lewitt[142], A. Li[30], B. Li[63b], C. Li[63a], C-Q. Li[112], H. Li[63a], H. Li[63b], H. Li[114a], H. Li[15], H. Li[63b], J. Li[63c], K. Li[14], L. Li[63c], M. Li[14,114c], S. Li[14,114c], S. Li[63d,63c], T. Li[5], X. Li[106], Z. Li[129], Z. Li[156], Z. Li[14,114c], Z. Li[63a], S. Liang[14,114c], Z. Liang[14], M. Liberatore[138], B. Liberti[77a], K. Lie[65c], J. Lieber Marin[84e], H. Lien[69], H. Lin[108], K. Lin[109], R.E. Lindley[7], J.H. Lindon[2], J. Ling[62], E. Lipeles[131], A. Lipniacka[17], A. Lister[167], J.D. Little[69], B. Liu[14], B.X. Liu[114b], D. Liu[63d,63c], E.H.L. Liu[21], J.B. Liu[63a], J.K.K. Liu[33], K. Liu[63d], K. Liu[63d,63c], M. Liu[63a], M.Y. Liu[63a], P. Liu[14], Q. Liu[63d,141,63c], X. Liu[63a], X. Liu[63b], Y. Liu[114b,114c], Y.L. Liu[63b], Y.W. Liu[63a], S.L. Lloyd[96], E.M. Lobodzinska[49], P. Loch[7], T. Lohse[19], K. Lohwasser[142], E. Loiacono[49], M. Lokajicek[134,*], J.D. Lomas[21], J.D. Long[165], I. Longarini[162], R. Longo[165], I. Lopez Paz[68], A. Lopez Solis[49], N.A. Lopez-canelas[7], N. Lorenzo Martinez[4], A.M. Lory[111], M. Losada[119a], G. Löschcke Centeno[149], O. Loseva[38], X. Lou[48a,48b], X. Lou[14,114c], A. Lounis[67], P.A. Love[93], G. Lu[14,114c], M. Lu[67], S. Lu[131], Y.J. Lu[66], H.J. Lubatti[141], C. Luci[76a,76b], F.L. Lucio Alves[114a], F. Luehring[69], O. Lukianchuk[67], O. Lundberg[147], B. Lund-Jensen[147,*], N.A. Luongo[6], M.S. Lutz[37], A.B. Lux[26], D. Lynn[30], R. Lysak[134], E. Lytken[100], V. Lyubushkin[39], T. Lyubushkina[39],

JHEP09(2024)005

M.M. Lyukova[148], M.Firdaus M. Soberi[53], H. Ma[30], K. Ma[63a], L.L. Ma[63b], W. Ma[63a], Y. Ma[124], J.C. MacDonald[102], P.C. Machado De Abreu Farias[84e], R. Madar[41], T. Madula[98], J. Maeda[86], T. Maeno[30], H. Maguire[142], V. Maiboroda[138], A. Maio[133a,133b,133d], K. Maj[87a], O. Majersky[49], S. Majewski[126], N. Makovec[67], V. Maksimovic[16], B. Malaescu[130], Pa. Malecki[88], V.P. Maleev[38], F. Malek[61,m], M. Mali[95], D. Malito[97], U. Mallik[81], S. Maltezos[10], S. Malyukov[39], J. Mamuzic[13], G. Mancini[54], M.N. Mancini[27], G. Manco[74a,74b], J.P. Mandalia[96], S.S. Mandarry[149], I. Mandić[95], L. Manhaes de Andrade Filho[84a], I.M. Maniatis[172], J. Manjarres Ramos[91], D.C. Mankad[172], A. Mann[111], S. Manzoni[37], L. Mao[63c], X. Mapekula[34c], A. Marantis[155,r], G. Marchiori[5], M. Marcisovsky[134], C. Marcon[72a], M. Marinescu[21], S. Marium[49], M. Marjanovic[123], A. Markhoos[55], M. Markovitch[67], E.J. Marshall[93], Z. Marshall[18a], S. Marti-Garcia[166], J. Martin[98], T.A. Martin[137], V.J. Martin[53], B. Martin dit Latour[17], L. Martinelli[76a,76b], M. Martinez[13,t], P. Martinez Agullo[166], V.I. Martinez Outschoorn[105], P. Martinez Suarez[13], S. Martin-Haugh[137], G. Martinovicova[136], V.S. Martoiu[28b], A.C. Martyniuk[98], A. Marzin[37], D. Mascione[79a,79b], L. Masetti[102], J. Masik[103], A.L. Maslennikov[38], P. Massarotti[73a,73b], P. Mastrandrea[75a,75b], A. Mastroberardino[44b,44a], T. Masubuchi[127], T.T. Mathew[126], T. Mathisen[164], J. Matousek[136], J. Maurer[28b], T. Maurin[60], A.J. Maury[67], B. Maček[95], D.A. Maximov[38], A.E. May[103], R. Mazini[151], I. Maznas[118], M. Mazza[109], S.M. Mazza[139], E. Mazzeo[72a,72b], C. Mc Ginn[30], J.P. Mc Gowan[168], S.P. Mc Kee[108], C.C. McCracken[167], E.F. McDonald[107], A.E. McDougall[117], J.A. Mcfayden[149], R.P. McGovern[131], R.P. Mckenzie[34g], T.C. Mclachlan[49], D.J. Mclaughlin[98], S.J. McMahon[137], C.M. Mcpartland[94], R.A. McPherson[168,x], S. Mehlhase[111], A. Mehta[94], D. Melini[166], B.R. Mellado Garcia[34g], A.H. Melo[56], F. Meloni[49], A.M. Mendes Jacques Da Costa[103], H.Y. Meng[158], L. Meng[93], S. Menke[112], M. Mentink[37], E. Meoni[44b,44a], G. Mercado[118], S. Merianos[155], C. Merlassino[70a,70c], L. Merola[73a,73b], C. Meroni[72a,72b], J. Metcalfe[6], A.S. Mete[6], E. Meuser[102], C. Meyer[69], J-P. Meyer[138], R.P. Middleton[137], L. Mijović[53], G. Mikenberg[172], M. Mikestikova[134], M. Mikuž[95], H. Mildner[102], A. Milic[37], D.W. Miller[40], E.H. Miller[146], L.S. Miller[35], A. Milov[172], D.A. Milstead[48a,48b], T. Min[114a], A.A. Minaenko[38], I.A. Minashvili[152b], L. Mince[60], A.I. Mincer[120], B. Mindur[87a], M. Mineev[39], Y. Mino[89], L.M. Mir[13], M. Miralles Lopez[60], M. Mironova[18a], M.C. Missio[116], A. Mitra[170], V.A. Mitsou[166], Y. Mitsumori[113], O. Miu[158], P.S. Miyagawa[96], T. Mkrtchyan[64a], M. Mlinarevic[98], T. Mlinarevic[98], M. Mlynarikova[37], S. Mobius[20], P. Mogg[111], M.H. Mohamed Farook[115], A.F. Mohammed[14,114c], S. Mohapatra[42], G. Mokgatitswane[34g], L. Moleri[172], B. Mondal[144], S. Mondal[135], K. Mönig[49], E. Monnier[104], L. Monsonis Romero[166], J. Montejo Berlingen[13], A. Montella[48a,48b], M. Montella[122], F. Montereali[78a,78b], F. Monticelli[92], S. Monzani[70a,70c], A. Morancho Tarda[43], N. Morange[67], A.L. Moreira De Carvalho[49], M. Moreno Llácer[166], C. Moreno Martinez[57], J.M. Moreno Perez[23b], P. Morettini[58b], S. Morgenstern[37], M. Morii[62], M. Morinaga[156], F. Morodei[76a,76b], L. Morvaj[37], P. Moschovakos[37], B. Moser[129], M. Mosidze[152b], T. Moskalets[45], P. Moskvitina[116], J. Moss[32,j], P. Moszkowicz[87a], A. Moussa[36d], E.J.W. Moyse[105], O. Mtintsilana[34g], S. Muanza[104], J. Mueller[132], D. Muenstermann[93], R. Müller[37], G.A. Mullier[164], A.J. Mullin[33], J.J. Mullin[131], D.P. Mungo[158], D. Munoz Perez[166], F.J. Munoz Sanchez[103], M. Murin[103], W.J. Murray[170,137], M. Muškinja[95], C. Mwewa[30], A.G. Myagkov[38,a], A.J. Myers[8], G. Myers[108], M. Myska[135], B.P. Nachman[18a], O. Nackenhorst[50], K. Nagai[129], K. Nagano[85], R. Nagasaka[156], J.L. Nagle[30,af], E. Nagy[104], A.M. Nairz[37], Y. Nakahama[85], K. Nakamura[85], K. Nakkalil[5], H. Nanjo[127], E.A. Narayanan[115], I. Naryshkin[38], L. Nasella[72a,72b], M. Naseri[35], S. Nasri[119b], C. Nass[25], G. Navarro[23a], J. Navarro-Gonzalez[166], R. Nayak[154], A. Nayaz[19], P.Y. Nechaeva[38], S. Nechaeva[24b,24a], F. Nechansky[134], L. Nedic[129], T.J. Neep[21], A. Negri[74a,74b], M. Negrini[24b], C. Nellist[117], C. Nelson[106], K. Nelson[108], S. Nemecek[134], M. Nessi[37,g], M.S. Neubauer[165], F. Neuhaus[102], J. Neundorf[49], J. Newell[94], P.R. Newman[21], C.W. Ng[132], Y.W.Y. Ng[49], B. Ngair[119a], H.D.N. Nguyen[110], R.B. Nickerson[129], R. Nicolaidou[138], J. Nielsen[139], M. Niemeyer[56], J. Niermann[56], N. Nikiforou[37], V. Nikolaenko[38,a], I. Nikolic-Audit[130], K. Nikolopoulos[21], P. Nilsson[30], I. Ninca[49], G. Ninio[154], A. Nisati[76a], N. Nishu[2], R. Nisius[112], J-E. Nitschke[51], E.K. Nkadimeng[34g], T. Nobe[156], T. Nommensen[150], M.B. Norfolk[142], B.J. Norman[35], M. Noury[36a], J. Novak[95], T. Novak[95], L. Novotny[135], R. Novotny[115], L. Nozka[125], K. Ntekas[162], N.M.J. Nunes De Moura Junior[84b], J. Ocariz[130], A. Ochi[86], I. Ochoa[133a], S. Oerdek[49,u], J.T. Offermann[40], A. Ogrodnik[136], A. Oh[103], C.C. Ohm[147], H. Oide[85], R. Oishi[156], M.L. Ojeda[37], Y. Okumura[156], L.F. Oleiro Seabra[133a], I. Oleksiyuk[57], S.A. Olivares Pino[140d], G. Oliveira Correa[13], D. Oliveira Damazio[30], J.L. Oliver[162], Ö.O. Öncel[55], A.P. O'Neill[20], A. Onofre[133a,133e], P.U.E. Onyisi[11], M.J. Oreglia[40], G.E. Orellana[92], D. Orestano[78a,78b], N. Orlando[13], R.S. Orr[158], L.M. Osojnak[131], R. Ospanov[63a], G. Otero y Garzon[31], H. Otono[90], P.S. Ott[64a], G.J. Ottino[18a], M. Ouchrif[36d], F. Ould-Saada[128], T. Ovsiannikova[141], M. Owen[60], R.E. Owen[137], V.E. Ozcan[22a], F. Ozturk[88], N. Ozturk[8], S. Ozturk[83], H.A. Pacey[129], A. Pacheco Pages[13], C. Padilla Aranda[13], G. Padovano[76a,76b], S. Pagan Griso[18a], G. Palacino[69], A. Palazzo[71a,71b], J. Pampel[25], J. Pan[175], T. Pan[65a], D.K. Panchal[11], C.E. Pandini[117], J.G. Panduro Vazquez[137], H.D. Pandya[1], H. Pang[15], P. Pani[49], G. Panizzo[70a,70c], L. Panwar[130], L. Paolozzi[57], S. Parajuli[165], A. Paramonov[6], C. Paraskevopoulos[54], D. Paredes Hernandez[65b], A. Pareti[74a,74b], K.R. Park[42], T.H. Park[158], M.A. Parker[33], F. Parodi[58b,58a], E.W. Parrish[118], V.A. Parrish[53], J.A. Parsons[42], U. Parzefall[55], B. Pascual Dias[110], L. Pascual Dominguez[101], E. Pasqualucci[76a], S. Passaggio[58b], F. Pastore[97], P. Patel[88], U.M. Patel[52], J.R. Pater[103], T. Pauly[37], C.I. Pazos[161], J. Pearkes[146], M. Pedersen[128], R. Pedro[133a], S.V. Peleganchuk[38], O. Penc[37], E.A. Pender[53], S. Peng[15], G.D. Penn[175], K.E. Penski[111], M. Penzin[38], B.S. Peralva[84d], A.P. Pereira Peixoto[141], L. Pereira Sanchez[146], D.V. Perepelitsa[30,af], G. Perera[105], E. Perez Codina[159a], M. Perganti[10], H. Pernegger[37], S. Perrella[76a,76b], O. Perrin[41], K. Peters[49], R.F.Y. Peters[103], B.A. Petersen[37], T.C. Petersen[43], E. Petit[104], V. Petousis[135], C. Petridou[155,d], T. Petru[136], A. Petrukhin[144], M. Pettee[18a], A. Petukhov[38], K. Petukhova[37], R. Pezoa[140f], L. Pezzotti[37], G. Pezzullo[175], A.J. Pfleger[37], T.M. Pham[173], T. Pham[107], P.W. Phillips[137], G. Piacquadio[148], E. Pianori[18a], F. Piazza[126], R. Piegaia[31], D. Pietreanu[28b], A.D. Pilkington[103], M. Pinamonti[70a,70c], J.L. Pinfold[2], B.C. Pinheiro Pereira[133a], J. Pinol Bel[13], A.E. Pinto Pinoargote[138,138], L. Pintucci[70a,70c], K.M. Piper[149], A. Pirttikoski[57], D.A. Pizzi[35], L. Pizzimento[65b], A. Pizzini[117], M.-A. Pleier[30], V. Pleskot[136], E. Plotnikova[39], G. Poddar[96], R. Poettgen[100], L. Poggioli[130], I. Pokharel[56], S. Polacek[136], G. Polesello[74a], A. Poley[145,159a], A. Polini[24b], C.S. Pollard[170], Z.B. Pollock[122], E. Pompa Pacchi[76a,76b], N.I. Pond[98], D. Ponomarenko[69], L. Pontecorvo[37], S. Popa[28a], G.A. Popeneciu[28d], A. Poreba[37], D.M. Portillo Quintero[159a], S. Pospisil[135], M.A. Postill[142], P. Postolache[28c], K. Potamianos[170], P.A. Potepa[87a], I.N. Potrap[39], C.J. Potter[33], H. Potti[150], J. Poveda[166], M.E. Pozo Astigarraga[37], A. Prades Ibanez[77a,77b], J. Pretel[168], D. Price[103], M. Primavera[71a], L. Primomo[70a,70c], M.A. Principe Martin[101], R. Privara[125], T. Procter[60], M.L. Proffitt[141], N. Proklova[131], K. Prokofiev[65c], G. Proto[112], J. Proudfoot[6], M. Przybycien[87a], W.W. Przygoda[87b], A. Psallidas[47], J.E. Puddefoot[142], D. Pudzha[55], D. Pyatiizbyantseva[38], J. Qian[108], D. Qichen[103], Y. Qin[13], T. Qiu[53], A. Quadt[56], M. Queitsch-Maitland[103], G. Quetant[57], R.P. Quinn[167], G. Rabanal Bolanos[62], D. Rafanoharana[55], F. Raffaeli[77a,77b], F. Ragusa[72a,72b], J.L. Rainbolt[40], J.A. Raine[57], S. Rajagopalan[30], E. Ramakoti[38], L. Rambelli[58b,58a], I.A. Ramirez-Berend[35], K. Ran[49,114c], D.S. Rankin[131], N.P. Rapheeha[34g], H. Rasheed[28b], V. Raskina[130], D.F. Rassloff[64a], A. Rastogi[18a], S. Rave[102], S. Ravera[58b,58a], B. Ravina[56], I. Ravinovich[172], M. Raymond[37], A.L. Read[128], N.P. Readioff[142], D.M. Rebuzzi[74a,74b], G. Redlinger[30], A.S. Reed[112], K. Reeves[27], J.A. Reidelsturz[174], D. Reikher[126], A. Rej[50], C. Rembser[37], M. Renda[28b], F. Renner[49], A.G. Rennie[162], A.L. Rescia[49], S. Resconi[72a], M. Ressegotti[58b,58a], S. Rettie[37], J.G. Reyes Rivera[109], E. Reynolds[18a], O.L. Rezanova[38], P. Reznicek[136], H. Riani[36d], N. Ribaric[52], E. Ricci[79a,79b], R. Richter[112], S. Richter[48a,48b], E. Richter-Was[87b], M. Ridel[130], S. Ridouani[36d], P. Rieck[120], P. Riedler[37], E.M. Riefel[48a,48b], J.O. Rieger[117], M. Rijssenbeek[148], M. Rimoldi[37], L. Rinaldi[24b,24a], P. Rincke[56,164], T.T. Rinn[30], M.P. Rinnagel[111], G. Ripellino[164], I. Riu[13], J.C. Rivera Vergara[168], F. Rizatdinova[124], E. Rizvi[96], B.R. Roberts[18a], S.S. Roberts[139], S.H. Robertson[106,x], D. Robinson[33], M. Robles Manzano[102], A. Robson[60], A. Rocchi[77a,77b], C. Roda[75a,75b], S. Rodriguez Bosca[37], Y. Rodriguez Garcia[23a], A. Rodriguez Rodriguez[55], A.M. Rodríguez Vera[118], S. Roe[37], J.T. Roemer[37], A.R. Roepe-Gier[139], O. Røhne[128], R.A. Rojas[105], C.P.A. Roland[130], J. Roloff[30], A. Romaniouk[38], E. Romano[74a,74b], M. Romano[24b], A.C. Romero Hernandez[165], N. Rompotis[94], L. Roos[130], S. Rosati[76a], B.J. Rosser[40], E. Rossi[129], E. Rossi[73a,73b], L.P. Rossi[62], L. Rossini[55], R. Rosten[122], M. Rotaru[28b], B. Rottler[55], C. Rougier[91], D. Rousseau[67], D. Rousso[49], A. Roy[165], S. Roy-Garand[158], A. Rozanov[104], Z.M.A. Rozario[60], Y. Rozen[153], A. Rubio Jimenez[166], A.J. Ruby[94], V.H. Ruelas Rivera[19], T.A. Ruggeri[1], A. Ruggiero[129], A. Ruiz-Martinez[166], A. Rummler[37], Z. Rurikova[55], N.A. Rusakovich[39], H.L. Russell[168], G. Russo[76a,76b], J.P. Rutherfoord[7], S. Rutherford Colmenares[33], M. Rybar[136], E.B. Rye[128], A. Ryzhov[45], J.A. Sabater Iglesias[57], H.F-W. Sadrozinski[139], F. Safai Tehrani[76a], B. Safarzadeh Samani[137], S. Saha[1], M. Sahinsoy[83], A. Saibel[166], M. Saimpert[138], M. Saito[156], T. Saito[156], A. Sala[72a,72b], D. Salamani[37], A. Salnikov[146], J. Salt[166], A. Salvador Salas[154], D. Salvatore[44b,44a], F. Salvatore[149], A. Salzburger[37], D. Sammel[55], E. Sampson[93], D. Sampsonidis[155,d], D. Sampsonidou[126], J. Sánchez[166], V. Sanchez Sebastian[166], H. Sandaker[128], C.O. Sander[49], J.A. Sandesara[105],

M. Sandhoff[174], C. Sandoval[23b], L. Sanfilippo[64a], D.P.C. Sankey[137], T. Sano[89], A. Sansoni[54], L. Santi[37,76b], C. Santoni[41], H. Santos[133a,133b], A. Santra[172], E. Sanzani[24b,24a], K.A. Saoucha[163], J.G. Saraiva[133a,133d], J. Sardain[7], O. Sasaki[85], K. Sato[160], C. Sauer[64b], E. Sauvan[4], P. Savard[158,ad], R. Sawada[156], C. Sawyer[137], L. Sawyer[99], C. Sbarra[24b], A. Sbrizzi[24b,24a], T. Scanlon[98], J. Schaarschmidt[141], U. Schäfer[102], A.C. Schaffer[67,45], D. Schaile[111], R.D. Schamberger[148], C. Scharf[19], M.M. Schefer[20], V.A. Schegelsky[38], D. Scheirich[136], M. Schernau[162], C. Scheulen[56], C. Schiavi[58b,58a], M. Schioppa[44b,44a], B. Schlag[146,l], K.E. Schleicher[55], S. Schlenker[37], J. Schmeing[174], M.A. Schmidt[174], K. Schmieden[102], C. Schmitt[102], N. Schmitt[102], S. Schmitt[49], L. Schoeffel[138], A. Schoening[64b], P.G. Scholer[35], E. Schopf[129], M. Schott[25], J. Schovancova[37], S. Schramm[57], T. Schroer[57], H-C. Schultz-Coulon[64a], M. Schumacher[55], B.A. Schumm[139], Ph. Schune[138], A.J. Schuy[141], H.R. Schwartz[139], A. Schwartzman[146], T.A. Schwarz[108], Ph. Schwemling[138], R. Schwienhorst[109], F.G. Sciacca[20], A. Sciandra[30], G. Sciolla[27], F. Scuri[75a], C.D. Sebastiani[94], K. Sedlaczek[118], S.C. Seidel[115], A. Seiden[139], B.D. Seidlitz[42], C. Seitz[49], J.M. Seixas[84b], G. Sekhniaidze[73a], L. Selem[61], N. Semprini-Cesari[24b,24a], D. Sengupta[57], V. Senthilkumar[166], L. Serin[67], M. Sessa[77a,77b], H. Severini[123], F. Sforza[58b,58a], A. Sfyrla[57], Q. Sha[14], E. Shabalina[56], A.H. Shah[33], R. Shaheen[147], J.D. Shahinian[131], D. Shaked Renous[172], L.Y. Shan[14], M. Shapiro[18a], A. Sharma[37], A.S. Sharma[167], P. Sharma[81], P.B. Shatalov[38], K. Shaw[149], S.M. Shaw[103], Q. Shen[63c], D.J. Sheppard[145], P. Sherwood[98], L. Shi[98], X. Shi[14], S. Shimizu[85], C.O. Shimmin[175], J.D. Shinner[97], I.P.J. Shipsey[129], S. Shirabe[90], M. Shiyakova[39,v], M.J. Shochet[40], D.R. Shope[128], B. Shrestha[123], S. Shrestha[122,ag], M.J. Shroff[168], P. Sicho[134], A.M. Sickles[165], E. Sideras Haddad[34g], A.C. Sidley[117], A. Sidoti[24b], F. Siegert[51], Dj. Sijacki[16], F. Sili[92], J.M. Silva[53], I. Silva Ferreira[84b], M.V. Silva Oliveira[30], S.B. Silverstein[48a], S. Simion[67], R. Simoniello[37], E.L. Simpson[103], H. Simpson[149], L.R. Simpson[108], N.D. Simpson[100], S. Simsek[83], S. Sindhu[56], P. Sinervo[158], S. Singh[158], S. Sinha[49], S. Sinha[103], M. Sioli[24b,24a], I. Siral[37], E. Sitnikova[49], J. Sjölin[48a,48b], A. Skaf[56], E. Skorda[21], P. Skubic[123], M. Slawinska[88], V. Smakhtin[172], B.H. Smart[137], S.Yu. Smirnov[38], Y. Smirnov[38], L.N. Smirnova[38,a], O. Smirnova[100], A.C. Smith[42], D.R. Smith[162], E.A. Smith[40], J.L. Smith[103], R. Smith[146], M. Smizanska[93], K. Smolek[135], A.A. Snesarev[38], H.L. Snoek[117], S. Snyder[30], R. Sobie[168,x], A. Soffer[154], C.A. Solans Sanchez[37], E.Yu. Soldatov[38], U. Soldevila[166], A.A. Solodkov[38], S. Solomon[27], A. Soloshenko[39], K. Solovieva[55], O.V. Solovyanov[41], P. Sommer[51], A. Sonay[13], W.Y. Song[159b], A. Sopczak[135], A.L. Sopio[98], F. Sopkova[29b], J.D. Sorenson[115], I.R. Sotarriva Alvarez[157], V. Sothilingam[64a], O.J. Soto Sandoval[140c,140b], S. Sottocornola[69], R. Soualah[163], Z. Soumaimi[36e], D. South[49], N. Soybelman[172], S. Spagnolo[71a,71b], M. Spalla[112], D. Sperlich[55], G. Spigo[37], B. Spisso[73a,73b], D.P. Spiteri[60], M. Spousta[136], E.J. Staats[35], R. Stamen[64a], A. Stampekis[21], E. Stanecka[88], W. Stanek-Maslouska[49], M.V. Stange[51], B. Stanislaus[18a], M.M. Stanitzki[49], B. Stapf[49], E.A. Starchenko[38], G.H. Stark[139], J. Stark[91], P. Staroba[134], P. Starovoitov[64a], S. Stärz[106], R. Staszewski[88], G. Stavropoulos[47], A. Stefl[37], P. Steinberg[30], B. Stelzer[145,159a], H.J. Stelzer[132], O. Stelzer-Chilton[159a], H. Stenzel[59], T.J. Stevenson[149], G.A. Stewart[37], J.R. Stewart[124], M.C. Stockton[37], G. Stoicea[28b], M. Stolarski[133a], S. Stonjek[112], A. Straessner[51],

J. Strandberg[147], S. Strandberg[48a,48b], M. Stratmann[174], M. Strauss[123], T. Strebler[104], P. Strizenec[29b], R. Ströhmer[169], D.M. Strom[126], R. Stroynowski[45], A. Strubig[48a,48b], S.A. Stucci[30], B. Stugu[17], J. Stupak[123], N.A. Styles[49], D. Su[146], S. Su[63a], W. Su[63d], X. Su[63a], D. Suchy[29a], K. Sugizaki[156], V.V. Sulin[38], M.J. Sullivan[94], D.M.S. Sultan[129], L. Sultanaliyeva[38], S. Sultansoy[3b], T. Sumida[89], S. Sun[173], O. Sunneborn Gudnadottir[164], N. Sur[104], M.R. Sutton[149], H. Suzuki[160], M. Svatos[134], M. Swiatlowski[159a], T. Swirski[169], I. Sykora[29a], M. Sykora[136], T. Sykora[136], D. Ta[102], K. Tackmann[49,u], A. Taffard[162], R. Tafirout[159a], J.S. Tafoya Vargas[67], Y. Takubo[85], M. Talby[104], A.A. Talyshev[38], K.C. Tam[65b], N.M. Tamir[154], A. Tanaka[156], J. Tanaka[156], R. Tanaka[67], M. Tanasini[148], Z. Tao[167], S. Tapia Araya[140f], S. Tapprogge[102], A. Tarek Abouelfadl Mohamed[109], S. Tarem[153], K. Tariq[14], G. Tarna[28b], G.F. Tartarelli[72a], M.J. Tartarin[91], P. Tas[136], M. Tasevsky[134], E. Tassi[44b,44a], A.C. Tate[165], G. Tateno[156], Y. Tayalati[36e,w], G.N. Taylor[107], W. Taylor[159b], R. Teixeira De Lima[146], P. Teixeira-Dias[97], J.J. Teoh[158], K. Terashi[156], J. Terron[101], S. Terzo[13], M. Testa[54], R.J. Teuscher[158,x], A. Thaler[80], O. Theiner[57], T. Theveneaux-Pelzer[104], O. Thielmann[174], D.W. Thomas[97], J.P. Thomas[21], E.A. Thompson[18a], P.D. Thompson[21], E. Thomson[131], R.E. Thornberry[45], C. Tian[63a], Y. Tian[56], V. Tikhomirov[38,a], Yu.A. Tikhonov[38], S. Timoshenko[38], D. Timoshyn[136], E.X.L. Ting[1], P. Tipton[175], A. Tishelman-Charny[30], S.H. Tlou[34g], K. Todome[157], S. Todorova-Nova[136], S. Todt[51], L. Toffolin[70a,70c], M. Togawa[85], J. Tojo[90], S. Tokár[29a], K. Tokushuku[85], O. Toldaiev[69], M. Tomoto[85,113], L. Tompkins[146,l], K.W. Topolnicki[87b], E. Torrence[126], H. Torres[91], E. Torró Pastor[166], M. Toscani[31], C. Tosciri[40], M. Tost[11], D.R. Tovey[142], I.S. Trandafir[28b], T. Trefzger[169], A. Tricoli[30], I.M. Trigger[159a], S. Trincaz-Duvoid[130], D.A. Trischuk[27], B. Trocmé[61], A. Tropina[39], L. Truong[34c], M. Trzebinski[88], A. Trzupek[88], F. Tsai[148], M. Tsai[108], A. Tsiamis[155], P.V. Tsiareshka[38], S. Tsigaridas[159a], A. Tsirigotis[155,r], V. Tsiskaridze[158], E.G. Tskhadadze[152a], M. Tsopoulou[155], Y. Tsujikawa[89], I.I. Tsukerman[38], V. Tsulaia[18a], S. Tsuno[85], K. Tsuri[121], D. Tsybychev[148], Y. Tu[65b], A. Tudorache[28b], V. Tudorache[28b], A.N. Tuna[62], S. Turchikhin[58b,58a], I. Turk Cakir[3a], R. Turra[72a], T. Turtuvshin[39], P.M. Tuts[42], S. Tzamarias[155,d], E. Tzovara[102], F. Ukegawa[160], P.A. Ulloa Poblete[140c,140b], E.N. Umaka[30], G. Unal[37], A. Undrus[30], G. Unel[162], J. Urban[29b], P. Urrejola[140a], G. Usai[8], R. Ushioda[157], M. Usman[110], F. Ustuner[53], Z. Uysal[83], V. Vacek[135], B. Vachon[106], T. Vafeiadis[37], A. Vaitkus[98], C. Valderanis[111], E. Valdes Santurio[48a,48b], M. Valente[159a], S. Valentinetti[24b,24a], A. Valero[166], E. Valiente Moreno[166], A. Vallier[91], J.A. Valls Ferrer[166], D.R. Van Arneman[117], T.R. Van Daalen[141], A. Van Der Graaf[50], P. Van Gemmeren[6], M. Van Rijnbach[37], S. Van Stroud[98], I. Van Vulpen[117], P. Vana[136], M. Vanadia[77a,77b], W. Vandelli[37], E.R. Vandewall[124], D. Vannicola[154], L. Vannoli[54], R. Vari[76a], E.W. Varnes[7], C. Varni[18b], T. Varol[151], D. Varouchas[67], L. Varriale[166], K.E. Varvell[150], M.E. Vasile[28b], L. Vaslin[85], G.A. Vasquez[168], A. Vasyukov[39], L.M. Vaughan[124], R. Vavricka[102], T. Vazquez Schroeder[37], J. Veatch[32], V. Vecchio[103], M.J. Veen[105], I. Veliscek[30], L.M. Veloce[158], F. Veloso[133a,133c], S. Veneziano[76a], A. Ventura[71a,71b], S. Ventura Gonzalez[138], A. Verbytskyi[112], M. Verducci[75a,75b], C. Vergis[96], M. Verissimo De Araujo[84b], W. Verkerke[117], J.C. Vermeulen[117], C. Vernieri[146], M. Vessella[105], M.C. Vetterli[145,ad], A. Vgenopoulos[102], N. Viaux Maira[140f],

T. Vickey[142], O.E. Vickey Boeriu[142], G.H.A. Viehhauser[129], L. Vigani[64b], M. Vigl[112], M. Villa[24b,24a], M. Villaplana Perez[166], E.M. Villhauer[53], E. Vilucchi[54], M.G. Vincter[35], A. Visibile[117], C. Vittori[37], I. Vivarelli[24b,24a], E. Voevodina[112], F. Vogel[111], J.C. Voigt[51], P. Vokac[135], Yu. Volkotrub[87b], J. Von Ahnen[49], E. Von Toerne[25], B. Vormwald[37], V. Vorobel[136], K. Vorobev[38], M. Vos[166], K. Voss[144], M. Vozak[117], L. Vozdecky[123], N. Vranjes[16], M. Vranjes Milosavljevic[16], M. Vreeswijk[117], N.K. Vu[63d,63c], R. Vuillermet[37], O. Vujinovic[102], I. Vukotic[40], I.K. Vyas[35], S. Wada[160], C. Wagner[105], J.M. Wagner[18a], W. Wagner[174], S. Wahdan[174], H. Wahlberg[92], J. Walder[137], R. Walker[111], W. Walkowiak[144], A. Wall[131], E.J. Wallin[100], T. Wamorkar[6], A.Z. Wang[139], C. Wang[102], C. Wang[11], H. Wang[18a], J. Wang[65c], P. Wang[98], R. Wang[62], R. Wang[6], S.M. Wang[151], S. Wang[63b], S. Wang[14], T. Wang[63a], W.T. Wang[81], W. Wang[14], X. Wang[114a], X. Wang[165], X. Wang[63c], Y. Wang[63d], Y. Wang[114a], Y. Wang[63a], Z. Wang[108], Z. Wang[63d,52,63c], Z. Wang[108], A. Warburton[106], R.J. Ward[21], N. Warrack[60], S. Waterhouse[97], A.T. Watson[21], H. Watson[53], M.F. Watson[21], E. Watton[60,137], G. Watts[141], B.M. Waugh[98], J.M. Webb[55], C. Weber[30], H.A. Weber[19], M.S. Weber[20], S.M. Weber[64a], C. Wei[63a], Y. Wei[55], A.R. Weidberg[129], E.J. Weik[120], J. Weingarten[50], C. Weiser[55], C.J. Wells[49], T. Wenaus[30], B. Wendland[50], T. Wengler[37], N.S. Wenke[112], N. Wermes[25], M. Wessels[64a], A.M. Wharton[93], A.S. White[62], A. White[8], M.J. White[1], D. Whiteson[162], L. Wickremasinghe[127], W. Wiedenmann[173], M. Wielers[137], C. Wiglesworth[43], D.J. Wilbern[123], H.G. Wilkens[37], J.J.H. Wilkinson[33], D.M. Williams[42], H.H. Williams[131], S. Williams[33], S. Willocq[105], B.J. Wilson[103], P.J. Windischhofer[40], F.I. Winkel[31], F. Winklmeier[126], B.T. Winter[55], J.K. Winter[103], M. Wittgen[146], M. Wobisch[99], T. Wojtkowski[61], Z. Wolffs[117], J. Wollrath[162], M.W. Wolter[88], H. Wolters[133a,133c], M.C. Wong[139], E.L. Woodward[42], S.D. Worm[49], B.K. Wosiek[88], K.W. Woźniak[88], S. Wozniewski[56], K. Wraight[60], C. Wu[21], M. Wu[114b], M. Wu[116], S.L. Wu[173], X. Wu[57], Y. Wu[63a], Z. Wu[4], J. Wuerzinger[112,ab], T.R. Wyatt[103], B.M. Wynne[53], S. Xella[43], L. Xia[114a], M. Xia[15], M. Xie[63a], S. Xin[14,114c], A. Xiong[126], J. Xiong[18a], D. Xu[14], H. Xu[63a], L. Xu[63a], R. Xu[131], T. Xu[108], Y. Xu[15], Z. Xu[53], Z. Xu[114a], B. Yabsley[150], S. Yacoob[34a], Y. Yamaguchi[85], E. Yamashita[156], H. Yamauchi[160], T. Yamazaki[18a], Y. Yamazaki[86], J. Yan[63c], S. Yan[60], Z. Yan[105], H.J. Yang[63c,63d], H.T. Yang[63a], S. Yang[63a], T. Yang[65c], X. Yang[37], X. Yang[14], Y. Yang[45], Y. Yang[63a], Z. Yang[63a], W-M. Yao[18a], H. Ye[114a], H. Ye[56], J. Ye[14], S. Ye[30], X. Ye[63a], Y. Yeh[98], I. Yeletskikh[39], B. Yeo[18b], M.R. Yexley[98], T.P. Yildirim[129], P. Yin[42], K. Yorita[171], S. Younas[28b], C.J.S. Young[37], C. Young[146], C. Yu[14,114c], Y. Yu[63a], J. Yuan[14,114c], M. Yuan[108], R. Yuan[63d,63c], L. Yue[98], M. Zaazoua[63a], B. Zabinski[88], E. Zaid[53], Z.K. Zak[88], T. Zakareishvili[166], S. Zambito[57], J.A. Zamora Saa[140d,140b], J. Zang[156], D. Zanzi[55], O. Zaplatilek[135], C. Zeitnitz[174], H. Zeng[14], J.C. Zeng[165], D.T. Zenger Jr[27], O. Zenin[38], T. Ženiš[29a], S. Zenz[96], S. Zerradi[36a], D. Zerwas[67], M. Zhai[14,114c], D.F. Zhang[142], J. Zhang[63b], J. Zhang[6], K. Zhang[14,114c], L. Zhang[63a], L. Zhang[114a], P. Zhang[14,114c], R. Zhang[173], S. Zhang[108], S. Zhang[91], T. Zhang[156], X. Zhang[63c], X. Zhang[63b], Y. Zhang[63c], Y. Zhang[98], Y. Zhang[114a], Z. Zhang[18a], Z. Zhang[63b], Z. Zhang[67], H. Zhao[141], T. Zhao[63b], Y. Zhao[139], Z. Zhao[63a], Z. Zhao[63a], A. Zhemchugov[39], J. Zheng[114a], K. Zheng[165],

X. Zheng[63a], Z. Zheng[146], D. Zhong[165], B. Zhou[108], H. Zhou[7], N. Zhou[63c], Y. Zhou[15], Y. Zhou[114a], Y. Zhou[7], C.G. Zhu[63b], J. Zhu[108], X. Zhu[63d], Y. Zhu[63c], Y. Zhu[63a], X. Zhuang[14], K. Zhukov[69], N.I. Zimine[39], J. Zinsser[64b], M. Ziolkowski[144], L. Živković[16], A. Zoccoli[24b,24a], K. Zoch[62], T.G. Zorbas[142], O. Zormpa[47], W. Zou[42], L. Zwalinski[37]

[1] *Department of Physics, University of Adelaide, Adelaide, Australia*
[2] *Department of Physics, University of Alberta, Edmonton AB, Canada*
[3] [(a)] *Department of Physics, Ankara University, Ankara;* [(b)] *Division of Physics, TOBB University of Economics and Technology, Ankara, Türkiye*
[4] *LAPP, Université Savoie Mont Blanc, CNRS/IN2P3, Annecy, France*
[5] *APC, Université Paris Cité, CNRS/IN2P3, Paris, France*
[6] *High Energy Physics Division, Argonne National Laboratory, Argonne IL, United States of America*
[7] *Department of Physics, University of Arizona, Tucson AZ, United States of America*
[8] *Department of Physics, University of Texas at Arlington, Arlington TX, United States of America*
[9] *Physics Department, National and Kapodistrian University of Athens, Athens, Greece*
[10] *Physics Department, National Technical University of Athens, Zografou, Greece*
[11] *Department of Physics, University of Texas at Austin, Austin TX, United States of America*
[12] *Institute of Physics, Azerbaijan Academy of Sciences, Baku, Azerbaijan*
[13] *Institut de Física d'Altes Energies (IFAE), Barcelona Institute of Science and Technology, Barcelona, Spain*
[14] *Institute of High Energy Physics, Chinese Academy of Sciences, Beijing, China*
[15] *Physics Department, Tsinghua University, Beijing, China*
[16] *Institute of Physics, University of Belgrade, Belgrade, Serbia*
[17] *Department for Physics and Technology, University of Bergen, Bergen, Norway*
[18] [(a)] *Physics Division, Lawrence Berkeley National Laboratory, Berkeley CA;* [(b)] *University of California, Berkeley CA, United States of America*
[19] *Institut für Physik, Humboldt Universität zu Berlin, Berlin, Germany*
[20] *Albert Einstein Center for Fundamental Physics and Laboratory for High Energy Physics, University of Bern, Bern, Switzerland*
[21] *School of Physics and Astronomy, University of Birmingham, Birmingham, United Kingdom*
[22] [(a)] *Department of Physics, Bogazici University, Istanbul;* [(b)] *Department of Physics Engineering, Gaziantep University, Gaziantep;* [(c)] *Department of Physics, Istanbul University, Istanbul, Türkiye*
[23] [(a)] *Facultad de Ciencias y Centro de Investigaciónes, Universidad Antonio Nariño, Bogotá;* [(b)] *Departamento de Física, Universidad Nacional de Colombia, Bogotá, Colombia*
[24] [(a)] *Dipartimento di Fisica e Astronomia A. Righi, Università di Bologna, Bologna;* [(b)] *INFN Sezione di Bologna, Italy*
[25] *Physikalisches Institut, Universität Bonn, Bonn, Germany*
[26] *Department of Physics, Boston University, Boston MA, United States of America*
[27] *Department of Physics, Brandeis University, Waltham MA, United States of America*
[28] [(a)] *Transilvania University of Brasov, Brasov;* [(b)] *Horia Hulubei National Institute of Physics and Nuclear Engineering, Bucharest;* [(c)] *Department of Physics, Alexandru Ioan Cuza University of Iasi, Iasi;* [(d)] *National Institute for Research and Development of Isotopic and Molecular Technologies, Physics Department, Cluj-Napoca;* [(e)] *National University of Science and Technology Politechnica, Bucharest;* [(f)] *West University in Timisoara, Timisoara;* [(g)] *Faculty of Physics, University of Bucharest, Bucharest, Romania*
[29] [(a)] *Faculty of Mathematics, Physics and Informatics, Comenius University, Bratislava;* [(b)] *Department of Subnuclear Physics, Institute of Experimental Physics of the Slovak Academy of Sciences, Kosice, Slovak Republic*
[30] *Physics Department, Brookhaven National Laboratory, Upton NY, United States of America*
[31] *Universidad de Buenos Aires, Facultad de Ciencias Exactas y Naturales, Departamento de Física, y CONICET, Instituto de Física de Buenos Aires (IFIBA), Buenos Aires, Argentina*
[32] *California State University, CA, United States of America*
[33] *Cavendish Laboratory, University of Cambridge, Cambridge, United Kingdom*

JHEP09(2024)005

[34] [(a)] *Department of Physics, University of Cape Town, Cape Town;* [(b)] *iThemba Labs, Western Cape;* [(c)] *Department of Mechanical Engineering Science, University of Johannesburg, Johannesburg;* [(d)] *National Institute of Physics, University of the Philippines Diliman (Philippines);* [(e)] *University of South Africa, Department of Physics, Pretoria;* [(f)] *University of Zululand, KwaDlangezwa;* [(g)] *School of Physics, University of the Witwatersrand, Johannesburg, South Africa*
[35] *Department of Physics, Carleton University, Ottawa ON, Canada*
[36] [(a)] *Faculté des Sciences Ain Chock, Université Hassan II de Casablanca;* [(b)] *Faculté des Sciences, Université Ibn-Tofail, Kénitra;* [(c)] *Faculté des Sciences Semlalia, Université Cadi Ayyad, LPHEA-Marrakech;* [(d)] *LPMR, Faculté des Sciences, Université Mohamed Premier, Oujda;* [(e)] *Faculté des sciences, Université Mohammed V, Rabat;* [(f)] *Institute of Applied Physics, Mohammed VI Polytechnic University, Ben Guerir, Morocco*
[37] *CERN, Geneva, Switzerland*
[38] *Affiliated with an institute covered by a cooperation agreement with CERN*
[39] *Affiliated with an international laboratory covered by a cooperation agreement with CERN*
[40] *Enrico Fermi Institute, University of Chicago, Chicago IL, United States of America*
[41] *LPC, Université Clermont Auvergne, CNRS/IN2P3, Clermont-Ferrand, France*
[42] *Nevis Laboratory, Columbia University, Irvington NY, United States of America*
[43] *Niels Bohr Institute, University of Copenhagen, Copenhagen, Denmark*
[44] [(a)] *Dipartimento di Fisica, Università della Calabria, Rende;* [(b)] *INFN Gruppo Collegato di Cosenza, Laboratori Nazionali di Frascati, Italy*
[45] *Physics Department, Southern Methodist University, Dallas TX, United States of America*
[46] *Physics Department, University of Texas at Dallas, Richardson TX, United States of America*
[47] *National Centre for Scientific Research "Demokritos", Agia Paraskevi, Greece*
[48] [(a)] *Department of Physics, Stockholm University;* [(b)] *Oskar Klein Centre, Stockholm, Sweden*
[49] *Deutsches Elektronen-Synchrotron DESY, Hamburg and Zeuthen, Germany*
[50] *Fakultät Physik, Technische Universität Dortmund, Dortmund, Germany*
[51] *Institut für Kern- und Teilchenphysik, Technische Universität Dresden, Dresden, Germany*
[52] *Department of Physics, Duke University, Durham NC, United States of America*
[53] *SUPA - School of Physics and Astronomy, University of Edinburgh, Edinburgh, United Kingdom*
[54] *INFN e Laboratori Nazionali di Frascati, Frascati, Italy*
[55] *Physikalisches Institut, Albert-Ludwigs-Universität Freiburg, Freiburg, Germany*
[56] *II. Physikalisches Institut, Georg-August-Universität Göttingen, Göttingen, Germany*
[57] *Département de Physique Nucléaire et Corpusculaire, Université de Genève, Genève, Switzerland*
[58] [(a)] *Dipartimento di Fisica, Università di Genova, Genova;* [(b)] *INFN Sezione di Genova, Italy*
[59] *II. Physikalisches Institut, Justus-Liebig-Universität Giessen, Giessen, Germany*
[60] *SUPA - School of Physics and Astronomy, University of Glasgow, Glasgow, United Kingdom*
[61] *LPSC, Université Grenoble Alpes, CNRS/IN2P3, Grenoble INP, Grenoble, France*
[62] *Laboratory for Particle Physics and Cosmology, Harvard University, Cambridge MA, United States of America*
[63] [(a)] *Department of Modern Physics and State Key Laboratory of Particle Detection and Electronics, University of Science and Technology of China, Hefei;* [(b)] *Institute of Frontier and Interdisciplinary Science and Key Laboratory of Particle Physics and Particle Irradiation (MOE), Shandong University, Qingdao;* [(c)] *School of Physics and Astronomy, Shanghai Jiao Tong University, Key Laboratory for Particle Astrophysics and Cosmology (MOE), SKLPPC, Shanghai;* [(d)] *Tsung-Dao Lee Institute, Shanghai;* [(e)] *School of Physics and Microelectronics, Zhengzhou University, China*
[64] [(a)] *Kirchhoff-Institut für Physik, Ruprecht-Karls-Universität Heidelberg, Heidelberg;* [(b)] *Physikalisches Institut, Ruprecht-Karls-Universität Heidelberg, Heidelberg, Germany*
[65] [(a)] *Department of Physics, Chinese University of Hong Kong, Shatin, N.T., Hong Kong;* [(b)] *Department of Physics, University of Hong Kong, Hong Kong;* [(c)] *Department of Physics and Institute for Advanced Study, Hong Kong University of Science and Technology, Clear Water Bay, Kowloon, Hong Kong, China*
[66] *Department of Physics, National Tsing Hua University, Hsinchu, Taiwan*
[67] *IJCLab, Université Paris-Saclay, CNRS/IN2P3, 91405, Orsay, France*
[68] *Centro Nacional de Microelectrónica (IMB-CNM-CSIC), Barcelona, Spain*

[69] Department of Physics, Indiana University, Bloomington IN, United States of America
[70] [(a)] INFN Gruppo Collegato di Udine, Sezione di Trieste, Udine; [(b)] ICTP, Trieste; [(c)] Dipartimento Politecnico di Ingegneria e Architettura, Università di Udine, Udine, Italy
[71] [(a)] INFN Sezione di Lecce; [(b)] Dipartimento di Matematica e Fisica, Università del Salento, Lecce, Italy
[72] [(a)] INFN Sezione di Milano; [(b)] Dipartimento di Fisica, Università di Milano, Milano, Italy
[73] [(a)] INFN Sezione di Napoli; [(b)] Dipartimento di Fisica, Università di Napoli, Napoli, Italy
[74] [(a)] INFN Sezione di Pavia; [(b)] Dipartimento di Fisica, Università di Pavia, Pavia, Italy
[75] [(a)] INFN Sezione di Pisa; [(b)] Dipartimento di Fisica E. Fermi, Università di Pisa, Pisa, Italy
[76] [(a)] INFN Sezione di Roma; [(b)] Dipartimento di Fisica, Sapienza Università di Roma, Roma, Italy
[77] [(a)] INFN Sezione di Roma Tor Vergata; [(b)] Dipartimento di Fisica, Università di Roma Tor Vergata, Roma, Italy
[78] [(a)] INFN Sezione di Roma Tre; [(b)] Dipartimento di Matematica e Fisica, Università Roma Tre, Roma, Italy
[79] [(a)] INFN-TIFPA; [(b)] Università degli Studi di Trento, Trento, Italy
[80] Universität Innsbruck, Department of Astro and Particle Physics, Innsbruck, Austria
[81] University of Iowa, Iowa City IA, United States of America
[82] Department of Physics and Astronomy, Iowa State University, Ames IA, United States of America
[83] Istinye University, Sariyer, Istanbul, Türkiye
[84] [(a)] Departamento de Engenharia Elétrica, Universidade Federal de Juiz de Fora (UFJF), Juiz de Fora; [(b)] Universidade Federal do Rio De Janeiro COPPE/EE/IF, Rio de Janeiro; [(c)] Instituto de Física, Universidade de São Paulo, São Paulo; [(d)] Rio de Janeiro State University, Rio de Janeiro; [(e)] Federal University of Bahia, Bahia, Brazil
[85] KEK, High Energy Accelerator Research Organization, Tsukuba, Japan
[86] Graduate School of Science, Kobe University, Kobe, Japan
[87] [(a)] AGH University of Krakow, Faculty of Physics and Applied Computer Science, Krakow; [(b)] Marian Smoluchowski Institute of Physics, Jagiellonian University, Krakow, Poland
[88] Institute of Nuclear Physics Polish Academy of Sciences, Krakow, Poland
[89] Faculty of Science, Kyoto University, Kyoto, Japan
[90] Research Center for Advanced Particle Physics and Department of Physics, Kyushu University, Fukuoka, Japan
[91] L2IT, Université de Toulouse, CNRS/IN2P3, UPS, Toulouse, France
[92] Instituto de Física La Plata, Universidad Nacional de La Plata and CONICET, La Plata, Argentina
[93] Physics Department, Lancaster University, Lancaster, United Kingdom
[94] Oliver Lodge Laboratory, University of Liverpool, Liverpool, United Kingdom
[95] Department of Experimental Particle Physics, Jožef Stefan Institute and Department of Physics, University of Ljubljana, Ljubljana, Slovenia
[96] School of Physics and Astronomy, Queen Mary University of London, London, United Kingdom
[97] Department of Physics, Royal Holloway University of London, Egham, United Kingdom
[98] Department of Physics and Astronomy, University College London, London, United Kingdom
[99] Louisiana Tech University, Ruston LA, United States of America
[100] Fysiska institutionen, Lunds universitet, Lund, Sweden
[101] Departamento de Física Teorica C-15 and CIAFF, Universidad Autónoma de Madrid, Madrid, Spain
[102] Institut für Physik, Universität Mainz, Mainz, Germany
[103] School of Physics and Astronomy, University of Manchester, Manchester, United Kingdom
[104] CPPM, Aix-Marseille Université, CNRS/IN2P3, Marseille, France
[105] Department of Physics, University of Massachusetts, Amherst MA, United States of America
[106] Department of Physics, McGill University, Montreal QC, Canada
[107] School of Physics, University of Melbourne, Victoria, Australia
[108] Department of Physics, University of Michigan, Ann Arbor MI, United States of America
[109] Department of Physics and Astronomy, Michigan State University, East Lansing MI, United States of America
[110] Group of Particle Physics, University of Montreal, Montreal QC, Canada
[111] Fakultät für Physik, Ludwig-Maximilians-Universität München, München, Germany
[112] Max-Planck-Institut für Physik (Werner-Heisenberg-Institut), München, Germany

JHEP09(2024)005

[113] *Graduate School of Science and Kobayashi-Maskawa Institute, Nagoya University, Nagoya, Japan*
[114] [(a)] *Department of Physics, Nanjing University, Nanjing;* [(b)] *School of Science, Shenzhen Campus of Sun Yat-sen University;* [(c)] *University of Chinese Academy of Science (UCAS), Beijing, China*
[115] *Department of Physics and Astronomy, University of New Mexico, Albuquerque NM, United States of America*
[116] *Institute for Mathematics, Astrophysics and Particle Physics, Radboud University/Nikhef, Nijmegen, The Netherlands*
[117] *Nikhef National Institute for Subatomic Physics and University of Amsterdam, Amsterdam, The Netherlands*
[118] *Department of Physics, Northern Illinois University, DeKalb IL, United States of America*
[119] [(a)] *New York University Abu Dhabi, Abu Dhabi;* [(b)] *United Arab Emirates University, Al Ain, United Arab Emirates*
[120] *Department of Physics, New York University, New York NY, United States of America*
[121] *Ochanomizu University, Otsuka, Bunkyo-ku, Tokyo, Japan*
[122] *Ohio State University, Columbus OH, United States of America*
[123] *Homer L. Dodge Department of Physics and Astronomy, University of Oklahoma, Norman OK, United States of America*
[124] *Department of Physics, Oklahoma State University, Stillwater OK, United States of America*
[125] *Palacký University, Joint Laboratory of Optics, Olomouc, Czech Republic*
[126] *Institute for Fundamental Science, University of Oregon, Eugene, OR, United States of America*
[127] *Graduate School of Science, Osaka University, Osaka, Japan*
[128] *Department of Physics, University of Oslo, Oslo, Norway*
[129] *Department of Physics, Oxford University, Oxford, United Kingdom*
[130] *LPNHE, Sorbonne Université, Université Paris Cité, CNRS/IN2P3, Paris, France*
[131] *Department of Physics, University of Pennsylvania, Philadelphia PA, United States of America*
[132] *Department of Physics and Astronomy, University of Pittsburgh, Pittsburgh PA, United States of America*
[133] [(a)] *Laboratório de Instrumentação e Física Experimental de Partículas - LIP, Lisboa;* [(b)] *Departamento de Física, Faculdade de Ciências, Universidade de Lisboa, Lisboa;* [(c)] *Departamento de Física, Universidade de Coimbra, Coimbra;* [(d)] *Centro de Física Nuclear da Universidade de Lisboa, Lisboa;* [(e)] *Departamento de Física, Universidade do Minho, Braga;* [(f)] *Departamento de Física Teórica y del Cosmos, Universidad de Granada, Granada (Spain);* [(g)] *Departamento de Física, Instituto Superior Técnico, Universidade de Lisboa, Lisboa, Portugal*
[134] *Institute of Physics of the Czech Academy of Sciences, Prague, Czech Republic*
[135] *Czech Technical University in Prague, Prague, Czech Republic*
[136] *Charles University, Faculty of Mathematics and Physics, Prague, Czech Republic*
[137] *Particle Physics Department, Rutherford Appleton Laboratory, Didcot, United Kingdom*
[138] *IRFU, CEA, Université Paris-Saclay, Gif-sur-Yvette, France*
[139] *Santa Cruz Institute for Particle Physics, University of California Santa Cruz, Santa Cruz CA, United States of America*
[140] [(a)] *Departamento de Física, Pontificia Universidad Católica de Chile, Santiago;* [(b)] *Millennium Institute for Subatomic physics at high energy frontier (SAPHIR), Santiago;* [(c)] *Instituto de Investigación Multidisciplinario en Ciencia y Tecnología, y Departamento de Física, Universidad de La Serena;* [(d)] *Universidad Andres Bello, Department of Physics, Santiago;* [(e)] *Instituto de Alta Investigación, Universidad de Tarapacá, Arica;* [(f)] *Departamento de Física, Universidad Técnica Federico Santa María, Valparaíso, Chile*
[141] *Department of Physics, University of Washington, Seattle WA, United States of America*
[142] *Department of Physics and Astronomy, University of Sheffield, Sheffield, United Kingdom*
[143] *Department of Physics, Shinshu University, Nagano, Japan*
[144] *Department Physik, Universität Siegen, Siegen, Germany*
[145] *Department of Physics, Simon Fraser University, Burnaby BC, Canada*
[146] *SLAC National Accelerator Laboratory, Stanford CA, United States of America*
[147] *Department of Physics, Royal Institute of Technology, Stockholm, Sweden*
[148] *Departments of Physics and Astronomy, Stony Brook University, Stony Brook NY, United States of America*

[149] *Department of Physics and Astronomy, University of Sussex, Brighton, United Kingdom*
[150] *School of Physics, University of Sydney, Sydney, Australia*
[151] *Institute of Physics, Academia Sinica, Taipei, Taiwan*
[152] [(a)] *E. Andronikashvili Institute of Physics, Iv. Javakhishvili Tbilisi State University, Tbilisi;* [(b)] *High Energy Physics Institute, Tbilisi State University, Tbilisi;* [(c)] *University of Georgia, Tbilisi, Georgia*
[153] *Department of Physics, Technion, Israel Institute of Technology, Haifa, Israel*
[154] *Raymond and Beverly Sackler School of Physics and Astronomy, Tel Aviv University, Tel Aviv, Israel*
[155] *Department of Physics, Aristotle University of Thessaloniki, Thessaloniki, Greece*
[156] *International Center for Elementary Particle Physics and Department of Physics, University of Tokyo, Tokyo, Japan*
[157] *Department of Physics, Tokyo Institute of Technology, Tokyo, Japan*
[158] *Department of Physics, University of Toronto, Toronto ON, Canada*
[159] [(a)] *TRIUMF, Vancouver BC;* [(b)] *Department of Physics and Astronomy, York University, Toronto ON, Canada*
[160] *Division of Physics and Tomonaga Center for the History of the Universe, Faculty of Pure and Applied Sciences, University of Tsukuba, Tsukuba, Japan*
[161] *Department of Physics and Astronomy, Tufts University, Medford MA, United States of America*
[162] *Department of Physics and Astronomy, University of California Irvine, Irvine CA, United States of America*
[163] *University of Sharjah, Sharjah, United Arab Emirates*
[164] *Department of Physics and Astronomy, University of Uppsala, Uppsala, Sweden*
[165] *Department of Physics, University of Illinois, Urbana IL, United States of America*
[166] *Instituto de Física Corpuscular (IFIC), Centro Mixto Universidad de Valencia - CSIC, Valencia, Spain*
[167] *Department of Physics, University of British Columbia, Vancouver BC, Canada*
[168] *Department of Physics and Astronomy, University of Victoria, Victoria BC, Canada*
[169] *Fakultät für Physik und Astronomie, Julius-Maximilians-Universität Würzburg, Würzburg, Germany*
[170] *Department of Physics, University of Warwick, Coventry, United Kingdom*
[171] *Waseda University, Tokyo, Japan*
[172] *Department of Particle Physics and Astrophysics, Weizmann Institute of Science, Rehovot, Israel*
[173] *Department of Physics, University of Wisconsin, Madison WI, United States of America*
[174] *Fakultät für Mathematik und Naturwissenschaften, Fachgruppe Physik, Bergische Universität Wuppertal, Wuppertal, Germany*
[175] *Department of Physics, Yale University, New Haven CT, United States of America*

[a] *Also Affiliated with an institute covered by a cooperation agreement with CERN*
[b] *Also at An-Najah National University, Nablus, Palestine*
[c] *Also at Borough of Manhattan Community College, City University of New York, New York NY, United States of America*
[d] *Also at Center for Interdisciplinary Research and Innovation (CIRI-AUTH), Thessaloniki, Greece*
[e] *Also at CERN, Geneva, Switzerland*
[f] *Also at CMD-AC UNEC Research Center, Azerbaijan State University of Economics (UNEC), Azerbaijan*
[g] *Also at Département de Physique Nucléaire et Corpusculaire, Université de Genève, Genève, Switzerland*
[h] *Also at Departament de Fisica de la Universitat Autonoma de Barcelona, Barcelona, Spain*
[i] *Also at Department of Financial and Management Engineering, University of the Aegean, Chios, Greece*
[j] *Also at Department of Physics, California State University, Sacramento, United States of America*
[k] *Also at Department of Physics, King's College London, London, United Kingdom*
[l] *Also at Department of Physics, Stanford University, Stanford CA, United States of America*
[m] *Also at Department of Physics, Stellenbosch University, South Africa*
[n] *Also at Department of Physics, University of Fribourg, Fribourg, Switzerland*
[o] *Also at Department of Physics, University of Thessaly, Greece*
[p] *Also at Department of Physics, Westmont College, Santa Barbara, United States of America*
[q] *Also at Faculty of Physics, Sofia University, 'St. Kliment Ohridski', Sofia, Bulgaria*
[r] *Also at Hellenic Open University, Patras, Greece*
[s] *Also at Imam Mohammad Ibn Saud Islamic University, Saudi Arabia*

JHEP09(2024)005

[t] *Also at Institucio Catalana de Recerca i Estudis Avancats, ICREA, Barcelona, Spain*
[u] *Also at Institut für Experimentalphysik, Universität Hamburg, Hamburg, Germany*
[v] *Also at Institute for Nuclear Research and Nuclear Energy (INRNE) of the Bulgarian Academy of Sciences, Sofia, Bulgaria*
[w] *Also at Institute of Applied Physics, Mohammed VI Polytechnic University, Ben Guerir, Morocco*
[x] *Also at Institute of Particle Physics (IPP), Canada*
[y] *Also at Institute of Physics, Azerbaijan Academy of Sciences, Baku, Azerbaijan*
[z] *Also at Institute of Theoretical Physics, Ilia State University, Tbilisi, Georgia*
[aa] *Also at National Institute of Physics, University of the Philippines Diliman (Philippines), Philippines*
[ab] *Also at Technical University of Munich, Munich, Germany*
[ac] *Also at The Collaborative Innovation Center of Quantum Matter (CICQM), Beijing, China*
[ad] *Also at TRIUMF, Vancouver BC, Canada*
[ae] *Also at Università di Napoli Parthenope, Napoli, Italy*
[af] *Also at University of Colorado Boulder, Department of Physics, Colorado, United States of America*
[ag] *Also at Washington College, Chestertown, MD, United States of America*
[ah] *Also at Yeditepe University, Physics Department, Istanbul, Türkiye*
[*] *Deceased*

JHEP09(2024)005